Cranfield
UNIVERSITY

Andrew Duncombe

Legibility of Machine Readable Codes Used for Gas Turbine Part Tracking

School of Engineering

EngD

2008–2012

Cranfield
UNIVERSITY

School of Engineering

EngD

2008–2012

Andrew Duncombe

Legibility of Machine Readable Codes Used for Gas Turbine Part Tracking

Supervisors: Prof P. Pilidis & Dr P. Laskaridis

Jan 2012

This thesis is submitted in partial fulfilment of the requirements for the degree of
Engineering Doctorate

Abstract

Gas turbines are comprised of many parts, which are often expensive and required to survive a harsh environment for significant periods (with or without reconditioning). To differentiate between parts, and facilitate keeping accurate historical records, they are often given a unique identification number. However, manually recording and tracking these is difficult. This has led to increased adoption of machine readable codes to help reduce or eliminate many of the issues currently faced (mostly human error). The harsh environment of a gas turbine means that typical methods of applying machine readable codes, such as printed adhesive labels, are simply not durable enough. Direct part marking (DPM) is necessary to ensure the desired longevity of the code over the part's useful life.

The research presented in this thesis was approached in two main phases. Firstly, the author sought to investigate the technical solutions available for the elements required of a part tracking system (encoding, marking and scanning). This included identifying the characteristics of each and their compatibility with one other (across elements). In conjunction with Alstom, criteria were identified that were used as a basis for comparison so that the preferred technical solutions could be determined. The outcome of this process was enhanced by the author developing a number of industrial contacts experienced in implementing part tracking systems.

The second phase related to the legibility of the codes. The harsh environment of a gas turbine results in surface degradation that may in turn reduce the legibility of any machine readable codes present. To better understand why read failures occur, the author first looked to the scanning process. Data Matrix symbols (marked via dot peen) require the scanner to capture an image for processing. Image capture is typically achieved using a charge-coupled device (CCD), each pixel of which induces a charge proportional to the incident illumination. This illumination is received via reflection from the surface of the part and hence the Data Matrix marked on it. Several surface features were identified that govern the way in which the part surface will reflect light back to the scanner: surface roughness, dot geometry and surface colour. These parameters are important because they link the degradation mechanisms occurring – broadly categorised as deposition, erosion or corrosion – with the scanning process. Whilst the degradation mechanisms are distinctly different in their behaviour, their effect on surface reflectivity is common in that they can all be characterised via the surface parameters identified. This was deduced theoretically and so the author completed tests (utilising shot blasting to change the surface roughness and oxidation to change its colour, independently) to show that these surface parameters do indeed change with the introduction of surface degradation and that there is a commensurate change in symbol legibility.

Based on the learning derived with respect to Data Matrix legibility, the author has proposed a framework for developing a tool referred to as a Risk Matrix System. This tool is intended to enhance the application of part tracking to gas turbine engines by enabling symbol durability to be assessed based on the expected operating conditions.

The research presented is the first step in fully understanding the issues that affect the legibility of symbols applied to gas turbine parts. The author's main contribution to learning has been the identification of knowledge from various other sources applicable to this situation and to present it in a coherent and complete manner. From this foundation, others will be able to pursue relevant issues further; the author has made a number of recommendations to this effect.

Acknowledgements

Nomenclature

AIM	Association for Automatic Identification and Mobility
BRDF	Bi-directional reflectance distribution function
BSI	British Standards Institute
CCD	Charge-coupled device
CCPP	Combined-cycle power plant
CFD	Computational fluid dynamics
CGR	Concept gate review
COPQ	Cost of poor quality
CPD	Continuing professional development
DEC	Deposition, erosion and corrosion
DGR	Design gate review
DPM	Direct part marking
ECC	Error correction code
ECM	Electro-chemical marking
EHS	Environment, health and safety
EOH	Equivalent operating hours
EPSRC	Engineering and Physical Sciences Research Council
FE	Finite Element
FEA	Finite element analysis
FIC	Fluoride ion cleaning
FGR	Feedback gate review
FMEA	Failure mode and effect analysis
FPI	Fluorescent Penetrate Inspection
GALE	Gas assisted laser etch
HRI	Human readable information
IGR	Initiation gate review
IP	Intellectual property
IPR	Intellectual property rights
KT	Knowledge transfer
LENS	Laser engineered net shaping
LISI	Laser inducted surface improvement
LLOC	Low-load operation capability
MRI	Machine readable information
OEM	Original equipment manufacturer
OFHC	Oxygen-free high thermal conductivity
PDQ	Product development quality
QE	Quantum efficiency
R&D	Research & development
RGR	Release gate review
RPN	Risk priority number
SAE	Society of Automotive Engineers
SC	Symbol contrast
SGR	Specification gate review
UV	Ultraviolet

Contents

Figures

Tables

Chapter 1

Introduction

This chapter is split into two parts. The first – Project Specification – covers the background to the project, including its rationale and the key objectives that were derived to satisfy the stakeholders, and the second – Research Methodology – indicates the broad methodology adhered to by the author in completing this Engineering Doctorate.

The work presented in this thesis was sponsored by Alstom (Switzerland) and the Engineering and Physical Sciences Research Council (EPSRC).

1.1 Project Specification

Gas turbine parts are often expensive and required to survive a harsh environment for significant periods of an engine's life. It is therefore desirable to have an accurate record of a part's history and current status. To help achieve this, parts are often given unique identifiers (serialisation); typically using alphanumeric strings that must be read and recorded manually by a human operator. With increasing product complexity and production volumes keeping track of parts in this manner has become fraught with difficulties, leading to errors that are costly both in terms of time and money. This thesis was born from Alstom wishing to investigate implementing an enhanced part tracking system, utilising machine readable codes, that would address many of these issues. The prominent drivers include:

- Improved data integrity of part status and history;
- Reduced time requirements for logging parts at critical stages of manufacture, operation and reconditioning; and
- Reduced human interaction.

Alstom is a commercial business and so does do not have the luxury of allowing its employees to thoroughly research every detail of every project – practical outcomes are ultimately required. As such, through this Engineering Doctorate, the author has aimed to support Alstom by offering an enhanced understanding of the process of scanning machine readable codes, including the impact of external stimuli, such as engine operating conditions, on symbol legibility. Where possible, the effects of these stimuli have been quantified in a practical manner so as to promote their usefulness in a commercial setting.

The main aim of this thesis and the key objectives derived to achieve it:

Aim
To identify quantifiable factors that indicate the effect of surface degradation mechanisms on code legibility with respect to surface reflectance.

Key objectives

- Research the available technical solutions and define the part tracking system via a robust selection process.
- Develop an understanding of the scanning process, including relevant theory.
- Identify parameters that relate the effects of degradation to the scanning process – to better mitigate read failures.
- Define the framework of a Risk Matrix System (based on prior learning) – intended as a practical tool for assessing code legibility.

1.1.1 Type of contribution

Cranfield University's senate guidelines on the academic standards required for theses identifies a number of ways in which a contribution to knowledge may be achieved:

"...through the discovery of new knowledge or the application of existing knowledge to new situations, the connection of previously unrelated facts, the development of a new theory or design, or the significant revision of older views or the improvement of an existing design."

The author's work presented in this thesis predominantly relates to "...the application of existing knowledge to new situations...". More specifically, the utilisation of theory with respect to surface reflectance, including roughness and colour, to help explain why the degradation of dot peen Data Matrix symbols during engine operation affects their legibility to the scanner.

1.2 Research Methodology

In carrying out a research project such as this it is preferable to develop an overarching methodology upon which the work is based (see figure 1.1). Of course it is difficult to foresee all possibilities and eventualities, therefore such a tool needs to be reviewed and developed throughout to ensure all objectives are met satisfactorily. The benefit of a methodology is that it provides structure and an opportunity to assess the relative merits and synergy of proposed research elements. In doing so, one hopes to avoid extraneous activities that do not contribute in a meaningful way to the research objectives.

An overview of figure 1.1:

Item 1 An important task in the beginning was to become familiar with the possible solutions available for a part tracking system. With the main components having been identified as encoding, marking and scanning it was then a matter of researching specific solutions within each of these for further appraisal. Information was sought via a number of means: literature, prior experience within Alstom, identifying trends with competitors and enquiring with companies experienced in implementing part tracking systems.
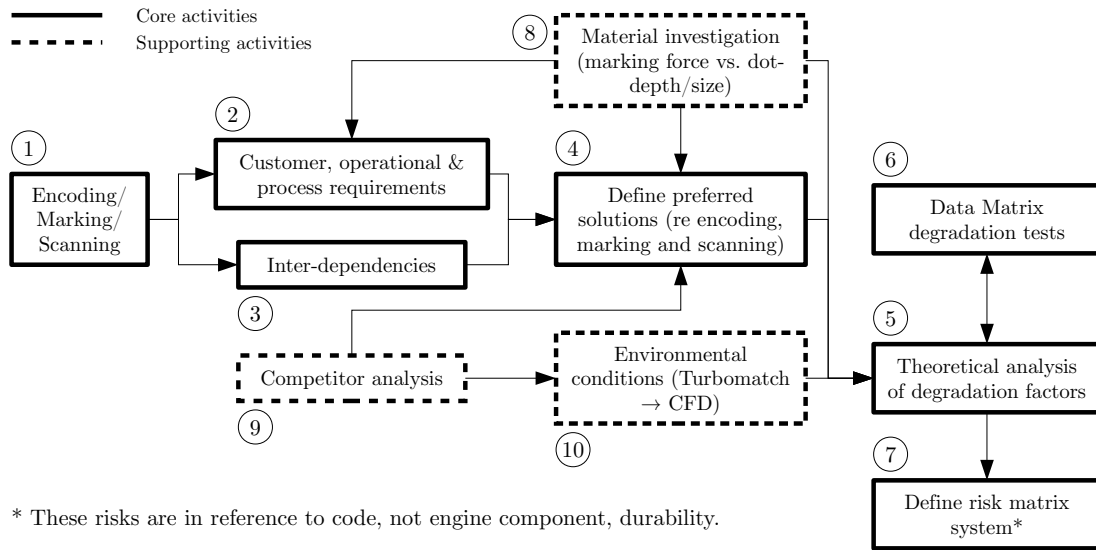
Figure 1.1: Project methodology

Item 2 As the research presented is intended to enhance Alstom's implementation of a part tracking system, possible solutions needed to be judged with their requirements in mind. Consequently, selection of the part tracking system's components was very much a two-way process. Maintaining an open dialogue helped to maximise the effectiveness of this process.

Item 3 Whilst researching the options available for comprising a part tracking system, it became apparent that there was a question of compatibility and consequently inter-dependency when selecting elements. This became an important outcome in its own right. The essence of the issue is to not define a solution for one component, such as marking, without consideration for the impact this choice has on those components remaining. This is to avoid being driven into making a choice that compromises the overall effectiveness of the part tracking system.

Item 4 Having gained a suitable understanding of the options available, ultimately a recommendation would be necessary to identify to Alstom a preferred solution for each component of the part tracking system. As before, this process was completed very much in unison with Alstom to ensure their requirements were met.

Item 5 The main question mark over the use of machine readable codes is their durability, with them needing to endure through manufacturing and reconditioning processes as well as engine operation. The intention of the theoretical analysis was to lay a foundation regarding the identification of parameters that can be used to characterise a code's condition with respect to scanning success or failure.

Item 6 To lend weight to the theoretical analysis, testing was planned that would highlight application of the theory to real examples. Specifically, with respect to code degradation and its impact on scanning legibility.

Item 7 A main outcome of the presented research is to provide the basis of a tool that can be used to assess not only the current legibility of a code, but also its expected

durability. This relies on empirical data to an extent, which is currently limited, so a framework has been proposed that Alstom can develop as their experience grows.

Item 8 The material investigation was intended to provide a method for determining optimum dot peen marking machine settings, so that Data Matrices could be applied quickly and accurately. It was envisaged this tool would be useful to Alstom by reducing the number of test marks required to define machine settings for different materials (i.e. of different hardness). This was entrusted to an MSc student – Faivre [27] – working under supervision.

Item 9 There are few gas turbine OEMs that have implemented a part tracking system utilising permanent machine readable codes (as opposed to adhesive labels, or similar). Nonetheless, this means that some have implemented one, or are attempting to do so, from whose experience it may be possible to learn. This included approaching suppliers of such systems to take advantage of their expertise.

Item 10 It was envisaged that computational analysis may serve to augment the limited availability of real data by enabling the simulation of code degradation, to then be referenced against the parameters identified by the theoretical analysis. The author's Turbomatch model of Alstom's GT26 engine was utilised by Papanikolaou [54], an MSc student working under supervision, who also completed a series of CFD analyses with respect to surface erosion.

Chapter 2

Literature

This chapter presents all the relevant literature gathered throughout the research period. This has predominantly involved developing an understanding of the overall part tracking process, which is comprised of three main elements: encoding, marking and scanning. Understanding the factors that cause a scan to succeed, or otherwise, then dictates the choice of physical properties used to characterise the degradation present.

Further, there is a discussion of failure mode and effect analysis (FMEA) as this serves as a basis for development of the Risk Matrix System intended for assessing code durability.

2.1   Encoding

Many types of machine readable code exist, some of which have been developed for particular applications. However, it is typical to be able to classify these as one of three types: linear, two-dimensional or three-dimensional. The latter is a pseudo-type in that it is typically a linear code that has been embossed in some way to provide depth, otherwise known as a 'bumpy bar code'. A particular type of scanner is used to read such codes that detects changes in the received angle of an emitted laser light, caused by the surface's varying profile. This is in comparison to the contrast detection method as employed with most other linear and two-dimensional codes. Linear codes have now been around for a long time having first seen use in the retail sector during the 1960s. This has resulted in the development of a number of different types, some for particular applications, such as postal systems. Two-dimensional codes are a more recent development that seek to improve on their linear predecessor. One of their main advantages is that they can store significantly more information, through the use of an extra dimension. This further implies that if they are storing a comparable amount of data to a linear code this can be achieved in less physical space.

As part of the research process a number of code types were selected for assessment with respect to their suitability for gas turbine part tracking. As this is a largely unexplored application for such codes – at least in the open literature – the preliminary selection was based largely upon those types that are typically used in industry. Those codes were: Code 39 (linear), Code 128 (linear), PDF417 (two-dimensional), Data Matrix (two-dimensional) and PosiCode (as a bumpy bar code) – see figure 2.1.

(a) Code 39   **(b)** Code 128

(c) PDF417   **(d)** Data Matrix

(e) PosiCode
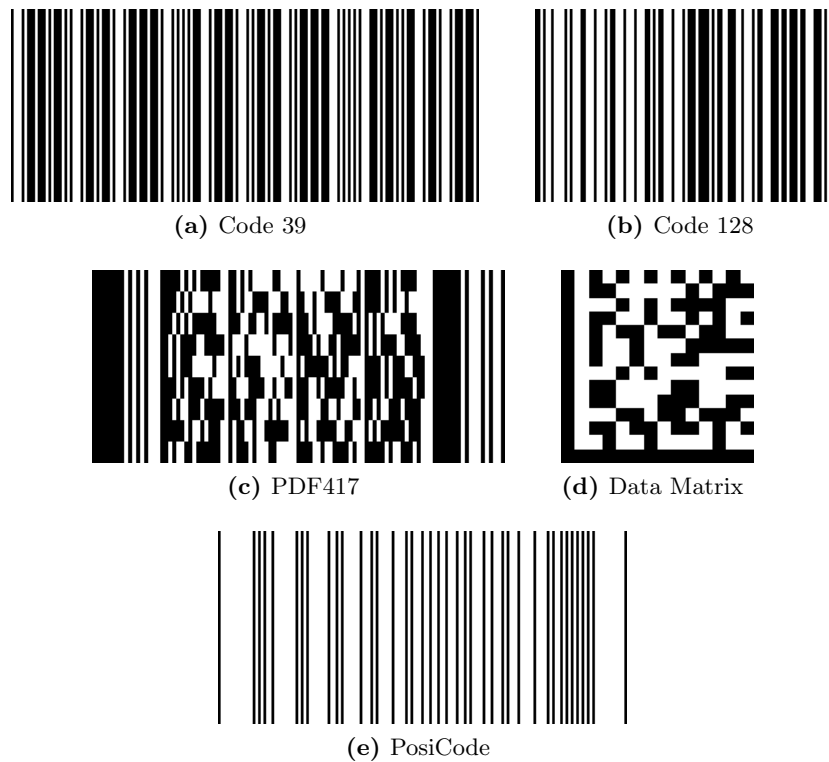
Figure 2.1: Examples of machine readable codes

2.1.1 Code 39 [18]

Code 39 is able to encode upper case letters (A–Z inclusive), digits (0–9 inclusive), and several special characters (such as the $ sign). It is a low density code (compared to Code 128, for example) and so the space required limits its use to larger items. It does not contain a check digit, however any incorrectly interpreted bar cannot generate another valid character. Nonetheless Code 39 sees widespread use and can be decoded by virtually any bar code scanner. Code 39 is restricted to the use of 44 characters, however full ASCII compatibility can be achieved. Symbols 0–9, A–Z, ".", and "-" maintain their Code 39 representations whilst lower case letters, additional punctuation marks, and control characters are represented by sequences of two Code 39 characters. Furthermore, although not typical, it is possible to use Code 39 with a modulo 43 check digit (referred to as Code 39 mod 43).

2.1.2 Code 128 [17]

Code 128 is a high density symbology, used extensively by industry (particularly in shipping and packaging). It is able to encode all 128 ASCII characters, meaning it can cope with alphabetic, numeric, and alphanumeric sequences. It has an additional feature that enables it to encode two numbers into a single character width, known as double density, which would further reduce the space occupied by the bar code. There are three sub-types of Code 128 (128A, 128B, and 128C) that may be invoked at any time within a bar code. These simply represent different character sets (e.g. 128C is for double density encoding of numeric data only — characters 00–99). A checksum digit is included at the

end of the bar code; this enables decoding software to verify whether it has been read correctly.

2.1.3   PDF417 [15]

Whilst PDF417 is a two-dimensional symbol, it is actually comprised of a number of rows that are similar to a linear bar code (from 3–90 of these can be stacked on one another). This format is in the public domain and so anyone can implement a PDF417 based system free of any licence fees. PDF417 has a number of useful features, including user specified dimensions for the narrowest vertical bar (i.e. x-dimension) and row height (i.e. y-dimension), and the ability to link symbols that are scanned in sequence (this allows more data to be stored than any one symbol can achieve alone).

2.1.4   Data Matrix [16]

A Data Matrix can provide much greater data capacity than a linear bar code, although this is in part determined by the chosen resolution (which can be up to 144×144, allowing 2,335 alphanumeric characters to be encoded). By utilising two dimensions for data storage its data density is also much improved, even when compared to a high density linear symbology like Code 128. Typically symbols will be square (with an even number of rows and columns), although rectangular configurations are possible. A particular advantage of the Data Matrix is its ability to incorporate error correction: error correction code (ECC) 200 is the latest version of the Data Matrix and supports advanced error checking and correction algorithms, such as Reed-Solomon [16]. Simply, Reed-Solomon involves oversampling a polynomial constructed from the data, leading to it being over-determined. Therefore if some of the points are not received correctly the original data can still be reconstructed. It is not too dissimilar to correcting or drawing a curve by interpolating through a number of known points. This means symbols that are significantly damaged or obscured can be still be decoded.

Approximately ten years ago an industrial drive began (particularly in aerospace) to enable tracking of parts throughout their useful lifetime using machine readable codes. Large organisations such as Airbus, Rolls-Royce [56], and the US Department of Defence [71] have been very proactive in implementing systems to achieve this, with the Data Matrix at their heart.

2.1.5   PosiCode [1]

PosiCode is a position-based symbology. This differs from the majority of bar codes, which operate on the principle of presence/absence. Presence/absence symbologies consider each character as a fixed number of rectangular modules, which may be either white or black. For example, each character of Code 128 comprises 11 modules of equal width and these are arranged as 3 bars alternating with 3 spaces (starting with a bar) – each bar or space may consist of 1–4 modules. However PosiCode de-couples the width of the bars from their position, with the centres of the bars arranged on a grid of equally spaced parallel lines (the distance between these is called the G-dimension and is analogous to the x-dimension of conventional codes). The data within the symbol is decoded based on the position of the bars, rather than their width (therefore the bars are uniform). The nature of PosiCode means it is suited to creating codes where controlling the bar width may be difficult.

Two variations of the code exist: PosiCode A and PosiCode B. PosiCode A is recommended where the mark width approaches the scanner resolution or if the accuracy of mark placement cannot be adequately controlled. PosiCode B is intended for applications where the mark width must exceed the G-dimension (typically in the range 1–2G) due to limitations of the chosen marking technique.

2.2 Marking

Gas turbine engines present a harsh environment where high temperatures and pressures are common place. This places a premium on durability when considering how codes should be applied to engine parts. More typical methods, such as printed adhesive labels, are simply not durable enough. This led the author to assess the applicability of direct part marking (DPM) techniques.

There are a number of DPM techniques, which can be broadly categorised as either intrusive or non-intrusive – some examples are shown in table 2.1. These are described in some detail in two NASA documents [50; 51], which serve as the basis for the following discussion. Intrusive markings can be considered a controlled defect as they involve altering the part's surface in some way (e.g. abrading, cutting, vaporising, etc.). If not done properly unacceptable material degradation can result and so intrusive methods are typically not recommended for safety critical applications. Non-intrusive markings, also known as additive markings, may be produced as part of the manufacturing process or by the addition of a layer of media to a part's surface (in such a way that material properties are not adversely affected).

Intrusive	Non-intrusive
Dot peen	Cast, forge and mould
Electro-chemical marking (ECM)	Ink jet
Engraving/milling	Laser bonding
Direct laser marking	Liquid metal jet

Table 2.1: Examples of intrusive and non-intrusive DPM techniques

Of the various DPM methods that exist, three were shortlisted for further consideration: dot peen, electro-chemical and laser. This was largely due to these methods seeing extensive use in industry already, thereby reducing the risk associated with implementing them as part of a part tracking system. The selection process is dealt with in detail in section 3.2.2.

2.2.1 Dot peen marking

Dot peen marking is a process whereby a conically tipped stylus is made to repeatedly strike against the surface of the target material, each contact causing an indentation. To ensure materials with a wide range of hardness can be marked a carbide stylus is typically utilised. Diamond tipped styli are also available, but require more careful use to ensure the tip does not become dislodged or misaligned. Actuation of the stylus is typically electromagnetic or pneumatic in nature, the former being preferred as any pulsing in the air system can impact marking accuracy. Translational movement of the stylus head is

best achieved with screws rather than belts to help reduce any possible backlash in the system.

The nature of the dot peen process means that it is best suited to marking Data Matrix codes, which are comprised of a number of modules – each of which corresponds to a single strike of the stylus. Varying the overall dimensions and/or number of rows and columns of the desired Data Matrix will change the required dot size. This can be accommodated by varying a number of parameters in combination:

- Stylus angle – typically 60, 90 or 120°
- Retract distance
- Impact force

2.2.2   Electro-chemical marking

ECM is a process that has been utilised since the 1940s and is compatible with all conductive metallic parts. It can be used to either etch or colour the material's surface. The former involves removing material from the target surface via electrolysis. Colouring is achieved in a similar manner to etching, except that an AC power source is required rather than DC. The target surface is coloured by oxidisation – no material is removed. Modern power units enable precise and repeatable marking, be it etching or colouring. If desired, it is possible to etch and then colour the same mark for improved contrast.

The shape of the mark is controlled by using a stencil. This means ECM is suited to applying a wide variety of codes, be they linear, two-dimensional, or otherwise. It is also a process that lends itself to marking curved surfaces, such as cylinders, which can be awkward via other means.

2.2.3   Laser marking

In a similar manner to ECM, laser marking can be broadly categorised in several ways: laser colouring, laser etching or laser engraving.

Laser colouring changes the colour of the marked surface without causing any material loss or damage. A relatively low power beam is used, traversing at a slow speed, to achieve the discolouration. Whilst a typically safe process, care must be exercised under certain circumstances, for example, where the material has received prior heat treatment. Marks applied correctly via laser colouring remain imperceptible to the touch and will appear smooth under low magnification ($\sim 10\times$).

Etching applies a greater level of heat to the surface than does colouring, causing local melting. An advantage of using increased power is that marks can be applied more quickly. This technique, however, is not recommended for safety critical parts because cracks may form in the metal during cooling and propagate into the surrounding surface material, leading to part failure. If a safety critical part has a coating applied then laser etching may be safely used so long as it does not penetrate beyond the surface coating (this is known as "coat and mark"). Due to local melting of the material, laser etched marks typically sit slightly proud of the surrounding surface and so are perceptible to the touch and visible under low magnification ($\sim 10\times$).

Engraving involves applying yet more heat than etching such that material is removed via vaporisation. This technique produces a deep, but light, marking, similar to electro-chemical etching. As this laser marking method uses the most power of the three described

here, it is also the quickest. Laser engraving cannot achieve the same levels of contrast as either colouring or engraving because the discoloured material is vaporised and ejected during the marking process. Like etching, this technique should be used with caution on safety critical parts as micro cracking can occur. Laser engraving may be suitable under such circumstances if used as part of a "coat and remove" process. This is where the part is coated in a contrasting colour that the engraving process partially removes to expose the underlying material. However, the identifying mark is only as resilient as the surface coating used. Laser etching is easily perceptible to the touch and visible under low magnification ($\sim 10\times$).

2.2.4 Material hardness

DPM methods such as dot peen involve striking the surface of a material to leave a mark. The size of the mark will, in part, depend upon the hardness of the target. There is no universal definition of hardness, but instead a number of empirically derived scales. Broadly speaking, the reason for there being no universal definition is due to the differing behaviour of materials to the application of loads on their surface. For example, a different impression on the surface will result if a load is applied statically rather than dynamically. These issues are discussed further in the MSc thesis of Faivre [27] – a summary of which is presented in section 3.3. Three of the most prominent scales used to describe material hardness are Brinell, Rockwell and Vickers:

Brinell [12]
  The indenter used for the Brinell test is a hard metal ball, of diameter D. This indenter is pressed into the surface of the target under an applied force F. Upon removal of the indenter, the mean diameter d ($= {}^{(d_1 + d_2)}/{}_2$) of the indentation left in the surface is measured (see figure 2.2a, page 12). Brinell hardness is proportional to the quotient obtained from dividing the applied force by the surface area of the indentation. The surface area is calculated using the depth h of the indentation, which is assumed to retain the shape of the ball indenter:

$$h = \frac{D}{2}(1 - \sqrt{1 - {}^{d^2}/{}_{D^2}})$$

$$\text{Brinell hardness} = 0.102 \times \frac{F}{\pi D h}$$

Vickers [13]
  There are three variants of the Vickers hardness test that are differentiated by the range of applied force (see table 2.2). The indenter used for all three test variants is diamond shaped in the form of a right pyramid with a square base – the angle between opposite faces at the vertex should be $136°$. This indenter is forced into the surface of the target under an applied force F. Upon removal, the diagonal of the indentation d left in the surface is measured (see figure 2.2b, page 12). Vickers hardness is proportional to the quotient obtained from dividing the applied force by the surface area of the indentation. The surface area of indentation is calculated based on the assumption that it retains the same shape and angle at its vertex as the indenter:

$$\text{Surface area of indentation} = \frac{d^2}{2\sin(\frac{136°}{2})}$$

$$\text{Vickers hardness} = 0.102 \times \frac{2F \sin(\frac{136°}{2})}{d^2} = 0.1891 \frac{F}{d^2}$$

Test force range (N)	Hardness symbol	Designation
$F \geq 49.03$	$\geq$ HV 5	Vickers hardness test
$1.961 \leq F < 49.03$	HV 0.2 to < HV 5	Low-force Vickers hardness test
$0.09807 \leq F \leq 1.961$	HV 0.01 to < HV 0.2	Vickers micro-hardness test

Table 2.2: Vickers hardness test variants [13]

Rockwell [14]

There are a number of different Rockwell hardness scales (A, B, C, D, E, F, G, H, K, N and T) that are differentiated by the type of indenter used and magnitude of the applied force (see table 2.3). However, all of them share the same principle of operation whereby the indenter is forced into the target surface in two steps: first under a preliminary force, followed by the application of an additional force. The permanent depth of indentation h is measured once the additional force has been removed, but with the preliminary force still in effect (see figure 2.2c, page 12). Rockwell hardness is calculated using the formula:

$$\text{Rockwell hardness} = N - \frac{h}{S}$$

where N and S are constants specific to the scale.

Rockwell hardness scale	Hardness symbol	Type of indenter	Preliminary test force F_0 (N)	Additional test force F_1 (N)
A	HRA	Diamond cone	98.07	490.3
B	HRB	Ball (1.5875 mm)	98.07	882.6
C	HRC	Diamond cone	98.07	1,373
D	HRD	Diamond cone	98.07	882.6
E	HRE	Ball (3.175 mm)	98.07	882.6
F	HRF	Ball (1.5875 mm)	98.07	490.3
G	HRG	Ball (1.5875 mm)	98.07	1,373
H	HRH	Ball (3.175 mm)	98.07	490.3
K	HRK	Ball (3.175 mm)	98.07	1,373
15N	HR15N	Diamond cone	29.42	117.7
30N	HR30N	Diamond cone	29.42	264.8
45N	HR45N	Diamond cone	29.42	411.9
15T	HR15N	Ball (1.5875 mm)	29.42	117.7
30T	HR30N	Ball (1.5875 mm)	29.42	264.8
45T	HR45N	Ball (1.5875 mm)	29.42	411.9

Table 2.3: Rockwell hardness test scales [14]

(a) Brinell [12]

(b) Vickers [13]
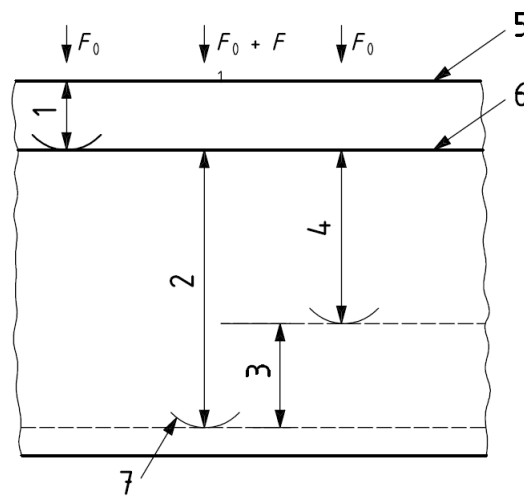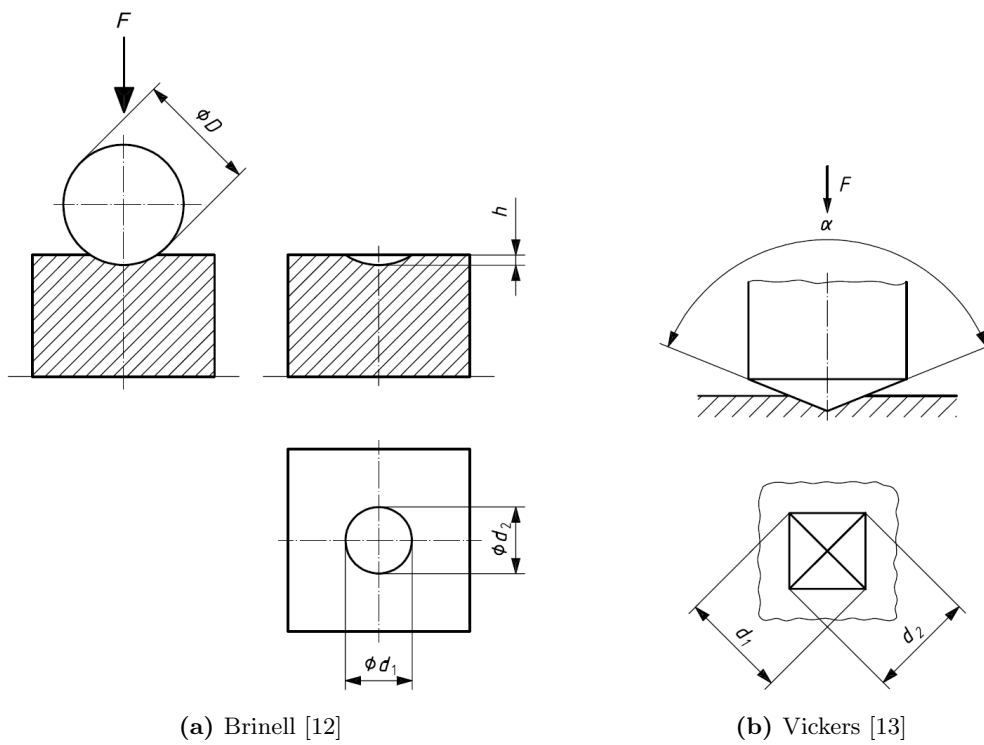
(c) Rockwell [14]

Key

1 – Indentation depth by preliminary force F_0
2 – Indentation depth by additional test force F_1
3 – Elastic recovery just after removal of additional test force F_1
4 – Permanent indentation depth h
5 – Surface of specimen
6 – Reference plane for measurement
7 – Position of indenter

Figure 2.2: Principles of several material hardness tests

2.3 Code Degradation

Gas turbine components are subject to a number of phenomena during typical running and those pertinent to this study may be considered under the broad terms of deposition, erosion and corrosion (DEC). These are caused by the presence of impurities in the flow, which may either be ingested by the engine (via the intake or fuel system) or originate from within (e.g. bearing oil). These impurities will be particles that may be in solid, liquid, or, for the hot section, gaseous form. Gaseous species will have been vaporized further upstream during combustion, but can condense back to liquid form on cooled turbine surfaces or within the main gas path as temperature and pressure drop through successive turbine stages.

Typically DEC is considered because of its impact on the main gas path and consequently engine performance. However, the main concern of this project is how these phenomena will impact any markings on engine components. For example, blades will not be marked on the aerofoil surface, but their root, and so the main area of interest in this instance will be below the blade platform, in and around the hub region.

2.3.1 Deposition

El-Batsh and Haselbacher [25] indicate that deposit build-up on surfaces exposed to particulate flow is the result of three primary processes: particle movement, particle sticking and particle detachment. They further identify a number of physical processes relevant to each of these (see figure 2.3). The particle movement processes listed in figure 2.3 have been summarised in table 2.4 on page 16.
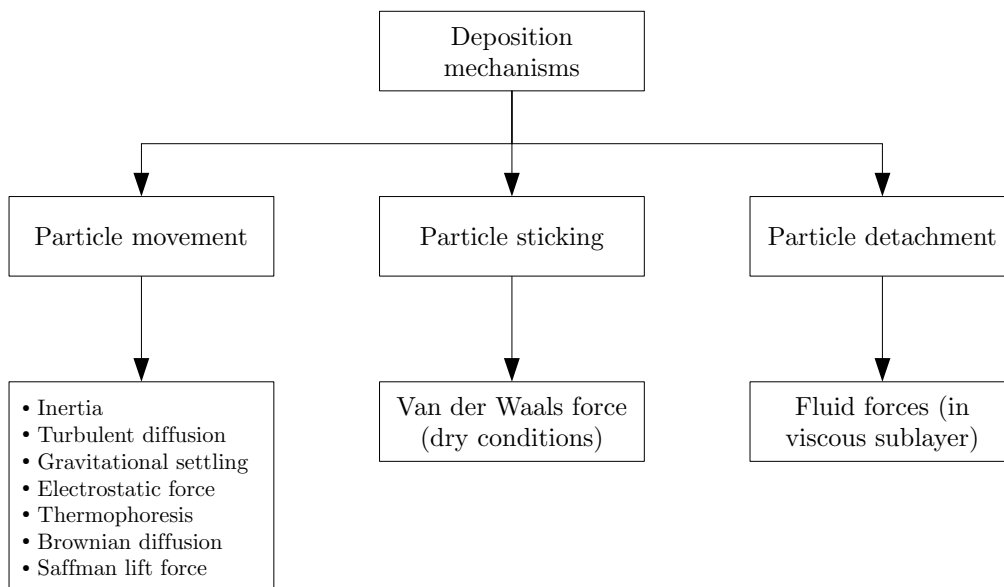

Figure 2.3: Particle deposition mechanisms [25]

Hamed et al. [34] suggest that the dominant mechanisms of particle delivery to turbine flow path surfaces are intertial impaction, turbulent diffusion/eddy impaction, Brownian diffusion, and thermophoresis. Inertial impaction is where particles have sufficient mass to

deviate from the gas flow streamlines, penetrate the aerofoil boundary layer, and impact on its surface. Turbulent diffusion is where smaller particles are entrained by the eddies of a boundary layer and swept towards the adjacent surface; however eddies will dissipate near a surface and so final impaction is the result of having sufficient inertia to coast towards it (eddy impaction). The variation of these two mechanisms with respect to particle size is depicted in figure 2.4. Brownian diffusion is relevant to extremely small particles where the random impacts can cause delivery to a nearby surface. Thermophoretic behaviour can occur near cooled surfaces, such as upstream turbine blades: if one considers a single particle in the thermal boundary layer, the energy of random impacts will be greater from its hot side – this produces a net average impact force towards the cooled surface.
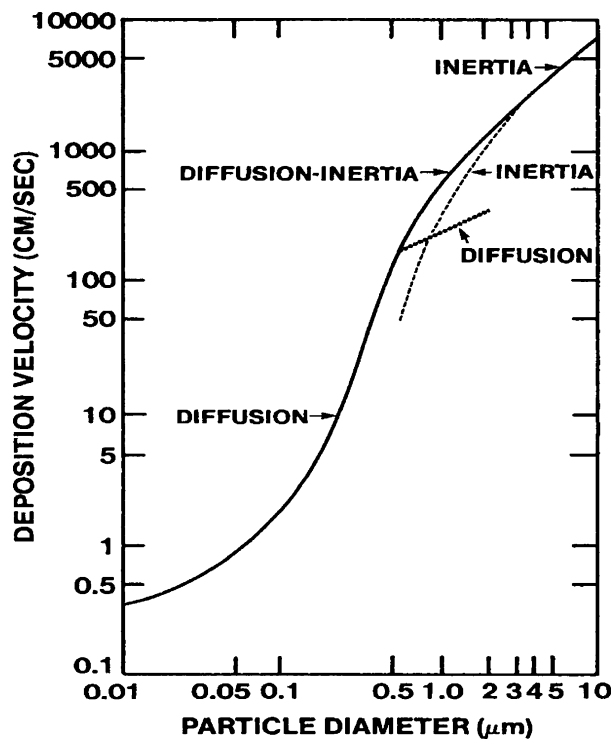
Figure 2.4: Variation in transport mechanism with particle size [34]

Once a particle has reached a surface, deposit build-up is governed by the balance of sticking and removal forces acting. Under dry conditions the van der Waals force is the major contributor to the former. Dahneke [24] investigated the rebound characteristics of spherical particles by measuring the ratio of reflected velocity to incident velocity (known as the coefficient of restitution). They found that this coefficient remained relatively constant for high incident velocities, but that the significance of the adhesion force increases as this velocity decreases and so the reflected velocity also decreases. At the point of zero rebound, the particle is captured. Brach and Dunn [9] developed an expression for the initial velocity below which rebound does not occur – the critical or capture velocity. In their model, this critical velocity depends upon the size of the particle and the material properties of both it and the surface it is impacting.

A particle attached to a surface will become detached if the removal forces of the fluid flow are sufficient. Detachment from smooth and rough surfaces is caused by the fluid dynamic moment in the viscous sublayer [25]. The mechanisms of particle detachment include rolling, sliding and lifting. Soltani and Ahmadi [64] showed that spherical particles are

released from a surface by rolling rather than sliding or lifting. They were able to derive an expression for the critical wall shear stress required for particle detachment. If the turbulent flow has a wall shear stress higher than this critical value then the particle will detach from the surface.

2.3.2 Erosion

Erosion is an important consideration as it has the potential to cause significant degradation to any codes marked on engine parts. It is caused by the impaction of suspended solid particles within the engine. These can manifest via a number of mechanisms, but typically they will either be ingested through the intake and/or produced as a combustion by-product. There are a number of factors that can affect the erosion process, including:

- Impingement angle
- Particle impact velocity
- Particle size, shape and concentration
- Mechanical properties of the particle and target surface
- Temperature of the target surface
- Exposure time

Hamed et al. [34] state that, in general, the erosion rate of a particular material will be governed by particle impact velocity and impingement angle. Ductile and brittle materials exhibit different characteristics regarding the variation of erosion rate with impingement angle (this is shown schematically in figure 2.5). This is because of the dominant mechanism occurring in each case: impactions will tend to cut a ductile material, whilst causing fracture in a brittle one.
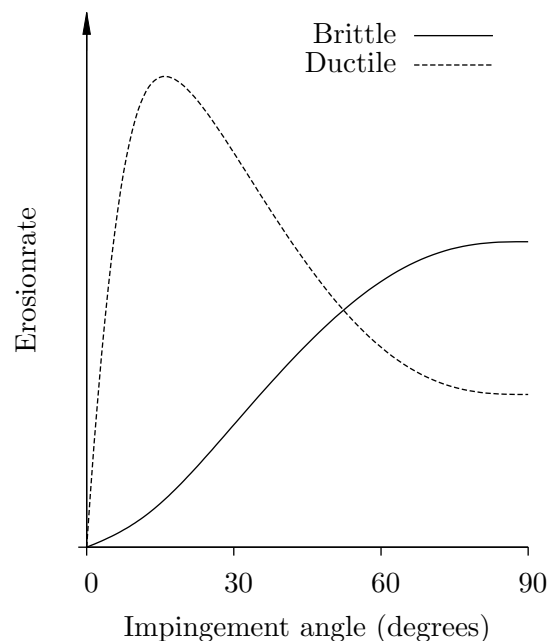
Figure 2.5: Variation of erosion rate with impingement angle [34]

Phenomenon	Description
Inertia	The mass of a particle prevents it from following exactly the same path as turning fluid streamlines (this becomes more pronounced with increasing particle mass).
Turbulent diffusion	The random fluctuations inherent to a turbulent boundary layer are responsible for the migration of entrained particles to the local surface. Smaller particles are particularly susceptible to this mechanism.
Gravitational settling	Particles suspended in a fluid will have a settling movement imparted by gravity. The extent of this effect will be, in part, due to the density of the containing fluid and the motion of each particle.
Electrostatic force	The charge of particles can influence how they interact due to the attractive or repulsive forces that may result, thereby affecting their relative motion.
Thermophoresis	This is the diffusive effect of temperature gradient on mixtures of varying particles. Thermal diffusion is considered "positive" when molecules migrate from hot to cold regions and "negative" when the opposite is observed. Typically heavier/larger species in a mixture will exhibit positive thermophoretic behaviour and lighter/smaller species negative.
Brownian diffusion	Brownian motion is the random movement of particles suspended in a liquid or gas. Even though a bulk fluid may be stationary, collisions will be occurring between its particles and those of the suspended matter, causing the latter to follow a random path. Diffusion is essentially the simultaneous, but independent, Brownian motion of many such suspended particles (e.g. a drop of ink diffusing in water where both have no apparent bulk movement).
Saffman lift force	Rotation will be induced in a particle subjected to a shear flow (i.e. velocity gradient). This rotation will give rise to a pressure distribution and therefore a force, causing translational motion.

Table 2.4: Summary of particle movement processes

Goodwin et al. [32] were able to show that erosion does increase with particle size, albeit up to a critical vale beyond which the rate of erosion tends to a constant. Further, the shape and strength of the particle can affect the form of the erosion curve. Typically angular particles will remove more material from the target surface than spherical, particularly for glancing impacts. Angular particles present a smaller contact area than do spherical, therefore the stress will be higher in the surface at impact and they are more likely to cause removal of material through cutting.

The mechanical properties of the particle and impact surface may affect erosion rate. For example, Tilly [68] showed that ductile erosion rates can be reduced by increasing the strength and hardness of the target material. However, brittle erosion apparently increases with hardness. This contradictory behaviour is not unexpected due to the differing mechanisms of ductile and brittle erosion. However, estimating erosion via a material's mechanical properties is not a certainty as it has been shown that commonly utilised parameters, such as Young's modulus, that relate to the strength or hardness of a material do not necessarily correlate well with erosion rate [63].

Wakeman and Tabakoff [72] show that, for the alloys tested, increasing the target temperature causes an increase in erosion rate for a given particle velocity (see figure 2.6a). This increase is also observed across the entire range of impingement angles (see figure 2.6b) – the profile of which remains similar, i.e. the peak erosion rate remains at approximately the same angle. Significantly increasing the temperature of a metal tends to have a negative effect on its mechanical properties, such as yield stress. For a ductile material this will likely cause an increase in erosion due to the surface being more susceptible to cutting and other deformation caused by impacting particles.

The exposure time of a surface to particle impacts will have an effect with respect to the volume loss rate of material. Usually this is considered a steady-state parameter, however Rao and Buckley [55], for example, show this not to be the case – they highlight a number of different ways in which volume loss rate can vary over time. Further, they present data for spherical particle impingement on an aluminium alloy specimen, which results in a so called type-III curve (see figure 2.7 on page 19). This behaviour is characterised by an initial incubation period, where the volume loss rate is minimal. This shortly translates to the acceleration period during which the volume loss rate peaks at a value above the steady-state. Once this peak value is attained there is a transition to the deceleration period during which time the volume loss rate reduces to its final steady-state value, at which point the steady-state phase commences.

Surface roughness (refer to section 2.3.2.1) characteristics have been measured after some erosion tests (Hamed et al. [35], for example), showing it to correlate closely with erosion rate in terms of its variation with impact angle, velocity, and particle size. Furthermore, eroded surface roughness does not appear to change beyond a certain limit even with continued mass removal by erosion. Surface roughness can be very important regarding the legibility of codes – if it and the individual symbol marks (e.g. individual dots of a Data Matrix) are too geometrically similar scanning can be severely compromised.

2.3.2.1 Surface roughness

Surface roughness is an important parameter across a wide range of engineering disciplines, such as optics, bearings and hydraulics, and is typically of the order of microns. There are myriad ways to define roughness, but one of the more prevalent measures is known as R_a roughness [20]. It is defined as the arithmetic mean of the absolute ordinate values $Z(x)$
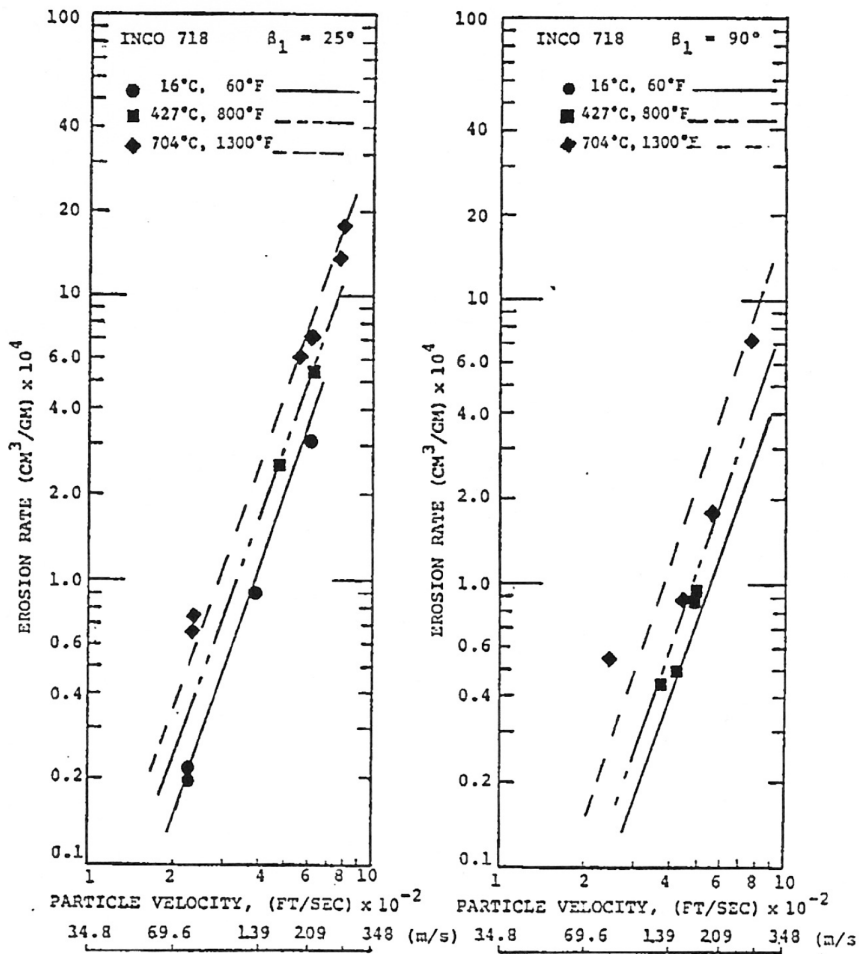
(a) INCO 718 erosion rate versus particle velocity for different sample temperatures
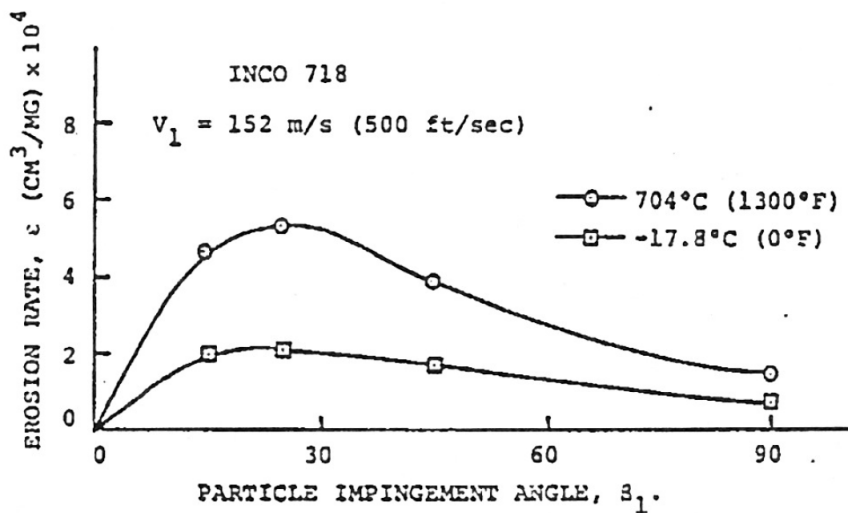
(b) Erosion rate versus impingement angle for two different temperatures

Figure 2.6: The effect of temperature on erosion rate [72]

Figure 2.7: Volume loss rate as a function of exposure time [55]

within a sampling length:

$$R_a = \frac{1}{l} \int_0^l \mid Z(x) \mid dx$$

Use of a roughness parameter enables the comparison of different surfaces. This is important because of the effect surface roughness can have with respect to the ratio of specular to diffuse reflection of light from a surface. This can affect the r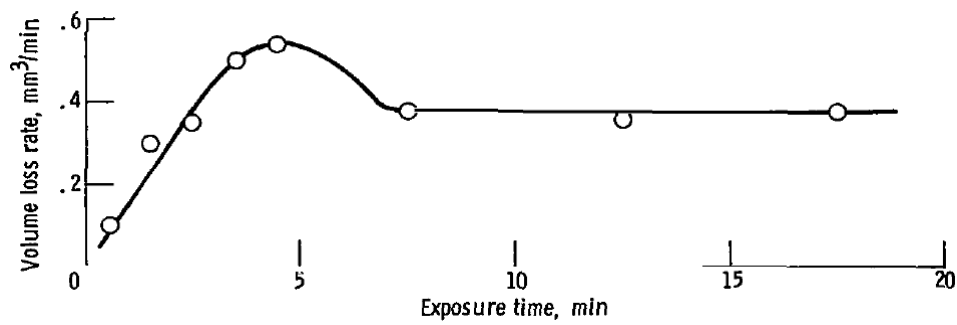eflective properties of a machine readable code applied to a part and therefore the quality of image captured by the scanning device. These issues are discussed further in section 2.4.2.

2.3.3 Corrosion

Corrosion encompasses a number of mechanisms whereby a material – usually a metal – disintegrates/decays through chemical reaction with its environment. Oxidation is a common form of corrosion that can readily occur to gas turbine parts; particularly in the engine's hot section where the elevated temperatures serve to increase the reaction rate. Such corrosion mechanisms are significant because they have the potential to compromise the legibility of machine readable markings applied to engine parts. Being chemical processes, attempts to mitigate their effects often involve the use of coatings in order to isolate the surface. However, coatings that may be used for corrosion protection or otherwise (such as thermal barriers) will hinder the scanning process. Therefore, surfaces chosen for marking will be more susceptible to these processes due to a relative lack of protection. Erosion can potentially amplify their effects through pitting, which results in more surface area for chemical reactions to occur over.

2.3.3.1 Thermal oxidation

All metals tend to form oxides, with the rate of reaction depending on temperature: higher temperatures cause it to increase. There is no single method applicable to calculating oxidation growth, a number of which are discussed by Kubaschewski and Hopkins [39, pp. 37–46]. The parabolic relationship provides a reasonable approximation of oxide growth with respect to ferrous metals, such as the mild steel used in this study. Schütze [60, p. 6] states that "the rate determining step when equilibrium has been established at the gas/oxide and oxide/metal phase boundaries is the diffusion of cations and/or anions of the oxide-forming elements and also of electrons via lattice defects (vacancies, interstitials) in the oxide scale" (presented schematically in figure 2.8a). Parabolic growth is based on

the assertion that oxide growth rate is inversely proportional to the scale thickness x and proportional to the scaling constant k_p.

$$\frac{dx}{dt} = \frac{k_p}{x} \tag{2.1}$$

Upon integration, 2.1 becomes

$$x^2 = 2k_p t \tag{2.2}$$

and thus the growth is parabolic (see figure 2.8b).
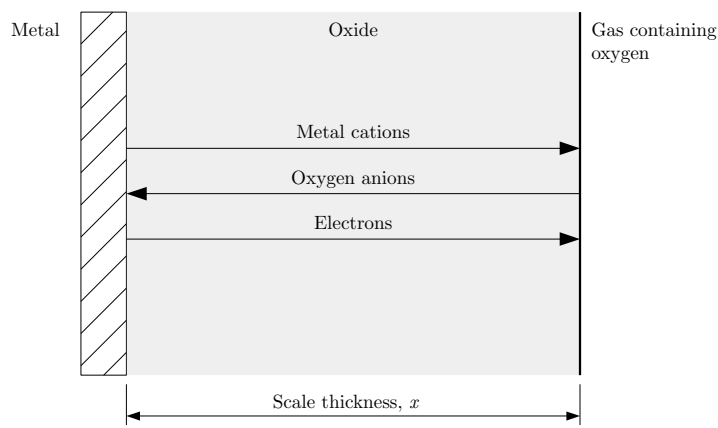
(a) Oxide diffusion schematic
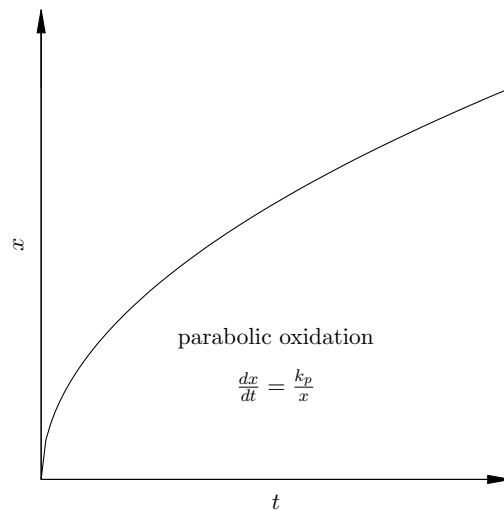
(b) Parabolic oxidation

Figure 2.8: Oxide growth [60, p. 7]

For temperatures up to ~ 570 °C the oxide layer produced on steel is comprised of two constituents: an under layer of magnetite (Fe_3O_4) and an over layer of haematite (Fe_2O_3) – see figure 2.9.

O$_2$

Fe$_2$O$_3$ (haematite)
Fe$_3$O$_4$ (magnetite)
Steel
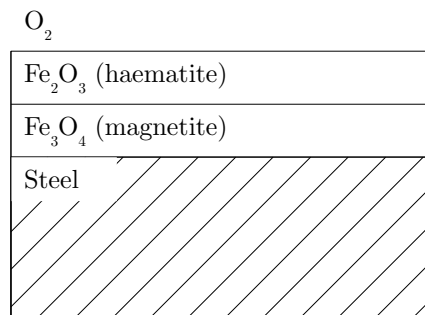
Figure 2.9: Schematic representation of the oxide layers that form on steel

With respect to colour, there are two distinct phases of oxide growth on metals. Initially, when the oxide layer is extremely thin (of the order of nanometres) it acts as a transparent film on the metal's surface. Depending on the film's thickness, light reaching the observer's eye will be coloured if the wavelengths subject to interference are within the visible region of the spectrum (refer to section 2.3.3.2). Once the oxide layer becomes thick enough to no longer allow the transmittance of light (i.e. it becomes opaque) then it will be the reflective properties of the oxide only that dictate its apparent colour. For example, steel oxides are primarily comprised of iron and as such are typically red/brown in colour.

2.3.3.2   Thin films

The perceived colour of thin oxide films on metallic surfaces can change dependent upon their thickness. Evans [26, pp. 58–99] describes the cause of this phenomenon: consider a metal plate covered by an oxide film of thickness y, as depicted in figure 2.10, and imagine that the monochromatic light shining upon the oxide's surface has a wavelength such that the ray ABC reflected at the film's outer surface is exactly out of phase with the ray $XYZBC$ that has been reflected at the inner surface. This wavelength is then the interference wavelength, denoted by the symbol λ_x. Due to the interference occurring between these two waves, the intensity of light emergent along BC will be abnormally low. The missing light is contained in the internally reflected ray BD, which will be exactly in phase with the externally incident ray A. This missing light will be further reflected at D and experience a further chance of escape at E, but if the film thickness remains uniform then destructive interference will occur once more with the externally reflected light WEF. This process will repeat, causing the missing light to remain imprisoned. Continued internal reflection will eventually cause conversion into heat, owing to the imperfect transparency of the oxide film, ultimately leading to complete extinction of the imprisoned light.

As the wavelength of the incident light varies from λ_x, be it less or more, then an increasing quantity of the imprisoned light can emerge after each internal reflection. If white light is allowed to shine on the surface, the reflected spectrum will show a minimum at λ_x, with the intensity rising on each side of that wavelength (see figure 2.11). The breadth of the interference band depends on the transparency of the film substance and reflectivity of the metal backing. The interference band will be narrower for a highly transparent oxide than for a nearly opaque one – a perfectly transparent film on a perfectly reflective backing should give a zero bandwidth (i.e. no interference colours).
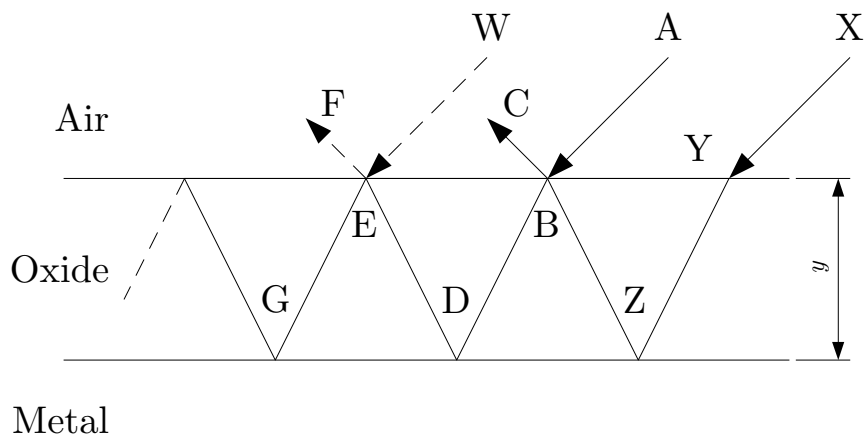
Figure 2.10: Light ray interaction with thin oxide films [26, p. 92]
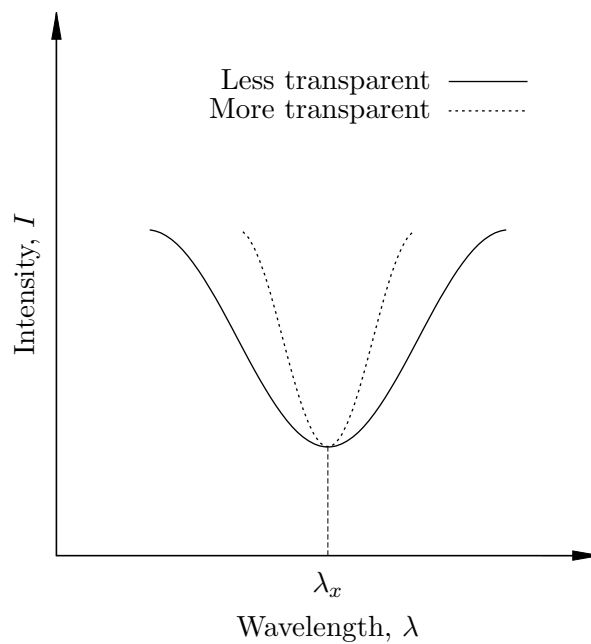

Figure 2.11: Variation of interference band breadth with film transparency [26, p. 93]

Kubaschewski and Hopkins [39, p. 100] state that for monochromatic light falling normally on a film covered metal, interference occurs when:

$$2\xi = \frac{\lambda}{2n},\ \frac{3\lambda}{2n},\ \frac{5\lambda}{2n}, \ldots \text{etc.} \tag{2.3}$$

where ξ = film thickness; λ = wavelength of the light in air; and n = refractive index of the film. If there is a difference in the phase-change produced by the two reflections, this can be regarded as an additional path difference c, giving:

$$\xi = \frac{\lambda}{4n} - c,\ \frac{3\lambda}{4n} - c,\ \frac{5\lambda}{4n} - c, \ldots \text{etc.} \tag{2.4}$$

For transparent films attached to metals it is usual to assume c is zero [26, p. 95], giving minimum reflectance at those thicknesses defined by equation 2.3.

2.3.3.3 Hot corrosion

Hot corrosion is the deposit-induced accelerated oxidation of a metal surface. In most practical situations, particularly those involving fossil fuel combustion products, this occurs through the formation of a salt deposit, usually a sulphate. Once a deposit has formed on the surface, the extent to which it affects corrosion resistance depends on whether or not it melts, its adherence and the extent to which it wets the surface [8]. It is usual for severe hot corrosion to only occur in the presence of liquid deposits.

The hot corrosion of most susceptible alloys occurs in two stages: initiation and propagation. During the initiation stage the rate of corrosion is slow (similar to that in the absence of the deposit), whilst the propagation stage is characterised by rapid, potentially catastrophic, corrosion. These two phases are illustrated in figure 2.12 for isothermal oxidation. Hot corrosion may be limited during the initiation stage by the protective action of an oxide scale on the alloy's surface. The extent of this protection depends on its ability to reduce the rate of corrosion reaction by acting as a diffusion barrier between the metal substrate and corrosive environment [60]. Oxide scales can arise naturally during operation or produced through deliberate pre-oxidation in oxygenated atmospheres at a suitable temperature. The propagation stage occurs because of alterations occurring during initiation, which may include: depletion of the element responsible for forming the protective oxide scale on the alloy, incorporation of a component from the deposit (e.g. sulphur) into the alloy, dissolution of oxides into the salt, and development of cracks or channels in the scale (reducing its effectiveness as a diffusion barrier) [8].

Given the importance of the oxide scale in abating the process of hot corrosion, alloying elements are added during the production of materials to promote the development of suitably protective oxide scales. Two of the most important alloying elements in this regard are Cr and Al [60], to promote formation of either a Cr_2O_3 or Al_2O_3 surface scale respectively. However, often it is not possible to achieve optimum protection against corrosion through alloying because the additions can have a deleterious effect on the material's mechanical properties. Therefore, many high temperature alloys are optimised with respect to their mechanical properties and then the finished components coated with a suitable corrosion protection layer, which can be regarded as an alloy itself (developed to form a suitable protective oxide scale).

Hot corrosion is often differentiated by the temperature range under which it occurs, referred to as either Type I or Type II [40]. Type I hot corrosion typically occurs between 800 and 950 °C; the lower threshold coinciding with the melting temperature of the salt
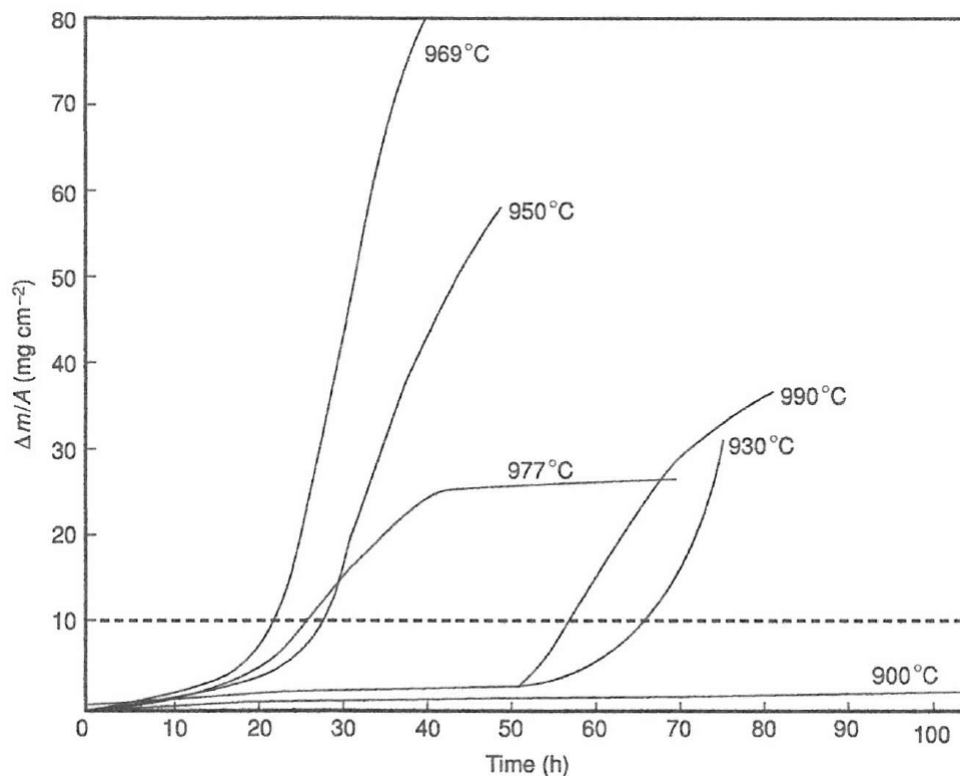
Note: These data consist of an initiation stage with small weight
changes and a propagation stage with larger weight changes (the
dashed line gives an arbitrary measure of the end of the initiation
stage).

Figure 2.12: Isothermal mass change versus time for IN-738 coated with 1 mg cm^{-2}
Na$_2$SO$_4$ in 1 atm O$_2$ [8]

deposit. Type II hot corrosion typically occurs at lower temperatures in the range between
670 and 750 °C. The specific temperature at which these two types of hot corrosion occur
will depend on a number of factors, including alloy composition and temperature cycle.

2.4   Scanning

The scanning process is key to a part tracking system based on machine readable codes;
failure at this stage renders the whole system useless. Codes applied to gas turbine parts
will likely become degraded in some way due to the conditions within the engine, thereby
reducing their legibility to the scanner. This places a premium on understanding the
scanning process to better manage how parts are handled so that symbol durability (and
by extension legibility) can be maximised.

Initial image capture is important because the quality of the image is related to the
likelihood of the symbol being decoded. The better the image quality, particularly with
respect to symbol contrast, the more likely a successful read will result – there will typically
be some pre-processing in an attempt to artificially improve the image, but of course this

can only provide a limited degree of correction. The part tracking system owner has no real control over the processing algorithms of the scanner's software, but may be able to affect the surface condition of the part. The latter is of direct significance because of the effect it can have on the quality of the captured image.

2.4.1 Operation

Scanning a two-dimensional code principally involves two steps: image capture followed by image processing. Image capture is typically achieved using a charge-coupled device (CCD). Simply, this is a sensor divided into a number of regions (pixels) that induce an electrical charge proportional to the ambient light incident upon them. From this information an image can be constructed for further processing in order to identify and retrieve the data from the code present. Because a CCD responds to the ambient light impinging on it, this raises questions regarding how the surface of the code can influence the light it reflects. The primary factors identified are surface roughness, dot geometry and surface colour.

Once an image has been captured, it must then be processed in order to identify the code's location and decipher its data. The finder pattern is used to identify the code and comprises two main features: the 'L' boundary and clock track [16]. Together, these features provide important information to the software such as matrix location, overall size, data capacity and module size. In order to distinguish these features correctly sufficient contrast is necessary to differentiate between 'on' and 'off' modules – contrast is defined as the difference in reflectance between the light and dark modules of a symbol. Once the code has been identified within an image, the software can then attempt to read it.

The specifics of the decoding process are not readily available from scanner manufacturers. This is because the capability of their decoding software is how they leverage competitive advantage for their products. However, there are some sources through which this process can be better understood. For example, the BSI standard that details the verification specification for two-dimensional symbols [10] indicates steps for obtaining images and processing them:

1. Obtain raw image – a plot of the actual reflectance values for each pixel of the light-sensitive array.

2. Produce reference grey-scale image by processing the raw image through a synthetic circular aperture – used for assessing the parameters symbol contrast, modulation and fixed pattern damage.

3. Produce a binarised image by applying a global threshold to the grey-scale image midway between R_{max} and R_{min} – used for assessing the parameters decode, axial non-uniformity and unused error correction.

4. Apply symbology reference decode algorithm – performs five tasks needed for subsequent measurement of the symbol quality parameters:

    (a) It locates and defines the area covered by the symbol in the image.

    (b) It creates a grid mapping of the data module nominal centres for sampling.

    (c) It determines the nominal grid centre spacings in each axis of the symbol (the symbol X dimension).

(d) It performs error correction, detecting if damage has caused any of the error budget to be consumed.

(e) It attempts to decode the symbol.

These five functions each facilitate processing of one or more of the symbol quality parameters.

One point of note is that BS 15415 [10] is intended for printed codes. Typically one would expect a printed code to have high contrast and to have square cells that are perfectly filled where required. Codes applied via DPM do not typically present the same ideal scenario; for example, dot peen data matrices, by the their nature, cannot produce connected dots. The AIM DPM quality guideline [2] was developed in an effort to better account for the additional complexities of DPM.

Codes marked via DPM typically have sub-optimal contrast, which can be exacerbated further if degradation occurs. This means that the image captured for decoding can be difficult to interpret in its raw form. Consequently it is typical for the scanner software to attempt to improve the image quality, particularly contrast, before proceeding to try and read the code. A leading scanner manufacturer filed a patent [49] that gives some indication of their approach to this problem. Key statements include:

- The captured image is pre-processed using smoothing, to reduce noise detrimental to symbol recognition, and sub-sampling, to reduce the data requirement and thus reduce processing time.

- Morphology is applied to the image prior to decoding to improve the reliability of symbol detection. The morphological filter is adapted for either dilation or erosion, depending on the contrast with respect to the background: for a dark symbol on a light background, erosion is used, and dilation when light on dark. This filtering removes some of the random artefacts induced by geometric distortions, non-uniform background and poor image quality. Artefacts can also make adjacent modules appear disconnected, which can impede symbol recognition and decoding.

- The decoding process utilises intensity and intensity-gradient information to first identify the symbol location, then determine distinguishing features (such as the finder pattern of a Data Matrix) and finally determine the encoded data.

A further patent [41] makes note of similar morphological operations for enhancing the scanned image's quality. It states that, depending on image polarity, erosion or dilation can be employed to help fill voids in the Data Matrix cells or increase/decrease cell feature size for improved measurement of cell placement. The open or close operation is noted with helping to remove noise spots without affecting cell size; thus not adversely affecting their measurement.

2.4.1.1 Charge-coupled device basics [47]

A charge-coupled device (CCD) is a photon detector, sub-divided into many small regions. The light detected by each of these regions (a pixel) can be combined to produce an image of interest. When a photon of light falls onto a pixel it will be converted into one (or more) electrons, the number of which will be directly proportional to the intensity of incident light. Clocking out the CCD enables the number of electrons at each pixel to be measured and the scene reconstructed.
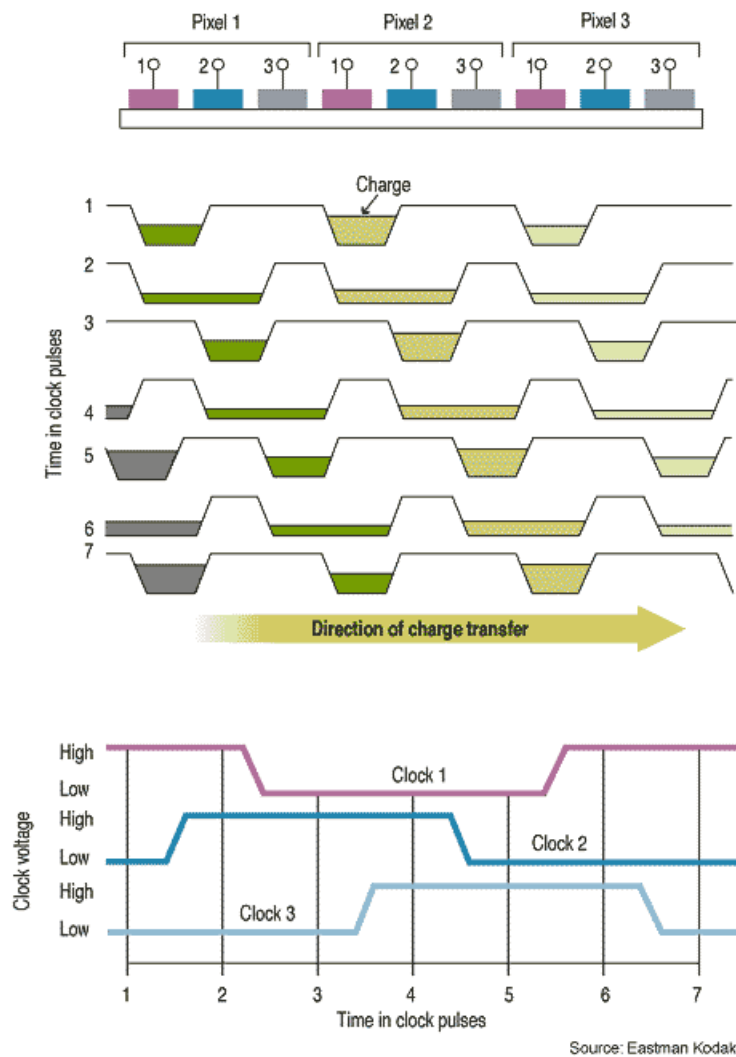
Figure 2.13: Charge transfer
(Image courtesy of http://spectrum.ieee.org)

A CCD is primarily silicon in its structure. Each pixel is defined by the positioning of the electrodes above the CCD itself. Applying a positive voltage to each electrode will attract all of the negatively charged electrons close to it (and any positively charged holes will be repelled). This results in a 'potential well' forming in which all the electrons produced by incoming photons will be stored. Each potential well has a finite capacity, so to prevent this from being reached light exposure should be controlled (for example, a shutter as used in a camera).

For an image to be constructed the charge at each pixel must be transferred out of the CCD – otherwise known as clocking out. This is typically achieved by transferring the charges downwards along the columns to the final row (the readout register). At each pixel there will be 3 electrodes; only one of these is required to form a potential well, but the others are needed to transfer charge. By holding these electrodes at a high or low voltage, either in combination or individually, charge may transferred across the CCD (this process is known as charge coupling – hence charge-coupled device – refer to figure 2.13). In the

readout register, the electrodes will be arranged to transfer charge horizontally along itself. Finally, the charge associated with each pixel must be measured. At the end of the readout register will be an amplifier to measure charge and convert it to a voltage. These values may then be digitised (a CCD is an analogue device) and processed by software to display an image.

Some parameters pertinent to CCD performance are summarised in table 2.5.

Parameter	Description
Quantum efficiency	Each pixel will not detect, and convert to an electrical charge, every photon falling onto it. The percentage of photons that are detected is called the quantum efficiency (QE) and may vary with wavelength.
Wavelength range	CCDs have a wavelength range of approximately 400–1,050 nm (blue to infra-red), with a peak sensitivity around 700 nm.
Dynamic range	Dynamic range defines the difference between the brightest and faintest source that a detector can accurately see in the same image. As a CCD converts photons into electrons, it is usually defined in terms of the maximum and minimum number of electrons that can be imaged. The minimum value will be affected by the inherent electrical noise associated with the physical structure of the CCD.
Linearity	A linear response would result in the number of detected photons producing the same number of electrons. Such a response is useful as it negates the need for additional processing to determine the 'true' intensity of an image.
Noise	CCD performance is impacted greatly by its noise response. Two main contributors to noise response are dark current (thermally generated noise) and readout noise (originating from the conversion of the charge of each pixel to a voltage). The latter determines the ultimate noise limit and dynamic range of the CCD; therefore much effort has been dedicated to reducing it.

Table 2.5: CCD parameters [47]

2.4.1.2 Image thresholding

Image thresholding is a technique by which one can convert a grey-scale image to binary (in this case black and white) and is a process that forms an important part of decoding Data Matrix symbols. Image thresholding requires the selection of a value that acts to separate the pixels in the grey-scale image. The way in which this threshold acts can vary, including [62, p. 83]:

- *Threshold above* – All pixels whose grey-level is above or equal to the threshold value become foreground pixels and the rest background.
- *Threshold below* – Opposite to threshold above.

- *Threshold inside* – A lower and upper threshold are defined with foreground pixels being selected between these two limits.
- *Threshold outside* – The opposite of threshold inside.

The threshold value can be defined manually in an interactive manner, but it is more useful to automate the process – such as in code scanning software – and so begs the question: how can this be achieved? Sezgin and Sankur [61] identify six different thresholding methods:

- histogram shape-based methods, where, for example, the peaks, valleys and curvatures of the smoothed histogram are analysed.
- clustering-based methods, where the grey-level samples are clustered in two parts as background and foreground (object), or alternatively modelled as a mixture of two Gaussians.
- entropy-based methods result in algorithms that use the entropy of the foreground and background regions, the cross-entropy between the original and binarised image, etc.
- object attribute-based methods search a measure of similarity between the grey-level and the binarised images, such as a fuzzy shape similarity, edge coincidence, etc.
- spacial methods use higher-order probability distribution and/or correlation between pixels.
- local methods adapt the threshold value on each pixel to the local image characteristics.

Given a histogram, the simplest case is where one is looking for a single threshold that separates the image into dark and light pixels (the clustering-based method by Otsu [53] is a popular choice). If the dark and light pixels of the grey-scale image are widely distributed, then this leads to a bimodal histogram (see figure 2.14a). With little overlap between the two distributions, the threshold value can be easily determined at a point in the valley between the two modes. However, if the distribution of light and dark pixels becomes less distinct (see figure 2.14b), the choice of threshold value becomes less obvious due to the valley disappearing as the histogram tends towards exhibiting a single mode. This progression of the histogram from two modes to one is symptomatic of the effect of surface degradation upon a symbol applied via DPM, such as a Data Matrix.
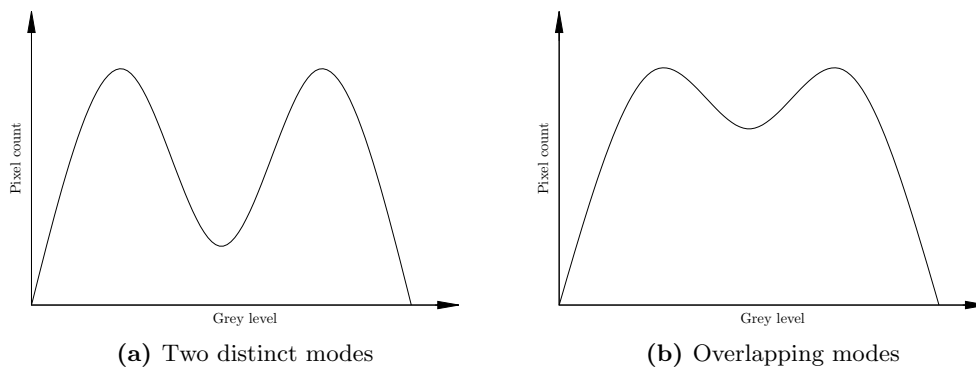

(a) Two distinct modes   **(b)** Overlapping modes

Figure 2.14: Example grey level image histograms [62, p. 85]

2.4.1.3 Grey-scale morphology

When scanning a high contrast and well defined Data Matrix, such as that printed onto a label, the captured image will be of high enough quality to negate the need for any processing prior to decoding. However, when Data Matrix codes are applied via DPM techniques the likelihood of achieving such idealised conditions is reduced, even for a freshly applied symbol – degradation exacerbates this issue further. One of the ways scanning software combats this issue is to apply morphological processes to the captured grey-scale image, prior to decoding, in order to enhance the features of interest and thereby increase the chance of achieving a successful read.

There are myriad morphological processes and ways to apply them, so only a brief summary of basic variants is presented [31, pp. 665–680]:

Erosion of an image f by a flat structuring element b at any location (x, y) is defined as the minimum value of the image in the region coincident with b when the origin of b is at (x, y). In equation form:

$$[f \ominus b](x, y) = \min_{(s,t) \in b} \{f(x + s, y + t)\} \tag{2.5}$$

That is to say, to find the erosion of f by b, we place the origin of the structuring element at every pixel location in the image and then select the minimum value of f from all those contained within the region coincident with b.

Dilation is the opposite to erosion whereby the structuring element is centred at every pixel location in the image and the maximum value is selected from all those contained within the region coincident with it. In equation form:

$$[f \oplus b](x, y) = \max_{(s,t) \in b} \{f(x + s, y + t)\} \tag{2.6}$$

Opening and closing Opening of an image f by structuring element b, denoted $f \circ b$, is simply the erosion of f by b, followed by a dilation of the result with b. In equation form:

$$f \circ b = (f \ominus b) \oplus b \tag{2.7}$$

Closing, denoted $f \bullet b$, is a dilation followed by an erosion. In equation form:

$$f \bullet b = (f \oplus b) \ominus b \tag{2.8}$$

It is expected that, in general, an eroded grey-scale image will be darker than the original because erosion using a flat structuring element will compute the minimum intensity value of f in every neighbourhood of (x, y) coincident with b. Further, the size of dark features will be increased and bright reduced; the degree to which this occurs depends on the size of the features with respect to the size of the structuring element. The effects of dilation are the opposite of those obtained with erosion.

The opening and closing of images can be interpreted by considering the function of an image $f(x, y)$ as a three-dimensional surface where the intensity values represent height over the xy-plane. The opening of f by b can be interpreted as pushing the structuring element up from below against the undersurface of f. At each location, the opening is the highest value reached by any part of b against the under surface of f. The complete opening is the set of all such values obtained by having the origin of b visit every (x, y)

coordinate of f. Closing involves the structuring element being pushed down on top of the curve while its origin is translated to all locations. Because the structuring element is too big to completely fit inside the peaks (for opening) or troughs (for closing) these will be clipped; the amount removed being proportional to how far the structuring element is able to reach into the peak. Figure 2.15 illustrates the effect of opening and closing by considering the intensity profile from a single row of an image. In general, openings are used to remove small bright details, whilst leaving the overall intensity levels and larger bright features of the image relatively undisturbed. Closing has the same affect, but on dark features.
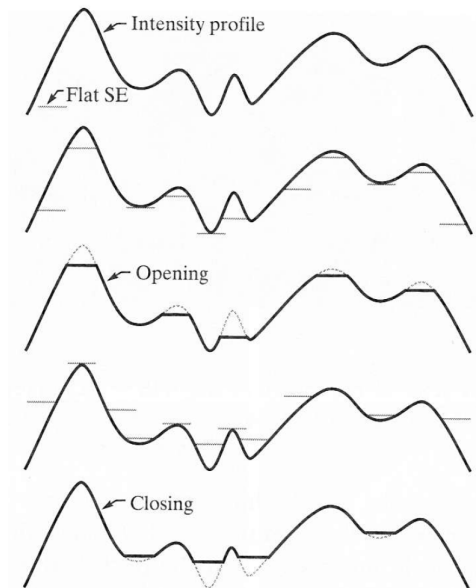
Note: For image opening the flat structuring element is pushed up underneath the signal, for closing it is pushed down along its top.

Figure 2.15: Image opening and closing in one dimension [31, p. 669]

Gonzalez and Woods [31, p. 670] give some examples of erosion, dilation, opening and closing being used in combination to form basic grey-scale morphological algorithms:

Morphological smoothing

Because opening suppresses bright details smaller than the specified structuring element, and closing those that are dark, they are often used in combination as morphological filters for image smoothing and noise removal.

Morphological gradient

Dilation and erosion can be used in combination with image subtraction to obtain the morphological gradient of an image, denoted by g, where

$$g = (f \oplus b) - (f \ominus b) \qquad (2.9)$$

Dilation will thicken regions in an image and erosion shrink them; their difference emphasises the boundaries between regions. So long as the structuring element is relatively small, homogeneous areas tend not to be affected and so are eliminated by the subtraction operation. The net result is an image where edges are enhanced and the homogeneous areas suppressed.

Top-hat and bottom-hat transformations

Top-hat and bottom-hat transformations (T_{hat} and B_{hat}, respectively) involve combining image subtraction with opening and closing operations, where

$$T_{hat}(f) = f - (f \circ b) \tag{2.10}$$

$$B_{hat}(f) = (f \bullet b) - f \tag{2.11}$$

These transformations enable the removal of objects from an image by using a structuring element in either the opening or closing operation that does not fit inside the object to be removed. The subtraction operation results in an image in which effectively only the removed components remain. The top-hat transformation is used for light objects on a dark background and the bottom-hat for dark on light.

Top-hat transformations are useful for correcting the effects of non-uniform illumination – uniform illumination plays a key role in the thresholding process described in section 2.4.1.2.

2.4.2 Surface reflectance

In section 2.4.1, contrast of the code in the captured image was identified as key to achieving a successful read. The CCD sensor of the scanner can only respond to the light incident upon it, and as such the reflective properties of the code and its surrounding surface will dictate the contrast that can be achieved. Two key factors that will affect this are: surface roughness and surface colour.

2.4.2.1 Roughness

Roughness is important due to how it can affect the ratio of specular to diffuse reflection from a surface [6]. The former is associated with highly polished surfaces where in the extreme any single incident ray of light will be reflected in a single outgoing direction. Diffuse reflection is where a single incident ray will be reflected in a number of outgoing directions; the amount of scattering being dependent on the surface roughness. These extremes can be undesirable due to their effect upon the observed contrast of the code: either glare induced by highly specular reflection or poor contrast when highly diffuse. Typically a surface will not exhibit purely specular or diffuse behaviour, but some mixture of the two. This intermediary behaviour is depicted in figure 2.16. The extent to which roughness affects the scatter of incident illumination depends on how the dimensions of the surface's facets compare to the wavelength of the light (refer to table 2.6 for a summary).

The behaviour just described with respect to surface roughness is particularly relevant to metals because they do not allow light to penetrate their outer surface (in fact, they absorb all incident radiation, but each excited electron immediately falls back to the state it came from, emitting exactly the same energy that was absorbed [67, p. 232]). However, many other materials do allow incident radiation to penetrate beyond their outer surface, giving rise to subsurface scattering. The incident ray is not wholly reflected at the particles of the outer surface, but rather 'walks' through the material, being further scattered at each subsequent particle interface. The significance of this is that those rays that are reflected via the subsurface do so in a random manner, leading to diffuse reflection. Specular reflection will still vary with surface roughness for materials of this type, but diffuse reflection will tend to dominate regardless. The importance of sub-surfacing scattering is made clear from attempts to accurately model real surfaces, such as that by Jensen et al.
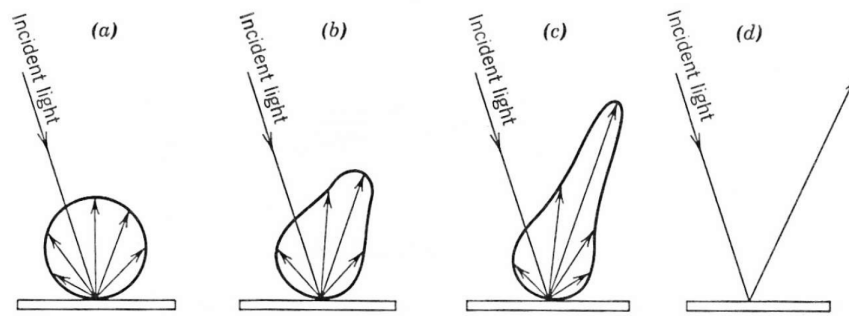
Note: A diffusing surface (as in *a*) tends to cause reflection equally in all directions. The smoother the surface (*b* and *c*), the more directional is the reflection until, with a perfectly smooth surface (*d*), all incident flux is reflected only at an angle equal to the angle of incidence.

Figure 2.16: The effect of optical smoothness on the scattering of incident light [21, p. 37]

Scenario	Outcome
Dimensions of the the surface facets are large compared with the wavelength of light	Surface reflectance is determined entirely by geometrical optics (i.e. the inclination of the facets)
Dimensions of the surface facets are comparable with the wavelength of light	Diffraction effects become important; surface reflectance is a function of both the inclination and size of the facets
Dimensions of the surface facets are small compared with the wavelength of light	Surface reflectance will be almost entirely determined by diffraction effects; surface roughness will then be the only important parameter

Table 2.6: Reflectance from a nominally plane surface [6]

[37]. They utilised the bidirectional surface scattering reflectance distribution function (BSSRDF) because it can describe the light transport between any two rays at a surface (*c.f.* the bidirectional reflectance distribution function – a simplification of the BSSRDF – that assumes the light entering a material leaves at the same point [52]). More pertinent to this thesis is that iron oxides, such as those that may develop on metallic gas turbine parts due to thermal oxidation, also display this behaviour of subsurface scattering. Torrent and Barrón [70], for example, have used diffuse reflectance spectra as a method for identifying different types of Fe oxides.

The data of table 2.6 indicates that if the geometry of a surface's features are similar to or larger in scale than the wavelength of the incident illumination then they can affect surface reflectance. In the case of a dot peen Data Matrix, for example, the individual dots will typically be of this scale. This suggests that their geometry and the surface roughness will simultaneously affect surface reflectance. Therefore both these parameters should be considered with respect to symbol legibility (in the context of the surface material, given

the distinct behaviour of metallics).

2.4.2.2   Colour

The perceived colour of an object is not a fixed property, but rather determined by the wavelengths of light leaving its surface to act as a stimulus for the observer. The characteristics of this stimulus will mainly depend upon the spectrum of incident illumination and the reflective properties of the surface itself. Additional factors that may alter the perceived colour include the ambient illumination and the colour properties of nearby objects.

Colour, whilst a complex concept, can, in fact, be precisely described using the three parameters hue, saturation (or chroma) and lightness (or brightness) [67, p. 11]:

Hue corresponds to the wavelength or frequency of the radiation, and is given a colour name such as red or yellow.

Saturation (or chroma) corresponds to the amount of white light mixed in with the hue – this allows pale colours to be described.

Lightness (or brightness) describes the intensity of the colour (i.e. the number of photons reaching the eye).

These three parameters can be represented in a three-dimensional coordinate system. The most typical form is cylindrical (see figure 2.17) where hue is defined via the cylinder's circumference, saturation its radius and lightness its axis.
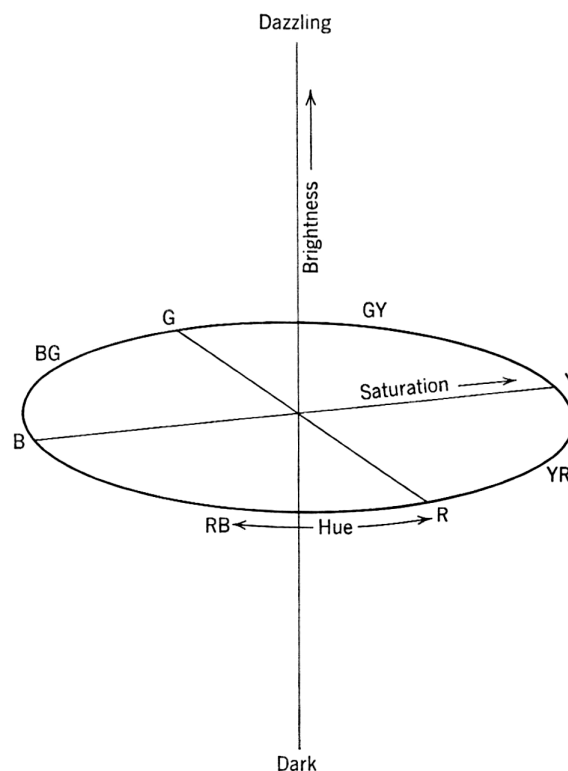
Figure 2.17: Dimensions of colour [21, p. 13]

Colour is important because it can have implications regarding the contrast of a code

applied to a part's surface. Typically this is not an issue immediately proceeding application, however the surface colour of the part will evolve through its operating life. Thermal oxidation is a good example of this, whereby a specific colour (quite different to the original metallic surface) can result, indicating a change in the reflectance and absorptance properties of the surface. The colour stimulus from a point on a surface will exhibit a certain spectrum, however attenuation of the reflected frequencies will occur, giving rise to a bright or dark response depending on if this attenuation is low or high.

The author suggests that lightness is particularly important with respect to symbol legibility because the scanning process utilises grey-scale imagery. A grey-scale image is monochromatic, each pixel of which carries intensity (i.e. lightness) information only. The variation in lightness across an image equates to contrast. For the symbol to remain legible, the contrast between it and the plain surface should be maximised where possible.

2.5 Standards

A number of standards have been derived with respect to the use of Data Matrix codes. These can vary in their nature from data encoding requirements, such as MIL-STD-130N [71], to marking requirements, such as SAE AS9132 [57]. Several of these that are particularly relevant have been summarised in the following sub-sections.

2.5.1 BS ISO/IEC 16022:2006 [16]

This document defines the requirements for the Data Matrix symbology, including "symbology characteristics, data character encodation, symbol formats, dimensions and print quality requirements". To briefly summarise:
Data Matrix is a two-dimensional symbology with the capability for error correction. The latest error correction code is ECC 200, which utilises the Reed-Solomon technique. A Data Matrix is comprised of a number of modules arranged in a rectangular (typically square) array. The central data region is surrounded by a finder pattern that is in turn surrounded on all sides by a quiet zone. The finder pattern and quiet zone are each one module wide (this is a minimum requirement of the latter). The finder pattern comprises an 'L' boundary and clock track, which together enable the scanning device to determine such parameters as location, physical size, orientation and resolution of the symbol. Some symbol attributes for ECC 200 are summarised in table 2.7. Symbol quality parameters are defined as: fixed pattern damage, scan and overall symbol grades, grid non-uniformity and decoding.

Symbol property	Square symbol	Rectangular symbol
Symbol size (row × col)	10 × 10–144 × 144	8 × 18–16 × 48
Total codewords (data/error)	3–1,558/5–620	5–49/7–28
Max. data capacity (num./alphanum./byte)	6–3,116/3–2,335/1–1,555	10–98/6–72/3–47
Max. correctable codewords (error/erasure)	2–310/0–590	3–14/0–25

Table 2.7: Data Matrix symbol attributes summary (ECC 200) [16]

2.5.2 BS EN ISO 15415:2005 [10]

This standard "specifies two methodologies for the measurement of specific attributes of two-dimensional bar code symbols". The two methods are necessary to accommodate both multi-row barcode and matrix symbologies. Methods are defined for evaluating and grading the measurements, leading to an overall assessment of symbol quality. Being able to grade the quality of a symbol is beneficial for diagnostic and process control purposes, and also helps to indicate the expected read performance. A brief summary of the assessment parameters used for two-dimensional matrix symbologies:

Decode The decode parameter tests whether the symbol's features are sufficiently correct to be readable.

Symbol Contrast This tests that the two reflective states of the symbol – light and dark – are sufficiently distinct.
$$SC = R_{max} - R_{min}$$

Modulation This is a measure of the uniformity of reflectance of the dark and light modules of the symbol. Insufficient modulation may increase the probability of modules being misinterpreted as light or dark.

Fixed pattern damage This tests that any damage to the fixed patterns of the symbol does not reduce the ability of the decode algorithm to locate and identify the symbol within the field of view (beyond an acceptable limit).

Axial non-uniformity The modules of a two-dimensional matrix nominally lie in a regular polygonal grid. The decode algorithm must map the centre positions of these modules in order to extract the symbol's data. Axial non-uniformity tests for uneven scaling of the symbol by measuring and grading the spacing of the mapping centres (i.e. sampling points).

Grid non-uniformity This measures and grades the largest vector deviation of the grid intersections from their ideal theoretical position.

Unused error correction This tests the extent to which damage to the symbol eroded the reading safety margin provided by error correction.

Additional parameters The *scan grade* is defined as the lowest grade of any of the measured parameters noted immediately above. The *overall symbol grade* is defined as the arithmetic mean of the scan grades of all images. *Print growth* tests that the graphical features comprising the symbol have not grown or shrunk from nominal so much as to hinder read performance.

2.5.3 SAE AS9132 [57]

This is a document that deals with the application of Data Matrix codes via direct part marking, specifically with respect to dot peening, laser marking and electro-chemical etching. For each of these marking methods the standard identifies the practical implications of using such techniques to mark a Data Matrix code and the subsequent impact on symbol quality. The reason for documenting the use of DPM techniques in this way is that such techniques present a challenge that is distinct from traditional printing. Consequently this standard serves to aid users in maintaining symbol quality when using one of these three marking techniques.

The requirements for dot peen marking include:

Nominal module size

Surface texture of the part will affect the quality of the symbol produced by dot peening. Table 2.8 and figure 2.18 show the minimum readable module size requirements with respect to the part's surface texture.

Symbol quality requirements

Geometric tolerances are summarised in table 2.9. Additional points of note include:

- Surface colour and consistency may be specified in order to maximise readability. Variation in surface colour should be minimised.
- A 120° style cone angle is preferred for both mark quality and stylus durability.
- The stylus point shall have a polished finish (surface texture should not exceed 0.8 μm or 32 μinch).
- Ovality of any dot shall not exceed 20 % of the module size (see figure 2.19). No more than 2 % of the total number of modules may contain dots outside of the ranges specified for dot size (see table 2.9) and ovality.
- The minimum dot size shall not be less than 0.132 mm (0.0054 inch).

2.5.4 AIM DPM Quality Guideline [2]

The AIM identified that existing specifications for matrix symbologies were not directly suited for symbol evaluation when using DPM techniques. Their guideline is complementary to, yet distinct from, the ISO/IEC 15415 print quality test specification document, more specifically: "It defines alternative illumination conditions, some new terms and parameters, modifications to the measurement and grading of certain parameters and the reporting of grading results."

All parameters in the print quality test specification of ISO/IEC 15415 apply, except for:

- A different method for setting the image contrast.
- A different method for creating the binary image.
- A new method for choosing the aperture size.
- An image pre-process methodology for joining disconnected modules in a symbol.
- A different process for determining the Modulation parameter renamed Cell Modulation.
- A different process for determining the Symbol Contrast parameter, which has been renamed Cell Contrast.
- A different process for computing Fixed Pattern Damage.
- A new parameter called Minimum Reflectance.

2.5.5 MIL-STD-130N [71]

This is a US Department of Defense (DoD) standard that provides "guidance regarding implementation of machine readable information (MRI) for item identification marking and automatic data capture". Information is also included regarding human readable information (HRI) markings, which may be in addition to or instead of MRI markings. It is expected that US DoD partners also adhere to this guidance, where applicable. There are a number of requirements covered by this document that are categorised as either 'general' or 'detailed'; a brief summary of these:

Surface texture (Ra)		Minimum module size	
Micro-inches	Micro-metres	Inches	Millimetres
32	0.8	0.0075	0.19
63	1.6	0.0087	0.22
95	2.4	0.0122	0.31
125	3.2	0.0161	0.41
250	6.3	0.0236	0.60

Table 2.8: Minimum readable module size by surface texture (Ra) [57]
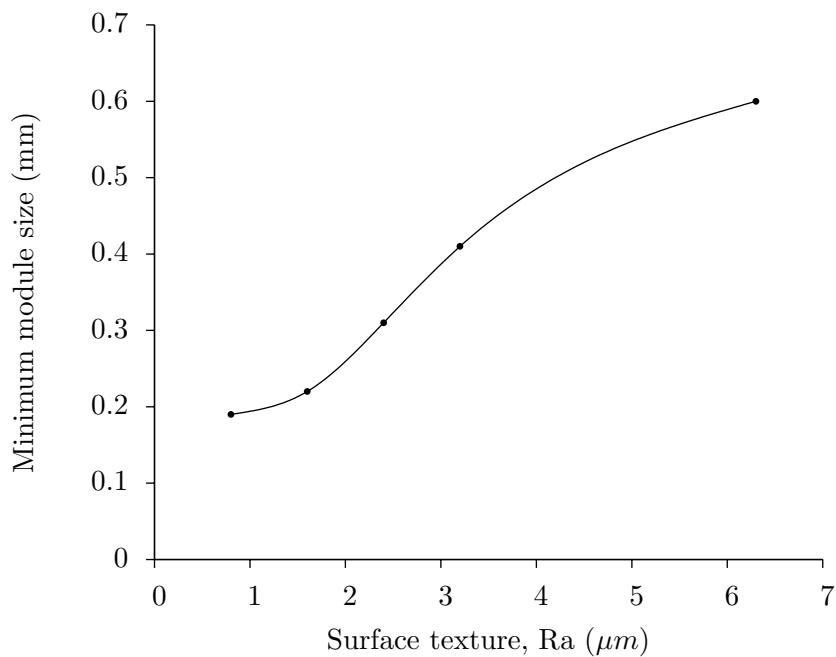
Figure 2.18: Minimum readable module size by surface texture (Ra) [57]

Characteristic	Requirement
Stylus angle	120°, 90°, 60° (±2°)
Stylus point radius	Subject to eng. design requirements
Dot size*	60 % to 105 %
Dot centre offset*	0 % to 20 %
Angle of distortion	±7°

* As a % of nominal module size

Table 2.9: Limits for dot size and dot centre offset [57]
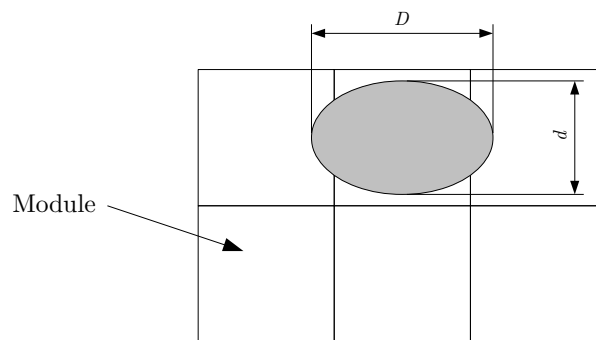
$D - d \leq 20$ % of the module size

Figure 2.19: Definition of ovality [57]

General requirements This section identifies: methods of application, such as marking an identification plate or the part directly; permanency of the code, which is expected to match that of the part it is applied to, including maintenance work where possible; and a number of HRI parameters for adherence.

Detailed requirements This section deals with: minimum information content, to enable item identification; MRI marking protocols, to ensure consistent application of information; data carriers, to define the allowed symbol types and quality criteria; and free text marking information, for when HRI is required in addition to or instead of MRI markings.

2.6 Failure Mode and Effect Analysis

McDermott et al. [46] state that "An FMEA is a systematic method of identifying and preventing product and process problems before they occur". Ideally, such analysis is performed during the product design or process development stages, however it can also be beneficial to retrospectively apply FMEA to existing products or processes.

FMEA analysis was first utilised in the aerospace industry in the 1960s, focusing specifically on safety issues. Its use then spread to other industries, such as chemical processing, as a key tool for improving safety. Analysing products and processes for potential failures is not exclusive to FMEA, but rather it serves to standardise the approach so that it can be used more universally within and between companies. The automotive industry has adapted FMEA to serve as a quality improvement tool, including the development of a technical specification – ISO/TS 16949 [19] – that states its goal as "...the development of a quality management system that provides for continual improvement, emphasizing defect prevention and the reduction of variation and waste in the supply chain."

The objective of FMEA is to identify those ways in which a product or process can fail. A failure is defined as when the product or process does not function as it should or when it malfunctions in some way. Failures are not limited to the product or process directly, but can also occur through user error – such errors should also be accounted for in the FMEA. The failures identified by an FMEA are known as failure modes, each of which

has a potential effect, with some effects more likely to occur than others. Further, each potential effect has a relative risk associated with it. The relative risk of a failure mode and its effect is determined by three factors:

Severity	The consequence of the failure should it occur.
Occurrence	The probability or frequency of the failure occurring.
Detection	The probability of the failure being detected before the impact of the effect is realised.

Each potential failure mode and effect is rated in each of the above three factors on a scale of 1–10 (low to high). Multiplying the ranking given to each of the three factors (severity × occurrence × detection) results in a risk priority number (RPN) for each potential failure mode and effect. The RPN indicates the relative risk associated with each failure mode and consequently enables them to be ranked in terms of the need for corrective action to reduce or eliminate the potential for failure. Once corrective action has been taken, a new RPN is determined by reevaluating the severity, occurrence and detection criteria. Corrective action should continue until the RPN is at an acceptable level with respect to the potential failure mode.

Chapter 3

Analysis

This chapter presents the analysis completed in support of the research topic. It is comprised of a number of different sections; a brief summary:

Section 3.1 – Gas Turbine Performance – Alstom GT26 (page 41)
  A performance analysis of Alstom's GT26 gas turbine engine using the Turbomatch software (developed by Cranfield University) was completed. The engine model was created by the author, but the analysis was carried out by Papanikolaou [54] – an MSc student – under the author's guidance.

Section 3.2 – Part Tracking System Selection (page 45)
  The process by which the preferred part tracking system technical solutions were selected in partnership with colleagues at Alstom is presented. The rationale for preferring one solution over the others is highlighted.

Section 3.3 – Indentation of Materials (page 56)
  Faivre [27], an MSc student who worked on their thesis in conjunction with the author, looked to identify metrics that would enable accurate prediction of the machine settings needed to mark a Data Matrix with dots of a particular diameter and depth. This section presents a summary of that student's analysis.

Section 3.4 – Degradation Causality (page 59)
  From reviewing the open literature, a means of relating the degradation mechanisms to the scanning process (via surface reflectance) was identified. This section explains the significance of this relationship.

Section 3.5 – Data Matrix Tests (page 62)
  Tests were performed that begin to show the behaviours identified via theory, in practice. These tests focused on the effects of erosion and oxidation (independently). The effect of degradation on surface reflectance was primarily assessed by observing the change in the grey level of images captured by the scanning device.

3.1   Gas Turbine Performance – Alstom GT26

The condition of codes on parts that are returned from service will depend heavily on the operating conditions of the engine. Cranfield University has developed proprietary software known as Turbomatch that has been utilised to model the performance of the Alstom GT26 engine. Modelling of this nature will not immediately provide all useful data regarding the degradation that may occur to any machine readable codes present, but can serve as a useful first iteration giving pertinent data such as temperatures, pressures and

mass flows.

The GT26 was selected because not only is it Alstom's most advanced engine, but because it also presents a configuration that is unique amongst its peers: sequential combustion. Typically a gas turbine engine has a single combustion stage that is proceeded by one or more turbines, depending on the number of shafts of the engine. With sequential combustion an additional combustion stage is introduced at an intermediate point of the expansion process. Heat addition is most efficient at high pressure so the second combustor is best introduced before too much expansion work has occurred. The reason for employing such a configuration is primarily two-fold: *i*) the specific output of the engine is improved (i.e. the same power output can be achieved for reduced mass flow over a simple cycle equivalent); and *ii*) benefits are realised for engine emissions, such as NOx, without compromising engine performance.

Saravanamuttoo et al. [59] state that "A substantial increase in specific work output can be obtained by splitting the expansion and reheating the gas between the high-pressure and low-pressure turbines." The relevant portion of the reheat cycle's T-s diagram is illustrated in figure 3.1. The increased turbine work of a reheat cycle is clear when one recalls that the vertical distance between lines of constant pressure increases with increasing entropy. Thus: $(T_3 - T_4) + (T_5 - T_6) > (T_3 - T_4^{'})$. Assuming that $T_3 = T_5$ then the optimum point in the expansion at which to reheat is when the pressure ratios for the high-pressure and low-pressure turbines are equal. This is why Alstom chose to apply reheat in the GT26 engine after the first of five expansion stages as it is typical to design for a pressure drop of $\sim$ 2:1 across each turbine stage.
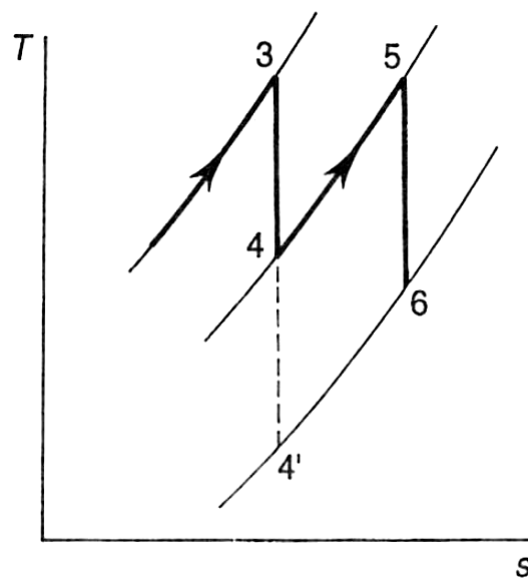
Figure 3.1: Reheat cycle T-s diagram [59, p. 50]

The configuration of the GT26 is illustrated in figure 3.2 and its operating parameters in table 3.1. Table 3.1 includes the equivalent values either specified for the Turbomatch model or obtained from it for comparison. Coupled to a generator, the GT26 produces electrical power at 50 Hz (it has a sister model – the GT24 – that is for the 60 Hz market).

The most significant deviation seen in the data of table 3.1 is between the efficiency obtained through Turbomatch versus that reported by Alstom. This is due to the Alstom
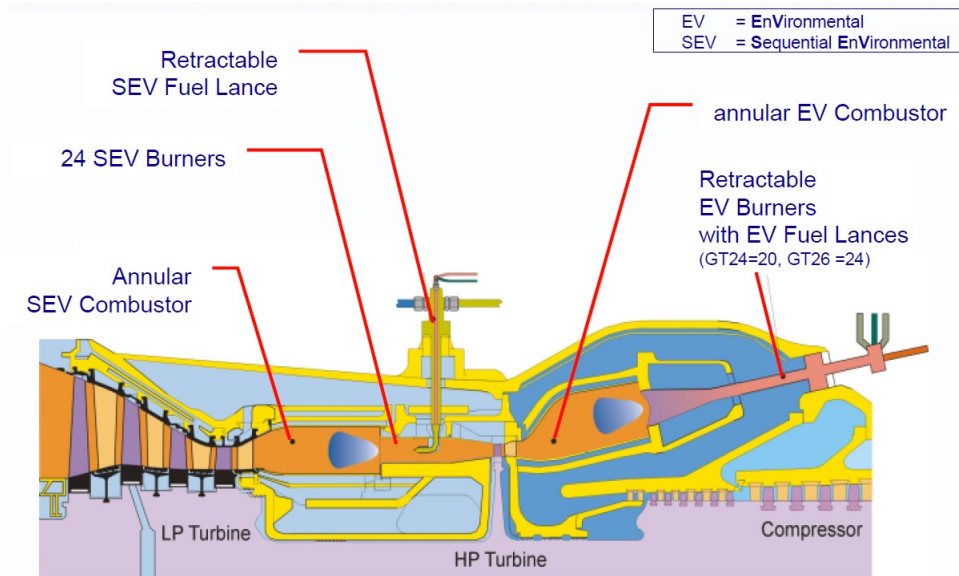
Figure 3.2: Alstom GT26 configuration
(Image courtesy of Alstom)

data being a gross electrical efficiency that will include losses due to the generator and, presumably, ducting and auxiliary components. The Turbomatch data already accounts for duct losses, at least at the inlet, so factoring for auxiliary and generator losses should yield a figure approximately equivalent to that quoted by Alstom. Gas Turbine World's 2005 publication of gas turbine performance specifications [28] suggests that generator and auxiliary losses can account for up to a 3% and 0.6% loss in available power (and heat rate) respectively. Adjusting the Turbomatch efficiency of 39.5% by these two factors yields a figure of 38.1% that is more comparable to that quoted by Alstom.

Engine parameter	Alstom	Turbomatch
Compressor pressure ratio	33.9	33.9
High pressure TET[a] (K)	–	1,565
Low pressure TET[a] (K)	–	1,565
Output (MW)	288.3	288.3
Efficiency[b] (%)	38.1	39.5
Exhasut gas flow (kg s^{-1})	650	650
Exhaust gas temperature (°C)	616	620

[a] These TET figures were defined through iteration.
[b] Alstom reports gross electrical efficiency; Turbomatch reports thermal efficiency.

Table 3.1: Alstom GT26 performance data
(Source: http://www.power.alstom.com)

Modelling the GT26 engine in Turbomatch presents a challenge because it is a single shaft engine and therefore both turbines are mechanically connected to the compressor – a

configuration that the software cannot naturally accommodate. The author circumvented this issue by adopting a similar approach to that proposed by Tordoir [69], which involves configuring the first turbine as a free (or power) turbine. A power output is specified for this free turbine so that the inlet parameters to the second combustor are at realistic levels. This power output is effectively mimicking the first turbine's contribution in driving the compressor and providing useful work. The value set must then be accounted for elsewhere in the model via constructs known as arithy bricks to ensure the overall engine performance is calculated as accurately as possible. For the sake of simplicity it was assumed that the free turbine only contributes to driving the compressor and so, ignoring the conversion of units, it was simply necessary to subtract its power output from the compressor work vector result so that the outcome could be specified as the compression work for the second (compressor) turbine – which is also providing all the auxiliary work. This technique is summarised in figure 3.3.
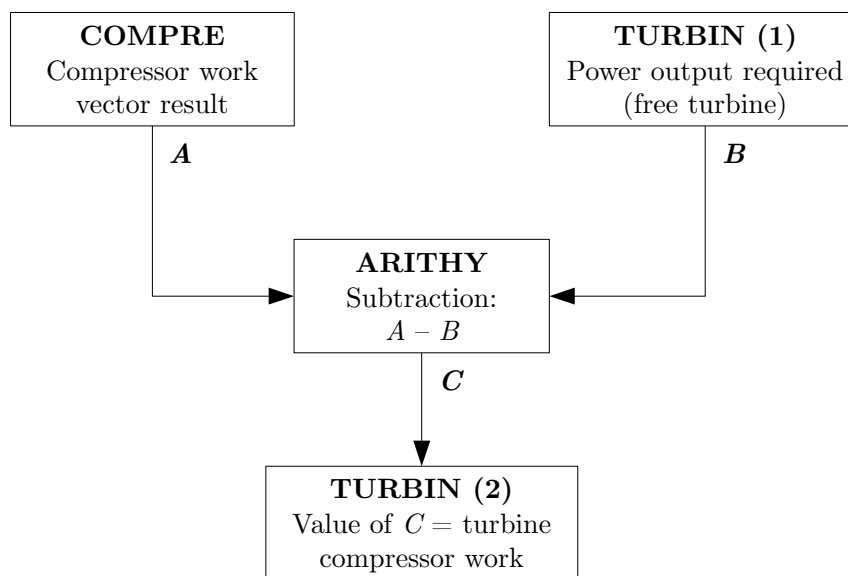
Figure 3.3: Summary of Turbomatch modelling technique

The Turbomatch model developed by the author was subsequently utilised by an MSc student – Christos Papanikolaou [54]. The author had an intellectual input to his thesis through helping to define its scope and supervise the student. Thus it was possible to ensure the work by Papanikolaou [54] would provide a positive contribution to this thesis, including a bilateral exchange of ideas and knowledge.

Turbomatch is not limited to design point simulation, but also allows off-design cases to be investigated. This latter function is of most interest as it enables the performance of an engine to be assessed over a wide variety of conditions through adjustment of ambient and engine specific parameters. A brief summary of the performance analysis completed by Papanikolaou [54]:

The effect of ambient pressure
This was achieved by varying altitude. As altitude is increased the static temperature and pressure fall. Pressure is the dominant effect causing a reduction in air density and hence a commensurate reduction in mass flow and shaft power. However,

assuming constant rotational speed with increasing altitude, the non-dimensional rotational speed $N/\sqrt{T_{in}}$ rises. This means the engine behaves as if N were rising, giving an increased pressure ratio. A higher pressure ratio results in increased thermal efficiency. Specific power of the engine is increased because the decrease in shaft power is exceeded by the decrease in mass flow.

The effect of ambient temperature

Increasing the ambient temperature causes the engine to operate at a reduced pressure ratio, thereby reducing both thermal efficiency and specific work, for a given TET. The specific work decreases because the reduction in shaft power exceeds that in mass flow. Decreasing the ambient temperature will have a favourable impact on these parameters.

The effect of compressor deterioration

This was evaluated via two separate analyses: one involved modifying compressor efficiency, the other flow capacity. Reducing compressor efficiency moves the operating line to the left, albeit modestly (i.e. lower pressure ratio and non-dimensional mass flow). The specific power reduces because the reduction in shaft power dominates that of mass flow. Reducing compressor flow capacity will lead to reduced mass flow. As with reducing compressor efficiency, this moves the operating line to the left, although the movement is more substantial. Since less mass is entering the compressor, pressure ratio also reduces, while specific power slightly increases because the decrease in shaft power is modest relative to the reduction in mass flow.

The effect of turbine deterioration

Reduced turbine efficiency means that for the same expansion ratio the engine produces less work. Thermal efficiency reduces as there is less useful work. Mass flow also decreases. Both of these contribute to reduced shaft power. The reduction in shaft power is greater than the reduction in mass flow so the specific power reduces.

The off-design performance of an engine is important as it may affect parameters relevant to the degradation mechanisms acting upon machine readable codes present in the engine. For example, as compressor performance deteriorates due to fouling if the power output is to be maintained the TET will need to be increased, which will then impact the corrosion and/or thermal oxidation of downstream parts.

3.2   Part Tracking System Selection

Selecting the preferred solutions for each component of the part tracking system – encoding, marking and scanning – followed a logical process (see figure 3.4).

This process went beyond simply identifying possible solutions, and sorting them according to their application. Three additional steps were incorporated to enhance the robustness of the outcome. The detail phase involved identifying the specific qualities of each solution. When looking at an encoding solution, for example, this would include parameters such as data density, compatible character set and error correction capabilities. Based on this more detailed appraisal, it was then necessary to identify the compatibility of solutions belonging to different components of the overall part tracking system. For example, a scanner designed for reading codes by contrast would not be suitable for use with bumpy bar codes. The benefit of the 'detail' and 'relate' phases is that the information they provide
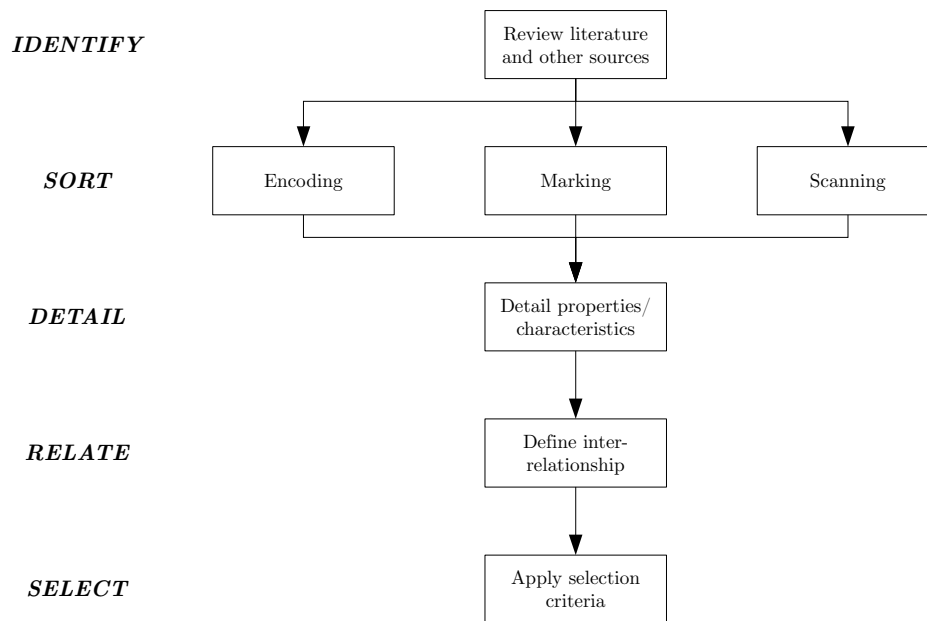
Figure 3.4: Selection process

enables the selection criteria to be applied in a robust manner. This aids identification of the most suitable solution for each component.

3.2.1 Encoding solution

An initial filtering process was carried out on the code types identified as of interest (refer to section 2.1). This was based on information obtained from the literature, existing experience and by observing what others have done in similar industries and/ or applications. The main criteria observed at this stage were the physical size and data capacity of the codes and their potential for withstanding engine operating conditions. Size is particularly significant as some engine parts present little space for applying a code, such as high pressure compressor blades. The differences between codes within each of the three types identified (linear, two-dimensional and three-dimensional) tend to be largely syntactic in nature. Consequently a single symbology was selected from within each type for further appraisal. These were:

Linear	Code 128
Two-dimensional	Data Matrix
Three-dimensional	PosiCode (as a bumpy bar code)

Examples of each of these are illustrated in figure 2.1 on page 6.

Two main tools were used for evaluating the three selected symbologies: *i*) a priority matrix to evaluate the code types against various influencing factors (see table 3.2); and *ii*) a pros versus cons analysis with respect to the intended application. Both tools were completed with input from both the author and colleagues at Alstom. The result of this process showed Data Matrix to be the preferred choice – a summary of the reasoning behind this decision is offered at the end of this section.

| | | | Code Type | | | | | |
| | | | Linear | | Two-dimensional | | Three-dimensional | |
#	Influencing factor	Weighting	Score	Product	Score	Product	Score	Product
1	Code size	10	7	70	9	90	7	70
2	Surface coatings	9	6	54	6	54	8	72
3	Error management	8	4	32	8	64	4	32
4	Durability	8	5	40	5	40	7	56
5	Data capacity	7	7	49	9	63	7	49
6	Scanner compatibility	5	9	45	7	35	5	25
				290		**346**		**304**

Weighting definition: 1–2 = Low importance; 3–5 = Medium; 6–8 = High; 9–10 = Highest.
Score definition: 1–2 = Unsatisfactory; 3–5 = Satisfactory; 6–8 = Good; 9–10 = Excellent.

Key:

1 Code size — The surface area requirement of the code type.

2 Surface coatings — The effect of surface coatings (from manufacturing/reconditioning processes) on code legibility (to the scanner).

3 Error management — The ability to detect and correct errors.

4 Durability — How well the code technology lends itself to resisting manufacturing/reconditioning processes and engine operating conditions - this excludes enhancements such as error correction.

5 Data capacity — The amount of information that a single code can contain.

6 Scanner compatibility — The number of options available when looking to select a scanner unit.

Table 3.2: Code type priority matrix

The main points arising from assessing each code are presented here (tabular summaries can be found on page 49: table 3.3 for Code 128, table 3.4 for Data Matrix and table 3.5 for PosiCode):

Code 128 [17] is already used extensively in industry. Its name is derived from the fact that it can encode all 128 ASCII characters, meaning it can cope with alphabetic, numeric and alphanumeric sequences. The advantages of Code 128 (and linear codes in general) are that it is well proven (although not for the particular application at hand), it is relatively uncomplicated and scanning technology is cheaper (compared to devices compatible with two-dimensional codes), with many different units available to choose from. However, linear codes in general are an ageing technology having been first developed in the 1950s. This leads to a number of drawbacks, including low data density, a lack of error correction (although some codes, including Code 128, do offer a checksum digit to at least validate the encoded string) and limited data capacity (at least where space is at a premium as in this instance). Whilst Code 128 is a high density linear symbology, it is still unable to compare favourably with two-dimensional codes; although this is to be expected as the latter have an additional dimension available for data storage. Finally, linear codes often require high levels of contrast (typically 80% and above) to achieve a successful scan; it is likely this would be difficult to achieve on used engine parts.

Data Matrix [16] has evolved a number of times, with the current standard characterised by the use of error correction code (ECC) 200, which incorporates advanced error checking and correction algorithms based on Reed-Solomon theory. This error correction capability enables symbols that have up to approximately 60% of their data obscured or damaged to still be decoded (without any loss of information). Other advantages of Data Matrix include: it's a proven technology (it has been adopted by major aircraft and gas turbine OEMs and governmental organisations such as the US DoD), verification of code quality is possible (reporting parameters such as symbol skew, for example) and has less stringent contrast requirements than linear codes. A particular advantage of Data Matrix is its error correction capability, however to maximise its usefulness marks must be consistently applied to a high quality. This requires more effort during initial implementation relative to perhaps a linear code, but thereafter the additional requirements should be minimal (a verification system to monitor mark quality for deviation outside of acceptable limits).

PosiCode [1] is a position-based symbology, which differs from the majority of bar codes that operate on the principle of presence/absence. Presence/absence orientated codes consider each character as a fixed number of rectangular modules (which will be 'on' or 'off'). However, PosiCode decouples the width of the bars from their position, with the bar centres arranged on a grid of equally spaced parallel lines. Data is encoded based on the position of the bars rather than their width (hence the bars are uniform). These characteristics make PosiCode particularly suited to application as a bumpy bar code because only the position of the bars need be detected by the scanner. The advantages of bumpy bar codes include: their use of existing linear codes (which are typically proven and reliable), that at least one GT OEM has used PosiCode-based identifiers on engine parts [33], that they are relatively uncomplicated and the method of scanning could help to negate some of the durability issues relevant to codes detected by contrast. However, applying

a linear code as a bumpy bar code does little to negate its shortcomings; most notably data density and size, which are particularly relevant to this application. Furthermore, bumpy bar codes have not seen such widespread application as their more traditional counterparts so there are very few scanner models available. This presents a risk if those models do not cope well with the condition of gas turbine parts throughout their life.

Pros	Cons
Proven under various applications	Relatively low data density
Relatively uncomplicated	No error correction
Scanning devices are cheaper	Ageing technology
Many compatible scanners available	Relatively limited data capacity
	Stringent contrast requirements

Table 3.3: Code 128 pros/cons summary

Pros	Cons
Proven (at least one major aero-engine OEM committed to this technology)	Accurate marking required to maximise benefits of error correction
Verification possible (using dot peen on flat surfaces only)	Unknown sensitivity to engine operation, manufacture and reconditioning processes
Incorporates error correction	
Higher data density than other solutions	
Less stringent contrast requirements	

Table 3.4: Data Matrix pros/cons summary

Pros	Cons
Does not rely on contrast scanning methods	Similar limitations to other linear codes
Proven use with at least one other GT OEM	Requires a particular scanner
Relatively uncomplicated	Unfavourable opinion from an independent professional

Table 3.5: PosiCode – as a bumpy bar code – pros/cons summary

Having completed the assessment process, it was concluded that Data Matrix would be the most suitable encoding solution for Alstom's part tracking system. A summary is presented of the main reasons for this decision:

Code size

Some gas turbine parts have very limited space available for placing an identifying

mark. Data Matrix is far more capable of accommodating this limitation than the other options considered.

Data capacity

Data Matrix offers sufficient data capacity within the available space, because of its excellent data density.

Durability

The error correction afforded by Data Matrix means it offers better resilience to physical degradation than the alternatives considered.

Scanner compatibility

Not all scanners are equally capable, therefore a choice is important to ensure a unit capable of scanning codes of varying physical condition can be found. A number of proven Data Matrix compatible models exist.

3.2.2   Marking solution

There are a significant number of DPM techniques available [50]. To enable the most suitable to be short-listed, from which to make a final recommendation, a number of influencing factors were identified so as to be able to score each technique. Furthermore, a weighting was associated with each factor to indicate its relative importance (refer to table 3.9 on page 53 and table 3.10 on page 54). This process led to three techniques being identified for more detailed consideration (including broader issues such as process requirements) before selecting one for implementation. These were: dot peen marking, electro-chemical marking (ECM) and laser marking. "Engraving/milling" and "cast, forge or mould" also scored well in principle, however they were not considered further because they would be more awkward and costly to integrate into existing production processes.

A brief discussion of each short-listed technique is presented here (tabular summaries can be found on page 51: table 3.6 for dot peen marking, table 3.7 for ECM and table 3.8 for laser marking):

Dot peen systems are of similar cost to ECM equivalents, but should prove cheaper to operate as essentially the stylus is the only consumable. It is a proven technique, particularly within the airframe and aero engine industries. Such systems are also relatively simple to operate and so parts can be marked within a matter of minutes. Some of the issues identified include:

- The need to monitor dot spacing (to prevent stress raisers from occurring).
- The stylus tip should be checked for wear as it has a significant impact on mark quality (this can be achieved through the use of a verification system).
- Dot depth is proportional to the module size (which, depending on the overall matrix dimensions, may have implications regarding durability).

ECM is an affordable means of marking parts that is relatively simple to implement. Importantly, it is a proven technique having been adopted by at least one major aero engine OEM for marking its parts [56]. However, there are health and safety issues to consider due to the chemicals used, which are also consumables and so contribute to operating costs. The latter may be exacerbated further by the fact that etching is more desirable due to the increased durability it affords over oxide marking.

Laser marking is advantageous regarding its ability to mark very hard materials, however it falls short in at least two key areas: system cost and questionable

Pros	Cons
Relatively low cost equipment (~ £3,500)	Dots should be gapped correctly to prevent stress raisers
Rapid marking	Condition of stylus tip can affect symbol quality – can monitor through verification
Proven technology	Dot depth proportional to matrix size
Complementary process to Data Matrix	
Verification possible	
Stylus is the only main consumable	

Table 3.6: Dot peen marking pros/cons summary

Pros	Cons
Relatively low cost equipment (~ £2,000)	Oxide marking not as robust as etching
Relatively simple to use	Etching and colouring require different electrolytes
Proven technology	No verification standard (for Data Matrix)
	EHS issues regarding chemical handling
	Chemical consumables contribute to higher operating costs

Table 3.7: Electro-chemical marking pros/cons summary

Pros	Cons
Able to mark *very hard* materials	Very costly (£25k–100k)
Proven technology	Can cause micro-cracking in metallic materials
	Dependent on the laser and method, a controlled environment may be required
	Power requirement will contribute to higher operating costs

Table 3.8: Laser marking pros/cons summary

applicability to safety critical parts. To purchase a laser marking system is more costly than ECM and dot peen by at least a factor of ten and colouring the surface will not produce a mark of sufficient durability, so etching or engraving is required which implies higher power. The latter introduces the possibility of micro-cracking in metallic materials due to the concentration of heat at the part's surface. The quality of mark produced by a laser system (including its durability) is not significantly better than that of the alternatives to warrant accepting these drawbacks.

Dot peen was selected from the three short-listed techniques. The main reasons for this include:

Code durability
Dot peen leaves an impression in the part's surface, which offers the potential to endure a modicum of material loss or deposition.

System cost
A dot peen machine is relatively cheap, particularly in comparison to laser equivalents.

System reliability
There are few moving parts in a dot peen machine and the only consumable of note is the stylus itself. This should result in a reliable system that is inexpensive to operate.

Marking speed
Once set up for a particular part and material combination then each Data Matrix can be marked in a matter of seconds – swapping parts in and out of the machine will be the time-limiting factor.

Perhaps even more important is that dot peen is particularly suited to marking Data Matrix symbols. This is a good example of how the compatibility of technical solutions should be kept in mind as earlier decisions can affect those later on in specifying the overall part tracking system. In this case, the fact that Data Matrix had been selected as the encoding method then provided a bias to the process of selecting the ideal marking method. Had a different code type been selected, then it is likely a different marking method would have been favoured.

3.2.3   Scanner solution

A paper-based comparison of different scanners is difficult, if not impossible. They must be trialled under the conditions they would be expected to operate and take consideration of other relevant factors, such as their ease of use in a production environment. Consequently, scanners were not directly evaluated as part of this thesis; the specificity of such a choice meant that such tests were left for Alstom to complete as they saw fit.

The main way in which scanners differentiate is their decoding algorithms, which dictate their ability to read degraded symbols. However, to compare and contrast them on this basis would not only be extremely time consuming in itself, but also extremely difficult due to the need for access to proprietary information that manufacturers are unlikely to share – it is the basis of their competitive advantage.

Alstom have conducted a number of trials to assess both the durability of dot peen Data Matrix codes applied to engine parts and enable comparison of primarily two different scanner models – the Cognex DataMan 7500 and IOSS DMH-100. These trials have included:

#	Influencing factor	Weighting	Cast, forge or mould		Laser bonding		LENS[a]		Liquid metal jet		Dot peen		ECM[b]		Engraving/ milling	
			S	P	S	P	S	P	S	P	S	P	S	P	S	P
1	Code durability	10	9	90	8	80	9	90	8	80	9	90	8	80	9	90
2	Code readability	10	8	80	9	90	9	90	8	80	8	80	8	80	8	80
3	System cost	9	8	72	6	54	5	45	6	54	8	72	9	81	8	72
4	Consistent marking	9	9	81	7	63	9	81	7	63	9	81	8	72	9	81
5	Consistent scanning	9	8	72	8	72	9	81	8	72	8	72	9	81	8	72
6	System reliability	8	9	72	8	64	8	64	8	64	9	72	8	64	8	64
7	System versatility	7	6	42	7	49	6	42	7	49	7	49	7	49	8	56
8	Marking speed	6	6	36	7	42	7	42	7	42	8	48	7	42	7	42
				545		**514**		**535**		**504**		**564**		**549**		**557**

DPM Technique

Weighting definition: 1–2 = Low importance; 3–5 = Medium; 6–8 = High; 9–10 = Highest.
Score definition: 1–2 = Unsatisfactory; 3–5 = Satisfactory; 6–8 = Good; 9–10 = Excellent.

Key:

1	Code durability	The likely durability of a code (marked using the indicated technique) to manufacturing and reconditioning processes and in-service conditions (i.e. its ability to stay in a readable condition).
2	Code readability	The clarity of a code marked using the indicated technique (e.g. colour and contrast).
3	System cost	The cost of purchasing and operating the marking equipment.
4	Consistent marking	The ability to consistently mark parts whilst maintaining quality requirements.

Continued in table 3.10 . . .

Table 3.9: Direct part marking priority matrix – *part a*

[a]Laser engineered net shaping
[b]Electro-chemical marking

			Laser colouring		Laser etching		Laser engraving		Laser shotpeening		LISI[a]		GALE[b]	
#	**Influencing factor**	**Weighting**	**S**	**P**	**S**	**P**	**S**	**P**	**S**	**P**	**S**	**P**	**S**	**P**
1	Code durability	10	7	70	8	80	8	80	8	80	8	80	8	80
2	Code readability	10	9	90	9	90	8	80	8	80	8	80	9	90
3	System cost	9	6	54	6	54	6	54	5	45	6	54	6	54
4	Consistent marking	9	9	81	9	81	9	81	8	72	8	72	9	81
5	Consistent scanning	9	9	81	9	81	8	72	8	72	8	72	9	81
6	System reliability	8	8	64	8	64	8	64	7	56	8	64	8	64
7	System versatility	7	6	42	7	49	6	42	6	42	6	42	6	42
8	Marking speed	6	6	36	7	42	8	48	6	36	7	42	7	42
				518		**541**		**528**		**483**		**506**		**534**

(DPM Technique)

Weighting definition: 1–2 = Low importance; 3–5 = Medium; 6–8 = High; 9–10 = Highest.
Score definition: 1–2 = Unsatisfactory; 3–5 = Satisfactory; 6–8 = Good; 9–10 = Excellent.

Key:

...Continued from table 3.9

5	Consistent scanning	The ability to scan codes consistently – this is related code readability.
6	System reliability	The reliability of the equipment (including maintenance requirements and consumable items).
7	System versatility	The ability to mark various materials and components (including surface finish, type – e.g. sheet metal or cast – and configuration)
8	Time requirements	The time it takes to mark each code (including setting the machine).

Table 3.10: Direct part marking priority matrix – *part b*

[a]Laser inducted surface improvement
[b]Gas assisted laser etch

- Reconditioning marked parts, including exposure to the most aggressive processes such as alumina blasting and grinding [7]
- Accelerated oxidation and corrosion testing of marked parts
- Running marked parts in the test engine at Alstom's facility in Birr, Switzerland (for approximately 1,000 operating hours, including 140 starts) [22]

Further to the above, Alstom have also marked a number of blade sets that will see service in customer engines. This is an ongoing process that will provide invaluable feedback once the parts are returned at the next service interval. Conducting such a variety of trials enables Alstom to assess the performance of different scanners with respect to reading Data Matrix codes in a wide variety of conditions. This is imperative in ensuring their final choice is the right one as failure to read degraded codes will clearly have significant repercussions for the viability of implementing an enhanced part tracking system.

3.2.4   Compatibility

The author would like to draw attention to the issue of compatibility and the importance of making it an explicit consideration during the selection process. It should not be an afterthought, but rather foremost in the minds of those determining the composition of the part tracking system. Each element of the overall system – encoding, marking or scanning – may have its own distinct solution, but this should not be determined in complete isolation from the others. By remaining mindful of this issue, the process can be made more effective by promoting a proactive rather than reactive methodology that helps to prevent repetition because the solutions preferred for particular elements are subsequently found to be incompatible. Figure 3.5 illustrates the compatibility of some of the more common technical solutions for encoding, marking and scanning.

To suitably account for compatibility requires thorough knowledge of the characteristics of the available technical solutions. This, coupled with a detailed set of requirements for the part tracking system, should result in a robust and efficient selection process that delivers a solution able to meet the customer's needs in a timely and cost effective manner.

3.2.5   Section conclusion

This section describes how the technical solutions for Alstom's proposed part tracking system were defined. A process was followed to help improve the robustness of the decisions that arose. The main phases were: identify, sort, detail, relate and select (refer to figure 3.4 on page 46). The advantages and disadvantages of the short-listed technical solutions have been presented, along with the rationale behind the preferred solutions identified.

Compatibility between technical solutions was explicitly identified as an important consideration. This helped to improve the decision process that the author, and colleagues at Alstom, enacted in order to identify the preferred technical solutions for the part tracking system.

The discussion presented hereafter (including subsequent chapters) is based on Data Matrix and dot peen having been selected for the encoding and marking solutions respectively.
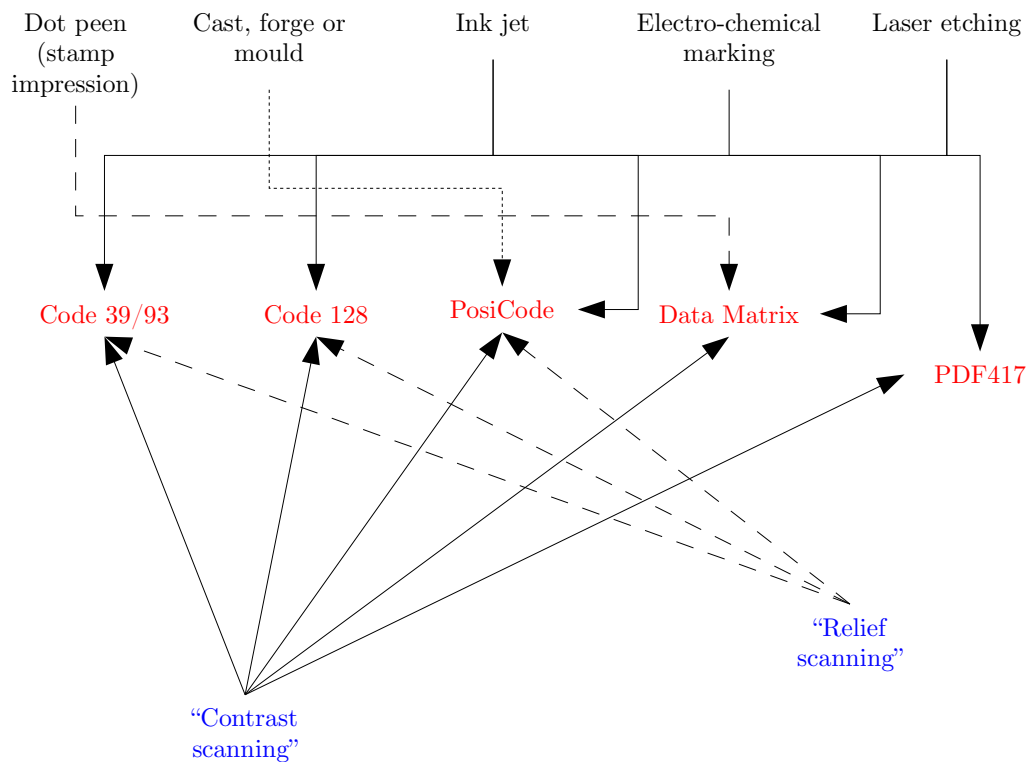
Figure 3.5: Example of compatibility between part tracking elements

3.3   Indentation of Materials

Marking a Data Matrix via dot peen involves adjusting the settings of the machine such that the resulting dots are of adequate size to provide optimum cell fill; this is typically a trial and error process. An MSc student – Stéphane Faivre [27] – completed a thesis, part of which involved him investigating a means of predicting the machine settings required for producing a dot of a certain size (i.e. diameter and, by extension, depth). The author had an intellectual input to his thesis through helping to define its scope and supervise the student. Thus it was possible to ensure the work by Faivre [27] would provide a positive contribution to the author's research, including a bilateral exchange of ideas and knowledge. This section presents a summary of his work.

The analysis of Faivre [27] comprised two main phases: *i*) proposal of a method for determining dot size; and *ii*) a means of relating the input parameters of said method back to the settings of the dot peen machine.

Metals can be deformed by an indenter under either static or dynamic conditions. The former is, in fact, quasi-static as some velocity is required, albeit very low, to indent a material's surface. Dynamic indentation refers to the situation where the indenter has a high velocity during the loading phase.

The mechanical behaviour of materials can be characterised by a stress-strain curve, typically comprised of two distinct regions representing elastic and plastic deformation. The elastic region is where any deformation caused by the application of a load can be recovered upon removal of that load. For most materials, this behaviour can be represented

by Hooke's law: $\sigma = E\varepsilon$. However, plastic deformation is of most interest in this thesis as it relates to permanent changes of a material's shape. Stéphane's review of the literature highlights the fact that certain materials' resistance to plastic flow increases when they are deformed under dynamic conditions, known as rate-dependency (see figure 3.6).
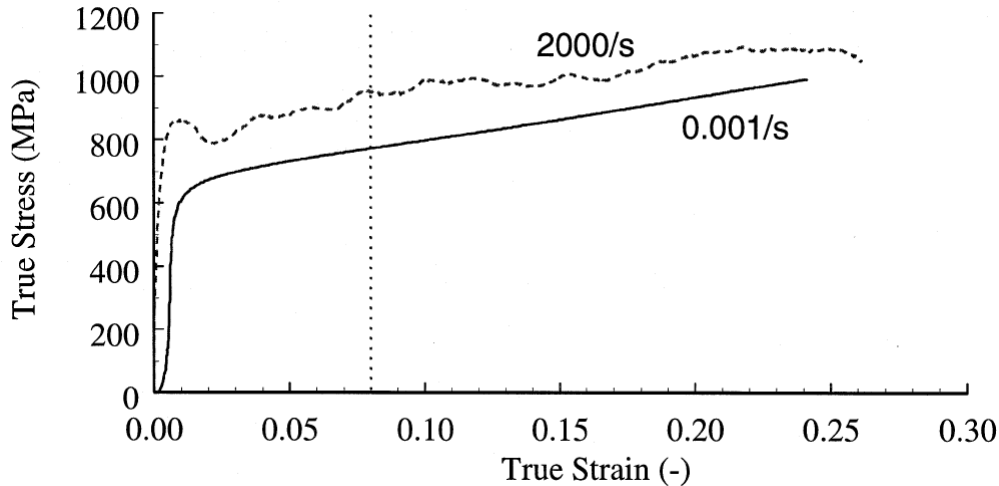
Figure 3.6: Stress-strain curves at quasi-static and high strain rates for 316 stainless steel [38]

Strain rate is the parameter used to define the loading rate at which a material is deformed. Nominal strain rate can be defined as the ratio of the indenter velocity to the size of the indentation [65]:

$$\text{Nominal strain rate} = \frac{\text{Velocity of the indenter}}{\text{Size of the indentation}}$$

However, during the impact of an indenter into a metallic surface, the velocity of the indenter is not constant – it will decrease until it reaches zero at the end of the loading phase. This means the choice of velocity to determine the strain rate is not obvious, but it is typical to use a value during the latter part of the loading phase where the deformed volume is largest. The effect of a non-static strain rate is that the material's resistance to plastic flow will vary. This effect can manifest as a higher loading requirement under dynamic conditions in order to achieve the same size of indentation as that achieved under static conditions. If this effect is negligible then the material is considered rate-independent, otherwise it is rate-dependent. Two models are noted by Faivre [27] as a means of accounting for the strain-rate dependency of metals in their stress-strain relationship: the Johnson-Cook model [48] and a further model proposed by Andrews et al. [5]. Faivre [27] utilised the Andrews et al. [5] model in his proposed solution to marking a dot of a specific size. Usefully, it can be adjusted for application to either rate-independent or rate-dependent materials.

Loading and unloading curves provide a more practical means of representing the elastic and plastic deformations occurring when an indenter impinges a surface. These curves plot the load at the interface between the indenter and material as a function of the depth of the indentation (see figure 3.7). As these curves indicate the residual indentation depth for a given process, by knowing the indenter geometry one can determine the geometry of the indentation in the plane of the surface (e.g. dot diameter for a conical indenter). The loading curve represents the elasto-plastic deformation of the material and, for static

indentations, this curve follows Kick's law [66]: $P = Ch^2$. The coefficient C depends not just on the material properties, but also the geometry of the indenter and so cannot be determined by purely analytical means. However, it can be determined by finite element analysis (FEA). FEA can, in fact, be used to determine the loading and unloading curves for a given material and indenter geometry pair. For rate-dependent materials, Kick's law is no longer valid as the coefficient C varies with the loading rate, however a correction for C can be applied so that agreement with Kick's law can be maintained. Further, varying the impact velocity will result in a family of loading and unloading curves with each one relating to a specific velocity. The unloading curve represents the elastic recovery only of the material. As such it is independent of the plastic deformation and, therefore, it is not influenced by the material's strain-rate dependency. The unloading curve is not completely linear – a non-linear portion exists at its end as the applied load tends back towards zero. However, as this portion is very small, the unloading curve is typically considered as linear throughout.

(a) Typical load-indentation curve [66]

(b) Numerical simulation of dynamic indentation repsonse of OFHC copper [44]
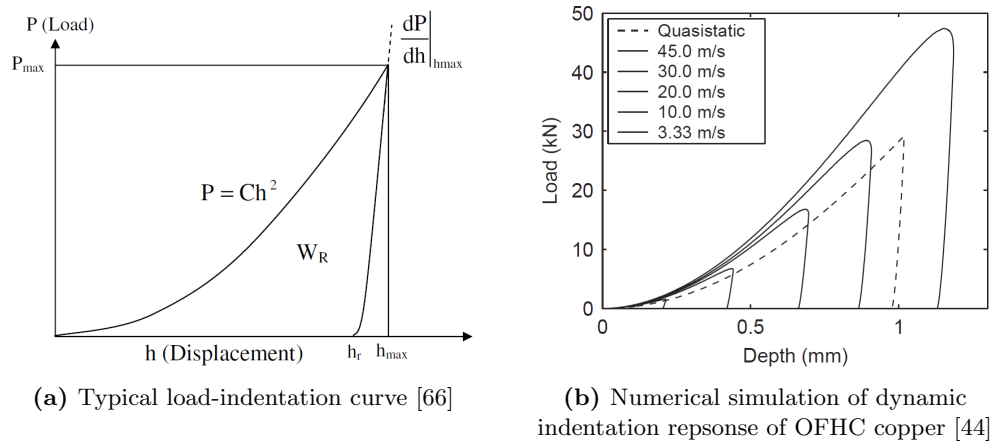
Figure 3.7: Loading and unloading curves

Based on the findings of his literature review, Faivre [27] proposed a means of relating the impact velocity of a conical indenter to the dimensions of the indentation. Given the significance of rate-dependency, two methods were proposed: one each for rate-independent and rate-dependent materials. For rate-independent materials a finite element model is used to determine the loading and unloading curves for each desired material and indenter geometry pair. From these curves the coefficients required for substitution into the Andrews et al. [5] model can be determined (remember that rate-independence means that the coefficients derived from these curves for each pairing can be used regardless of the strain-rate). For the application at hand the geometry of the indentation is to be specified, so the method of Andrews et al is effectively inversed such that the impact velocity becomes the output. In the case of rate-dependent materials a similar approach, albeit accounting for additional relevant factors such as the variability of the coefficient C in Kick's law, is discussed, but deemed impractical to solve analytically. To do so requires the derivation of certain parameters via an FE model, so it is suggested to simply use such a model directly to determine the required impact velocity. This essentially remains a trial and error process, however, assuming the computational expense of the model is not great then performing a batch run of varying indenter velocities for each material and indenter geometry pair potentially remains more practical than physically marking and measuring

a large number of samples. A diagrammatic summary of the two methods proposed by Faivre [27] is shown in figure 3.8.

Finally, it was necessary to consider how the required impact velocity could be related back to the settings of the dot peen machine, namely the impulse force applied to the stylus and the distance of the stylus from the part's surface. This was achieved via a one-dimensional analysis – the dot peen stylus is constrained to vertical motion only – using Newton's second law and the conservation of energy. The resulting relationship was:

$$F_0 = \frac{m}{\Delta t}(v_{imp}^2 - 2gh_1)^{1/2}$$

where

$$
\begin{aligned}
F_0 &= \text{Impulse force} \\
m &= \text{Mass of the stylus} \\
\Delta t &= \text{Time period over which } F_0 \text{ acts} \\
v_{imp} &= \text{Impact velocity} \\
g &= \text{Gravity} \\
h_1 &= \text{Distance between the stylus and marking surface}
\end{aligned}
$$

In the dot peen machine control software, the force setting is simply called "Depth" and does not have a known physical meaning. Therefore test specimens should be marked for each value of "Depth" and the resulting dot measured for determining impact velocity and hence the impulse force F_0 applied by the machine. This process is more easily achieved using a rate-independent material. The value of h_1 can be specified directly in the control software (known as the "lift-off" setting) and so in this case there is no need for conversion.

3.4   Degradation Causality

This section presents the causal relationship identified as a basis for assessing the impact of code degradation – in the form of deposition, erosion and corrosion – on the scanning process. The primary issue to overcome in achieving this has been to identify the causal relationship between these two extremes. The conclusion of this analysis was that a number of surface properties, namely surface roughness, dot geometry and surface colour, provide the causal link with regard to the effect of degradation on symbol legibility.

3.4.1   Interrelationship

Understanding how degradation affects the scanning process was of paramount importance. Without such a framework it would be difficult to identify and rationalise parameters for use in assessing the current degradation of a machine readable code.

The process began by understanding the basic operation of charge-coupled device (CCD) sensors, which are typical of scanners for two-dimensional codes like Data Matrix. By virtue of its response to incident ambient light, the next step was to understand how the code's surface properties could alter the ambient light it reflects towards the CCD sensor. Those surface properties identified, such as roughness and colour, may be affected by the degradation mechanisms known to act. In much the same way that multiple sources of degradation may be broadly categorised using the descriptors deposition, erosion and
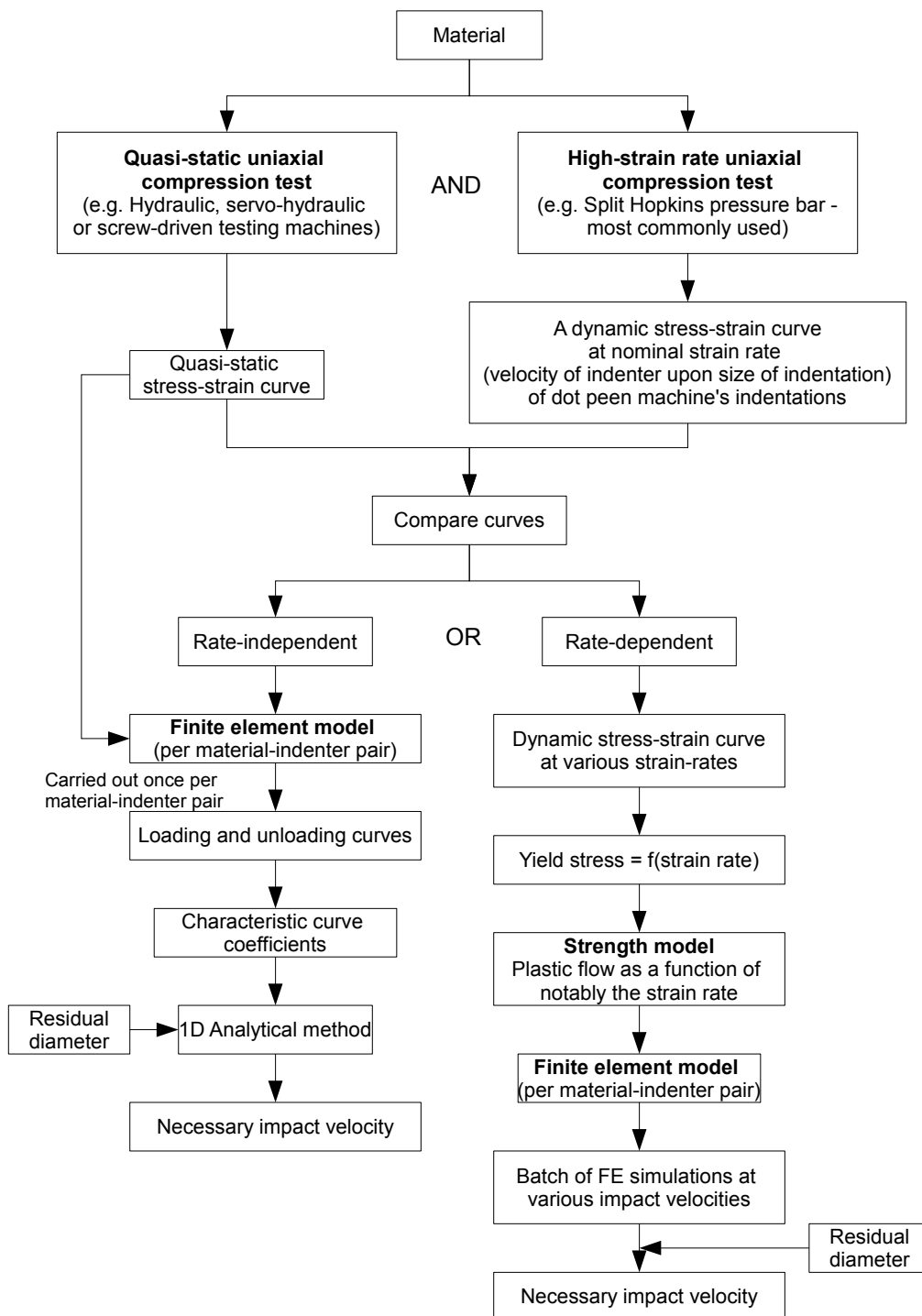
Figure 3.8: Summary of material investigation methodology [27]

corrosion, so too can the impact of these mechanisms on the surface's reflective properties be characterised by reference to surface roughness, dot geometry and surface colour. These surface properties provide measurable parameters for characterising a code's current level of degradation (see figure 3.9).
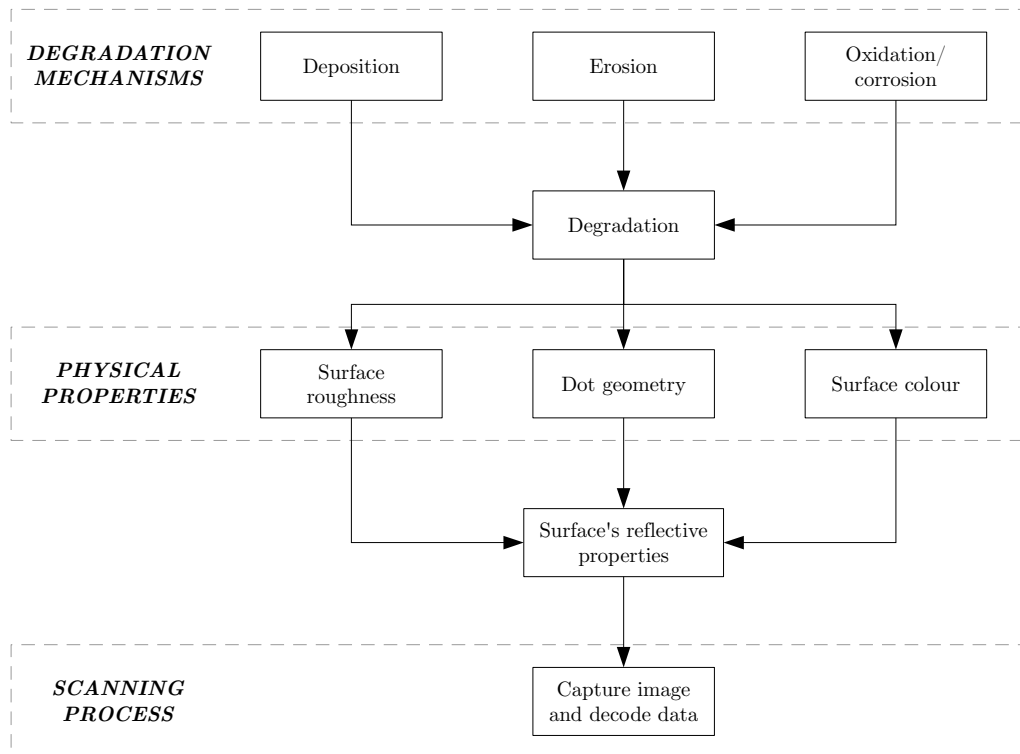
Figure 3.9: Interrelationship of factors

A brief description of the three main elements of figure 3.9:

Degradation mechanisms These are the predominant sources of damage gas turbine parts can be expected to experience (both during operation and reconditioning cycles). The contribution from each can be expected to vary based on a number of factors, including, but not limited to, the type of part, the code's size and location, operating parameters (e.g. firing temperature) and environmental factors (e.g. geographical location). Codes can be located on parts to help mitigate the potential for damage. For example, a turbine blade can be marked on its foot to avoid the main gas path.

Physical properties The degradation mechanisms will cause the physical properties of the code to change relative to its original condition. The reflectivity of the code and its surrounding surface is critical for the scanning process because image capture relies on the light received from the target surface. Therefore these properties present the means by which to link code legibility with the degradation mechanisms occurring.

Scanning process This is the critical phase of the part tracking process; failure to achieve a successful scan renders the system useless. Success is based on

understanding the relative significance of the degradation mechanisms, how the surface properties are affected and therefore the quality of the captured image. Successfully decoding the image primarily relies on the contrast level so that the code is distinguishable from the background surface. Reduced dot depth and diameter as a result of deposition, increased roughness from erosion and discolouration from oxidation/corrosion will typically all serve to reduce image contrast and hence decrease code legibility.

3.4.2   Impact of degradation

Several physical properties have been identified as important with respect to surface reflectance. It is feasible for the degradation mechanisms occurring to impact one, or a number of, these physical properties, leading to a change in legibility of the Data Matrix symbol applied to the surface. What is less clear is the degree to which these degradation mechanisms will degrade the surface and how long this will take during engine operation. Further compounding the issue is the likelihood that more than one of the physical parameters will be affected during the life of the part to which the Data Matrix symbol has been applied. Developing this knowledge is paramount for understanding the real changes in legibility that may occur for different parts installed in different engine models. Theory, such as that presented in this thesis, can help with initial estimations of symbol durability (in terms of remaining readable by the scanner), but feedback from inspecting marked parts that have experienced typical conditions (over a typical service interval) will be important for validating any estimations. This issue is discussed further in chapter 4.

3.4.3   Section conclusion

This section explicitly identified the importance of surface reflectance in the relationship that exists between the degradation mechanisms occurring and the scanning process. This outcome shows that maintaining the physical properties of the surface such that they yield reflective characteristics conducive to achieving a successful scan is important. Ultimately, this involves maintaining contrast between the dots of the matrix and the surrounding plain surface as much as possible.

How degradation accumulates over the life of a part marked with a Data Matrix is important as this will dictate symbol durability. It will be important to understand the types of degradation occurring and at what rate. This knowledge can help to define marking parameters (such as matrix size and its location on the part) so as to maximise through-life legibility. Data Matrix allows for some degradation through its error correction feature and scanner software can attempt to maximise image quality prior to processing through using such techniques as image morphology. However, these systems are limited in their capability; they cannot be relied upon to mitigate against all circumstances with respect to symbol degradation.

3.5   Data Matrix Tests

To reinforce the theory put forward in section 3.4 regarding the impact of degradation mechanisms on code legibility, tests were completed to demonstrate it in practice. The primary aim of these tests was to show that as the surface properties change with increased

degradation, the legibility of the symbol is indeed altered. Data for erosion and oxidation are presented in this section to demonstrate the effect of changes in roughness and colour respectively. Deposition was not investigated at this time because a means of consistently applying a deposit to the surface of the Data Matrix symbols (including a suitable media) was not available. However, some of the potential effects with regard to deposition are hypothesised with respect to the available data in section 3.5.4.

3.5.1 Test process

Exotic materials and processes were not used as the intention was not to reproduce the exact operating conditions of a gas turbine at this stage, but rather to demonstrate the theory of section 3.4 in practice. Mild steel plate was selected for marking the Data Matrix codes on, using the dot peen method. The dot peen machine used is shown in figure 3.10.

(a) Machine and controller   **(b)** Plate in situ
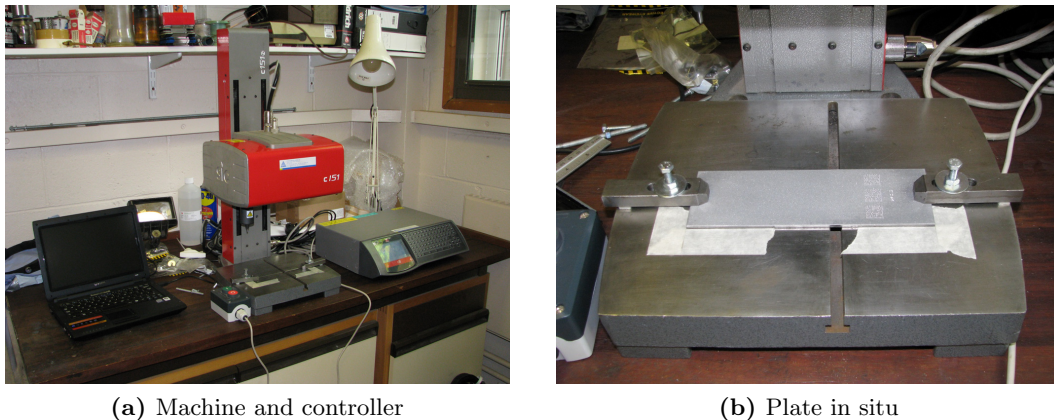
Figure 3.10: Dot peen machine

Because it was required to subject codes to varying levels of degradation a number of mild steel plates were cut for marking. Each plate was marked with the same set of Data Matrix codes comprising five different sizes of square matrix ranging from 4–12 mm (outside dimension), with each size of matrix being marked three times over to enable repeat readings (see table 3.11 and figure 3.11).

Once sufficient plates had been marked they were then degraded. Some received erosive damage using a shot blaster (primarily to induce a change in surface roughness), whilst others were heated to induce oxidation (and hence a change in surface colour). The manner in which these processes were applied to the samples is summarised in figure 3.12. The surface roughness produced by shot blasting primarily depends on system pressure, distance to the target and size of the blast media (these parameters are quantified in table 3.12). Varying levels of degradation were achieved by altering the number of times the blasting nozzle was tracked across the surface of the code. The shot blaster used is shown in figure 3.13. The thickness of the oxide layer is governed by the heating temperature and period of exposure. In order to estimate these parameters some preliminary tests were completed using the same mild steel material as the Data Matrix codes were applied to. This process is detailed further in section 3.5.1.1 and the parameters used are summarised in table 3.13.

Once the process of degradation was complete, the codes were analysed in several ways:

Outer dimension (mm)	Symbol size (row × col)	Module size (mm)
4	14 × 14	0.29
6	14 × 14	0.43
8	14 × 14	0.57
10	14 × 14	0.71
12	14 × 14	0.86

Stylus cone angle: 90°
Stylus tip radius: 0.3 mm

Table 3.11: Data matrix specifications
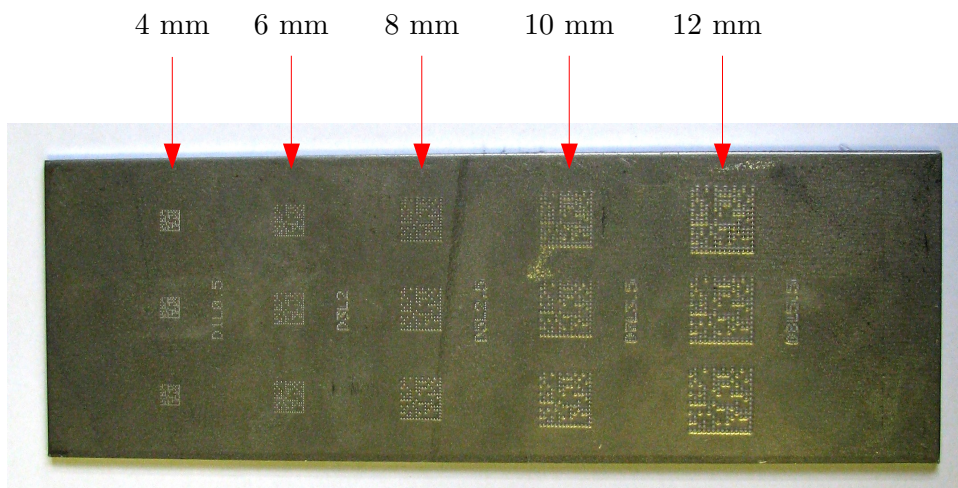
Figure 3.11: Steel plate showing marking arrangement

Pressure (bar)	Nozzle distance (cm)	Blast media (grit size)
3.5	∼ 7–10	30–40
3.5	∼ 7–10	60–80

Note: 30–40 grit is coarser than 60–80 grit [11]

Table 3.12: Shot blasting parameters
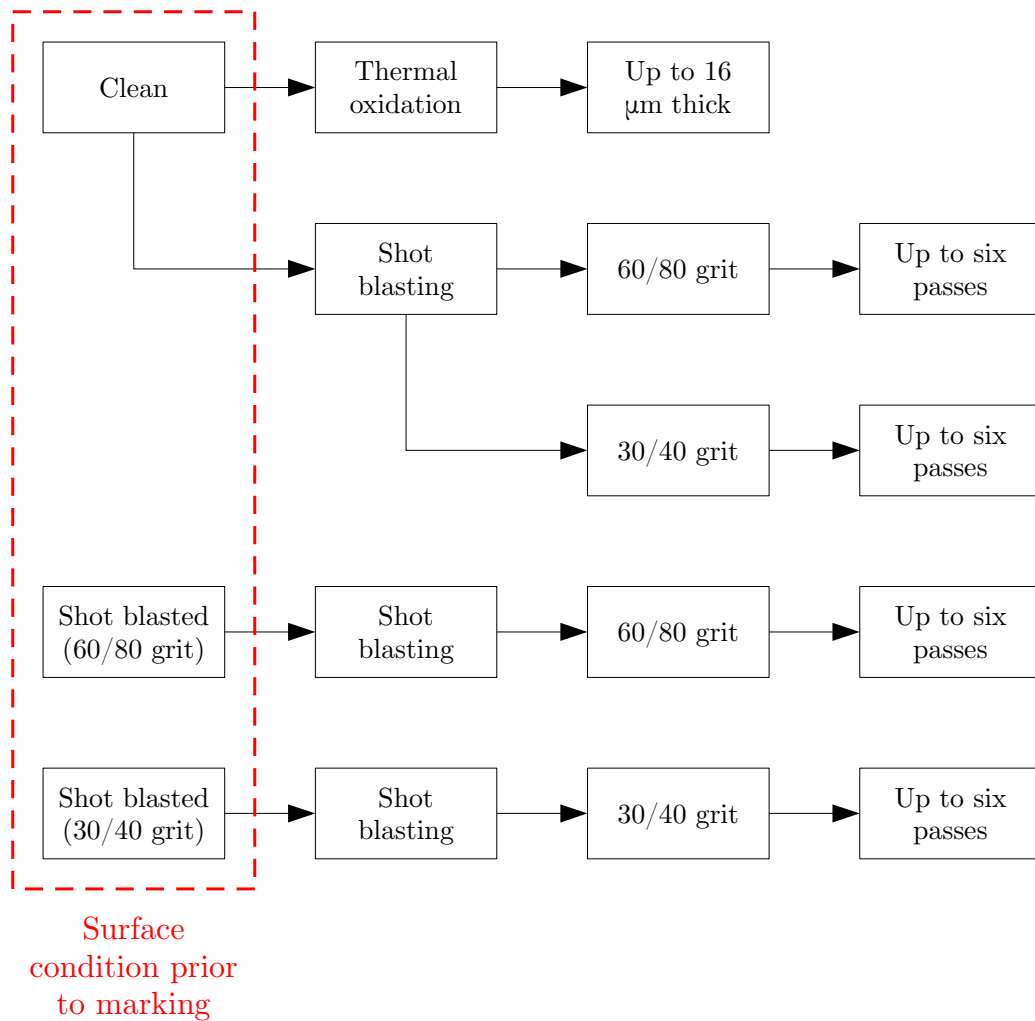
Figure 3.12: A summary of the degradation processes applied to the Data Matrix samples

(a) Cabinet   **(b)** Nozzle assembly
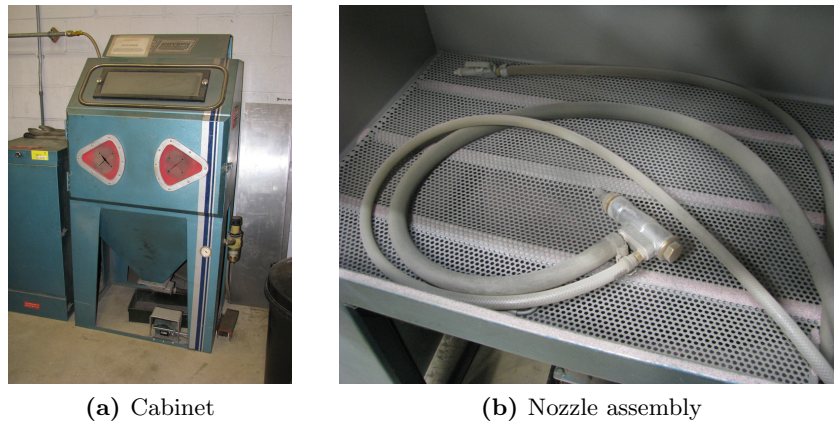
Figure 3.13: Shot blaster

Temperature ($^\circ$C)	Exposure time (hours)	Oxide thickness (μm)
500	2.2	~ 4
500	12.8	~ 8
500	76.1	~ 16

Table 3.13: Oxidation parameters

   i. They were scanned to check for read success/failure;
  ii. The images captured by the scanner were analysed for contrast;
 iii. A confocal microscope was used to measure geometry; and
 iv. A surface profilometer was used to measure surface roughness.

When the scanner attempts to read a code the captured grey-scale image can be displayed on the attached computer. Each of the images was saved for further processing in MATLAB whereby a row of the image could be defined and the intensity data extracted for plotting. This enabled the relative reflectance of the dots versus that of the plain surface to be assessed, which equates to contrast. The scanner used is shown in figure 3.14. The confocal microscope enabled the geometry of individual dots to be captured. This three-dimensional data enabled comparison of dots from matrices that had been exposed to varying amounts of degradation (the intention being to look for changes in geometry). Finally, a surface profilometer was used to measure surface roughness adjacent to the Data Matrix codes.

3.5.1.1 Thermal oxidation calculations

Preliminary tests were employed in order to estimate the temperature and period of exposure required to produce an oxide layer of a certain thickness. Equation 2.2 (p. 20) shows that oxide growth depends on the scaling constant k_p and time t. The scaling constant actually varies with temperature (see Kubaschewski and Hopkins [39, p. 174], for example) and so the preliminary tests involved heating plates at three different temperatures, and for three different time periods at each temperature. Once the heating
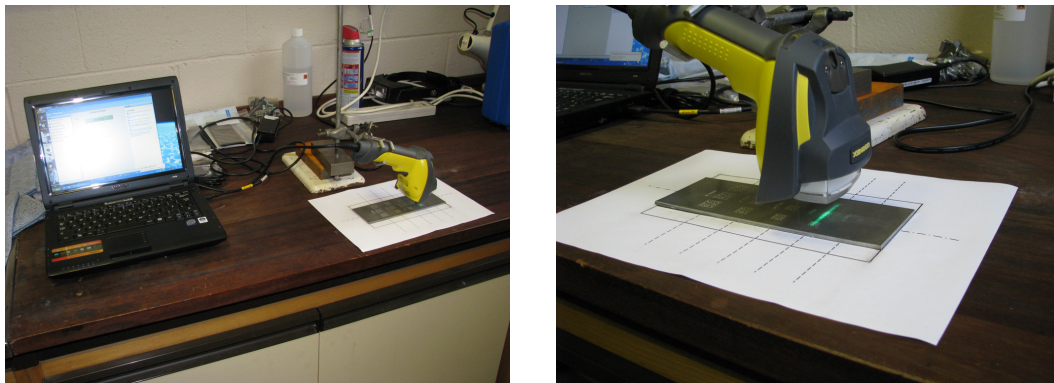
(a) Scanner and laptop

(b) Template used for aligning the plates

Figure 3.14: Data Matrix scanner

process had been completed the plates were allowed to cool and were then cut in order to measure, under high magnification, the thickness of the oxide layer that had grown (see figure 3.15 for an example). The data collected is summarised in table 3.14.
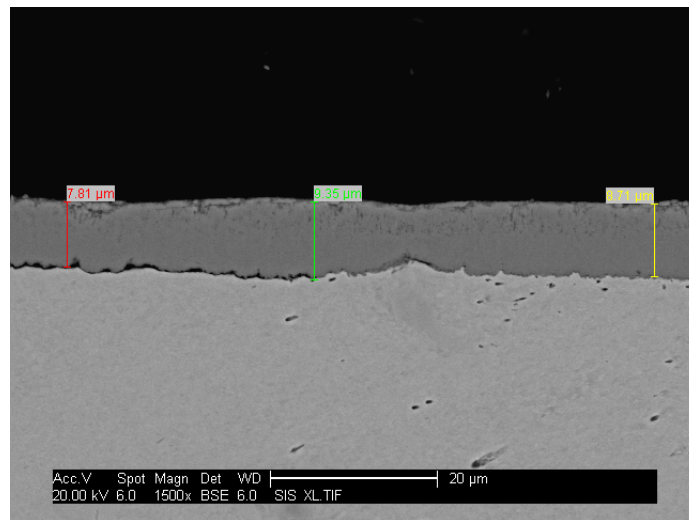
Figure 3.15: Oxide growth measured after heating at 500 °C for 20 hours

Based on the assumption that the preliminary data of table 3.14 follows the form

$$y = ax^n \tag{3.1}$$

a power regression analysis was performed to determine the constants a and n.
Taking logs of equation 3.1 yields:

$$\log y = n \log x + \log a \tag{3.2}$$

which is equivalent to

$$Y = mX + c \tag{3.3}$$

Temp. (°C)	Exposure (hours)	Oxide thickness (μm)				$\log(k_p)$ ($g^2cm^{-4}sec^{-1}$)
		Pt. 1	**Pt. 2**	**Pt. 3**	**Avg.**	
300	5	–	–	–	–	–
300	20	–	–	–	–	–
300	50	–	–	–	–	–
400	5	0.90	–	–	0.90	−10.91
400	22	1.54	0.67	0.96	1.06	−11.41
400	50	2.18	2.82	2.82	2.61	−10.98
500	5	5.38	5.64	6.28	5.77	−9.29
500	20	7.81	9.35	8.71	8.62	−9.55
500	50	14.25	14.25	14.73	14.41	−9.50

Table 3.14: Preliminary oxidation data

The sum of the squares S is given by

$$S = \sum_{1}^{n}(Y_i - mX_i - c)^2 \qquad (3.4)$$

Differentiating equation 3.4 with respect to m and c (and equating to zero for S to be a minimum):

$$\frac{\partial S}{\partial m} = -2\sum_{1}^{n} X(Y - mX - c) = 0 \qquad (3.5a)$$

$$\therefore \quad \sum XY - m\sum X^2 - c\sum X = 0 \qquad (3.5b)$$

and

$$\frac{\partial S}{\partial c} = -2\sum_{1}^{n}(Y - mX - c) = 0 \qquad (3.5c)$$

$$\therefore \quad \sum Y - m\sum X - nc = 0 \qquad (3.5d)$$

Using the 500 °C data from table 3.14 as an example, table 3.15 shows the factors calculated for subsequent substitution into equation 3.5b and 3.5d.

	X	**log X**	**Y**	**log Y**	**(log X) × (log Y)**	**(log X)^2**
	5	0.6990	5.77	0.7609	0.5319	0.4886
	20	1.3010	8.62	0.9357	1.2173	1.6927
	50	1.6990	14.41	1.1587	1.9685	2.8865
SUM	–	3.6990	–	2.8533	3.7177	5.0677

Table 3.15: Power regression example data

Substituting the appropriate data from table 3.15 into equation 3.5b and 3.5d gives:

$$3.7177 - 5.0677m - 3.699c = 0 \tag{3.6a}$$
$$2.8553 - 3.669m - 3c = 0 \tag{3.6b}$$

Solving equation 3.6a and 3.6b simultaneously yields the constants a and n for satisfying equation 3.1:

$$m = n = 0.3891$$
$$c = \log a \Rightarrow a = 10^c = 10^{0.4721} = 2.9652$$
$$\therefore \quad y = 2.9652x^{0.3891}$$

By the same method, the 400 °C data gives: $y = 0.4059x^{0.4195}$. The oxide grown at 300 °C was too thin to measure even at extremely high magnification. However, this did not hinder the subsequent tests as it was decided to use only a single temperature, that of 500 °C (see table 3.13 on page 66 for a summary).

3.5.2 Scanning data

After completing the process of degradation, all the codes were scanned from a fixed position so that the conditions were consistent. Identification of successes and failures was necessary to help validate the key properties identified as significant – surface roughness, dot geometry and surface colour – by the analysis described in section 3.4. The scan results are provided in appendix B.
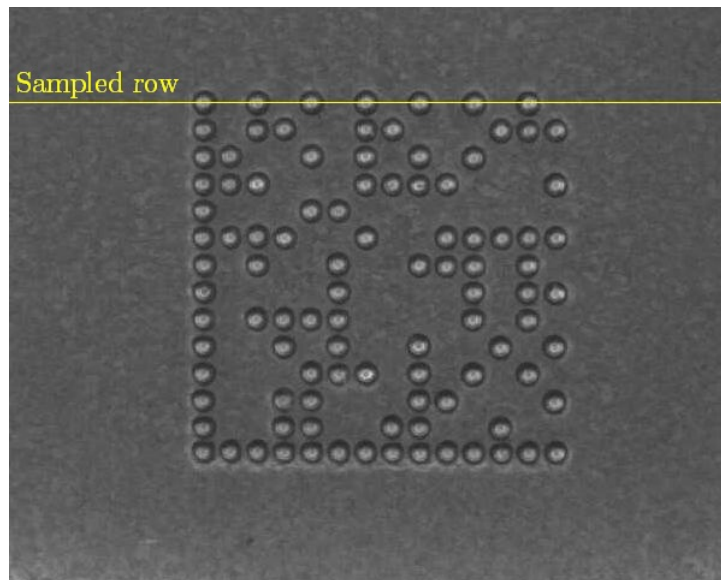
Description: a 10 mm matrix marked on a clean surface; no degradation applied.

Figure 3.16: An example of the image row selected for extracting intensity data

The images captured by the scanner (see appendix C for some examples) were saved for processing through MATLAB, which involved defining a row of the image for extracting

intensity data. The row number was selected to coincide with the upper clock track of the symbol (see figure 3.16) so that the output included reflectance of both dots and the plain surface. The intensity data extracted from the row highlighted in figure 3.16 is shown in figure 3.18 on page 72. This data on its own is not sufficient to definitively identify whether a code is readable or not, but does indicate symbol contrast, which is important to achieving a successful read.

3.5.2.1 Data Matrix codes applied to a clean surface

Those codes that were applied to a clean surface, with no subsequent degradation, serve as a reference point for the other samples tested. As expected, these codes could be scanned easily, irrespective of their size. In this instance the surface is relatively smooth (refer to table 3.16) and therefore the reflection of incident light tends to be specular rather than diffuse. The light source of the scanner predominantly directs light at a glancing angle towards the plate. This angle combined with the low scatter from the plain surface means the majority of the incident light is reflected away from the image sensor. The dots, however, serve to direct a higher proportion of this light back towards the sensor. This results in the dots appearing brighter than the surrounding plain surface. This behaviour is illustrated in figure 3.17. Analysing the grey-scale image captured by the scanner shows how the grey level varies across the upper clock track of one of the symbols. Figure 3.18 is typical of the response seen from the codes marked on a clean surface, with clear peaks evident that coincide with the presence of a dot. This confirms that the amount of light being received by the image sensor from these areas is greater than from elsewhere on the surface.
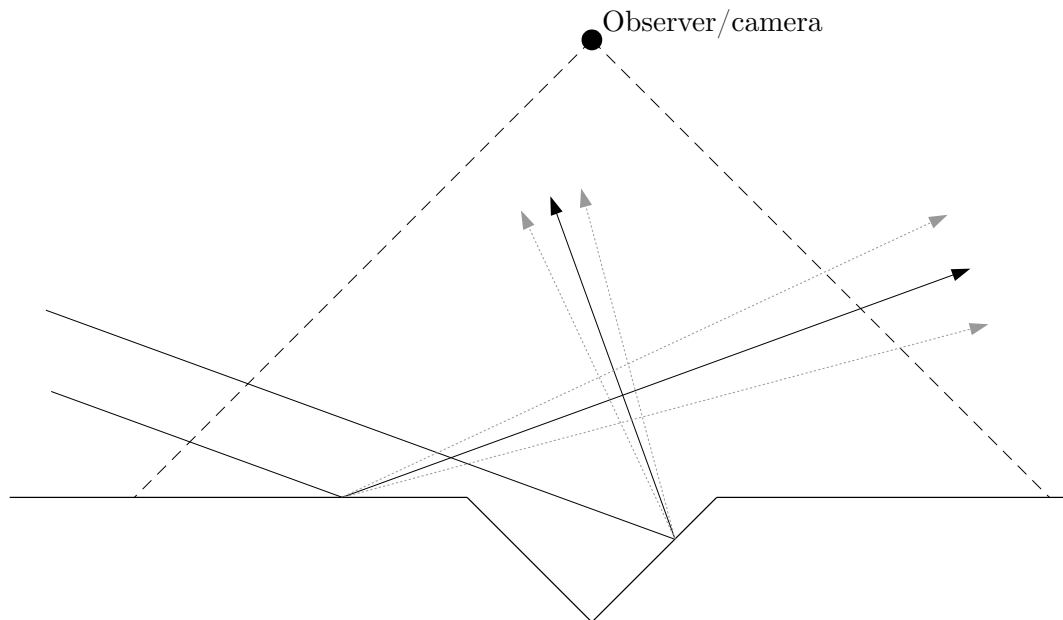
Figure 3.17: A schematic representation of the relative reflection from a Data Matrix dot and the plain surface (assuming predominantly specular behaviour)

Shot blasting codes that have been applied to a clean surface has a noticeable affect on their legibility to the scanner. The severity of this effect was dependent on the grit size of

the blast media used. As expected, the coarser (30/40) grit presented more issues for the scanner with only the two largest – 10 and 12 mm – matrices remaining consistently legible. The symbols blasted with the finer (60/80) grit did fare better, but not significantly so; the 8 mm matrix was now more consistently legible, but the two smallest matrices remained intolerant of the induced surface damage. Different samples of clean marks were blasted up to six times using each grit size. The roughness remained approximately constant and the amount of material removed from the surface was small, meaning that the scanning results between samples, based on the degree to which they had been exposed to shot blasting, did not change significantly. Where disparities are evident is likely due to the manual nature of the shot blasting process that meant it was difficult to ensure absolute consistency. Increasing the roughness of bare metal samples like this causes increased scatter of the reflected incident light. This increased scatter affects both the dots and plain surface, meaning their reflectance becomes more similar. The result is that the contrast evident between the dots and plain surface is reduced, which makes it harder for the scanning software to identify the symbol in the image. Looking at the grey level it is clear there is a distinct reduction in contrast between the dots of the upper clock track and surrounding surface, along with increased noise throughout the signal, when surface roughness is increased. Figure 3.19 shows the grey level profile from a symbol that remained readable after shot blasting. It indicates that after shot blasting the dots are actually reflecting less light back towards the image sensor relative to the plain surface and so now appear as troughs in the grey level profile. This is possibly due to there being an increased likelihood of incident light reflecting more than once within a dot before reaching the scanner's sensor (in comparison to the plain surface). Consequently, more diffusion is likely to occur of light impinging on the dots, which in turn reduces the proportion that will be reflected back towards the scanner's image sensor. This is not necessarily an issue in itself – the scanning software can cope equally well if the symbol is 'dark on light' or 'light on dark' – but what is significant is that the magnitude to which the dot grey level deviates from that of the background is significantly reduced (i.e. the contrast has dropped). Not all the matrices are equally affected, those that are larger (and hence have larger dots) are better able to cope with increased surface roughness (see figure 3.20). This behaviour suggests that the scale of the roughness in comparison to dot size is important (this is implied in an SAE technical standard [57], albeit in relation to applying Data Matrix codes to already rough surfaces). Where the scale of the roughness is too similar to that of the dots, then the noise introduced by the increase in diffuse reflection becomes too great. Figure 3.21 illustrates the grey level profile of a symbol that was not readable after shot blasting. This potentially relates to the behaviour outlined in table 2.6 (page 33), which identifies the importance of macro- and micro-scale geometry with respect to surface reflectance. The larger dots, having a larger surface area, are able to impart a greater macro-scale effect that helps to overcome the increased diffusion (due to increased roughness).

Thermal oxidation can have a significant impact on the legibility of Data Matrix codes depending on how well developed the oxide becomes. In the very early stages of growth where the oxide layer is only a thin film, the effect on legibility is negligible none of the symbols proved difficult for the scanner to read. In this state the oxide is largely transparent such that the incident light can still reach and reflect from the metal's surface (albeit tinted, depending on the oxide thickness relative to the light's wavelength – see section 2.3.3.2). Oxide layers that act as tints in this way exhibit a thickness of the order of nanometres. Further, three other oxide layers of approximately 4, 8 and 16 μm were grown. At these increased values of thickness the incident light can no longer penetrate

to the metal surface so reflectance is now governed by the properties of the oxide. As discussed in section 2.4.2, the influence of surface roughness on the ratio of specular to diffuse reflection is most applicable to metallic surfaces. Most other materials exhibit largely diffuse reflection even when smooth. This is true of the oxide layers that were grown for these tests. For the 4 μm sample the oxide layer that grew was not consistent over the plate's entire surface and so in the majority of cases it was still possible to achieve sufficient contrast for a successful scan – the grey level profile of one of these symbols is illustrated in figure 3.22. However, for the two thickest samples the oxide had grown over the entire surface, preventing nearly all of the codes from being read – only two symbols with 8 μm of growth could be read intermittently. Not only does the oxide hinder scanning by inducing diffuse reflection of incident light, but its dark red/brown colour (being an iron oxide) implies there is also increased absorption occurring. So not only is less light being reflected from the surface, but that which is reflected is highly diffuse. This behaviour causes reduced contrast between the symbol and plain surface, and hence read failures occur. This reduction in contrast is similar to that observed with increased surface roughness, however it appears that in the case of thermal oxidation, dot size offers no mitigation against reduced legibility. The oxide layer induces a high degree of scatter simply due to the way in which non-metallic surfaces reflect light (i.e. there is little progression in the severity of this effect as there is with increasing roughness). This, coupled with the dark colour of the oxide, presents a very low contrast image for the scanning software to interpret. Typical grey level profiles for the thicker oxide layers are illustrated in figure 3.23.
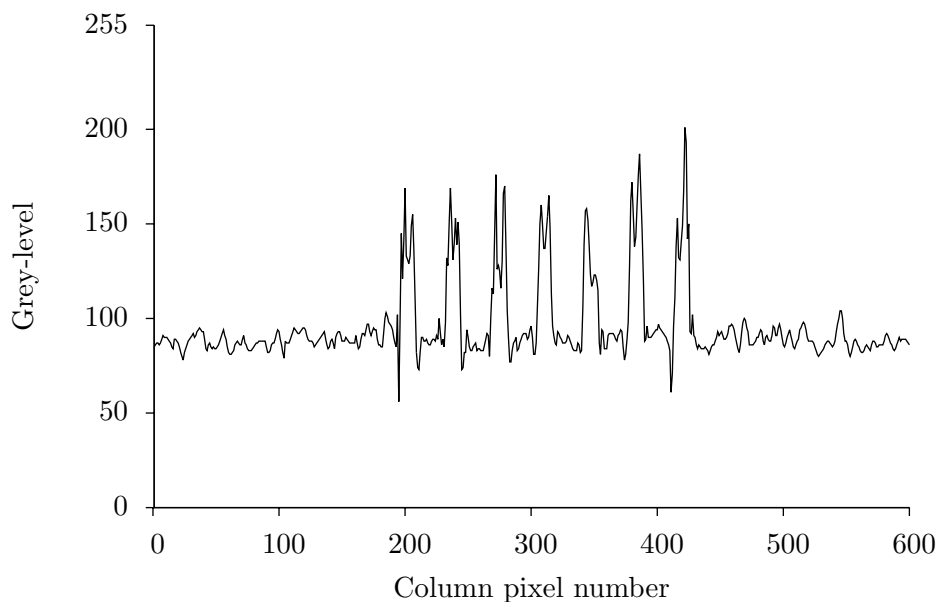
Figure 3.18: Intensity data – 8 mm matrix – clean marking surface (*Degradation: none*)
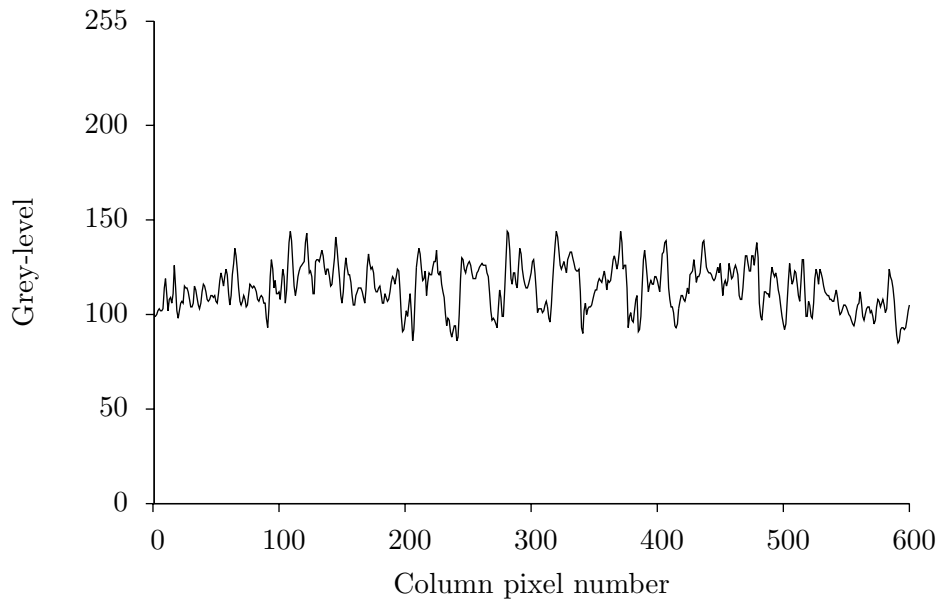
Figure 3.19: Intensity data showing the effect of increased surface roughness on symbol reflectance (symbol readable) – 8 mm matrix – clean marking surface (*Degradation:* shot blasting with 60/80 grit – two passes)
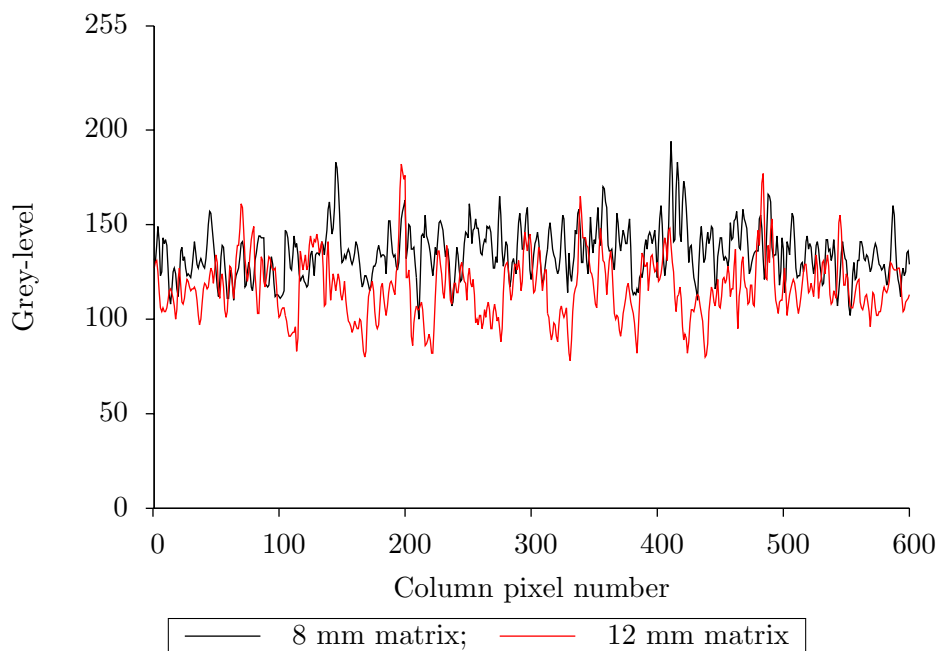
Figure 3.20: Intensity data showing the effect of increased matrix size on symbol reflectance for rough surfaces (symbol readable) – clean marking surface (*Degradation:* shot blasting with 30/40 grit – three passes)
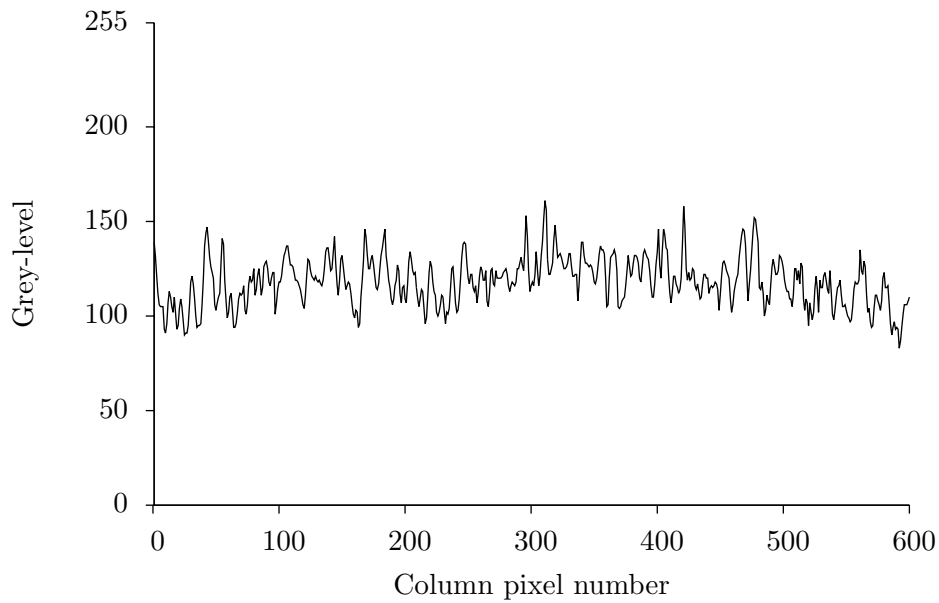
Figure 3.21: Intensity data showing the effect of increased surface roughness on symbol reflectance (symbol not readable) – 8 mm matrix – clean marking surface (*Degradation: shot blasting with 30/40 grit – two passes*)
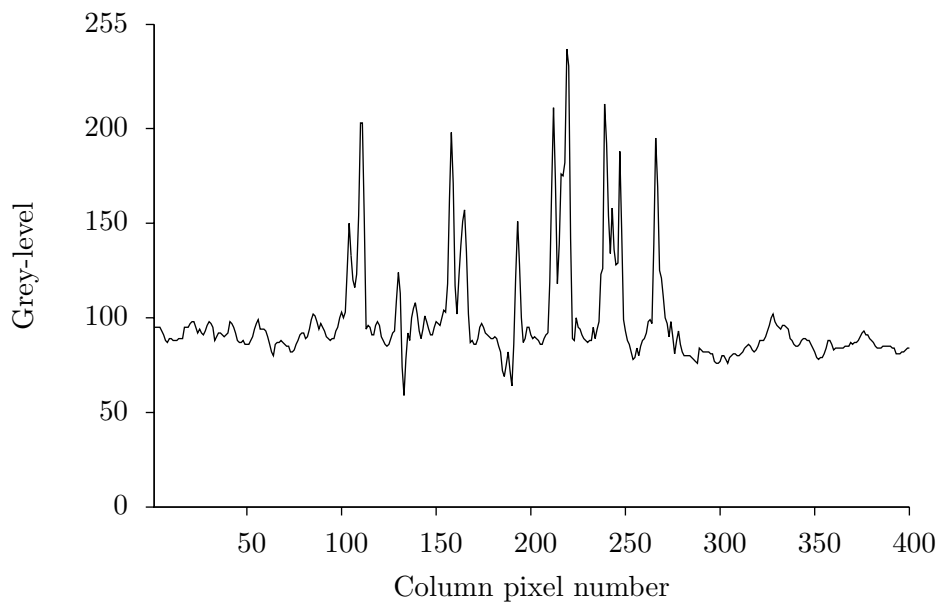
Figure 3.22: Intensity data showing the effect of 'light' oxidation on symbol reflectance – 6 mm matrix – clean marking surface (*Degradation:* thermal oxidation ~ 4 μm thickness)
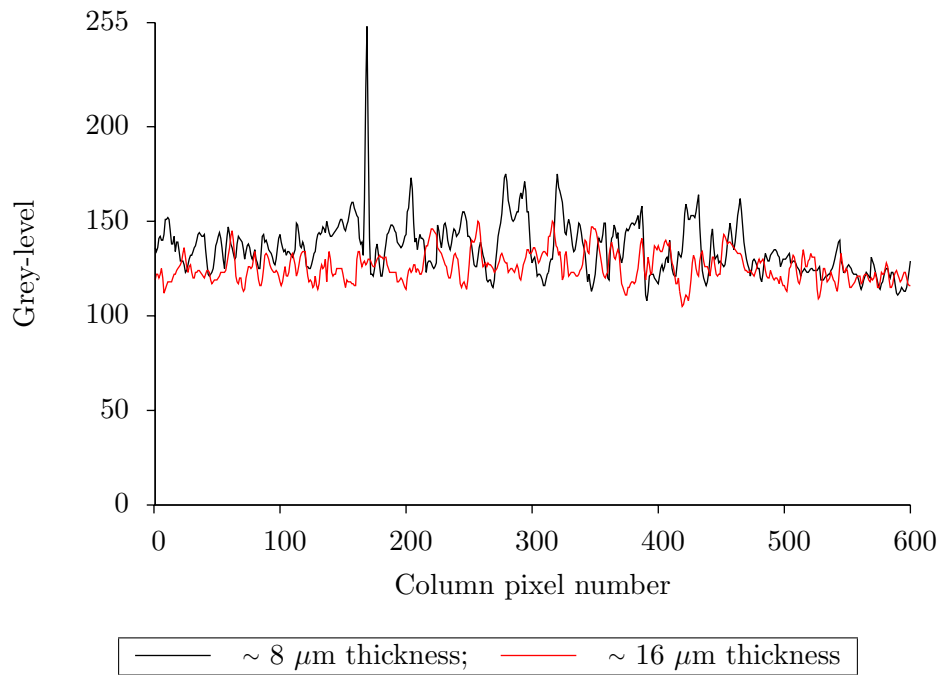
Figure 3.23: Intensity data showing the effect of 'heavy' oxidation on symbol reflectance – 10 mm matrices – clean marking surface (*Degradation:* thermal oxidation)
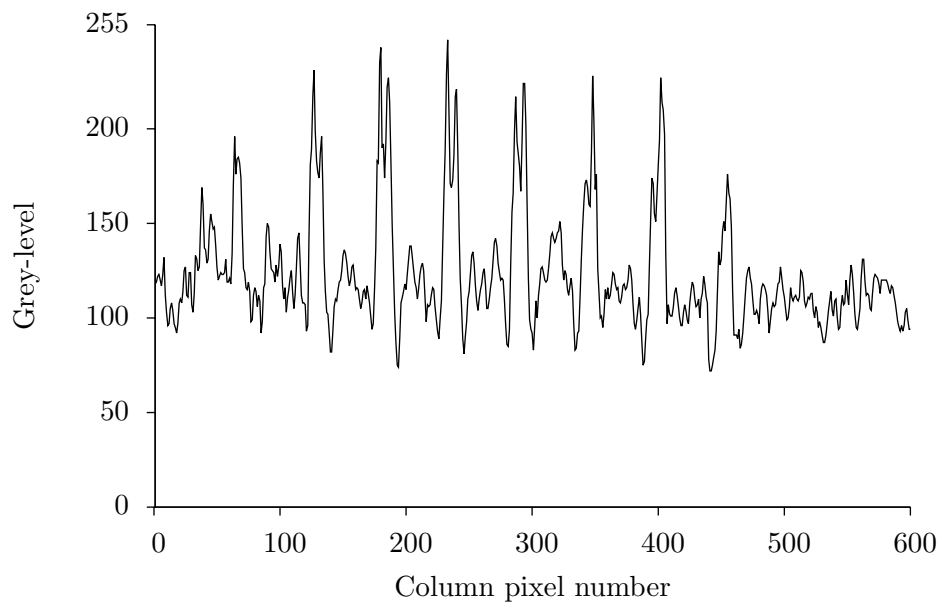
Figure 3.24: Intensity data showing the effect of marking an already rough surface on symbol reflectance – 12 mm matrix – blasted marking surface with 30/40 grit (*Degradation:* none)
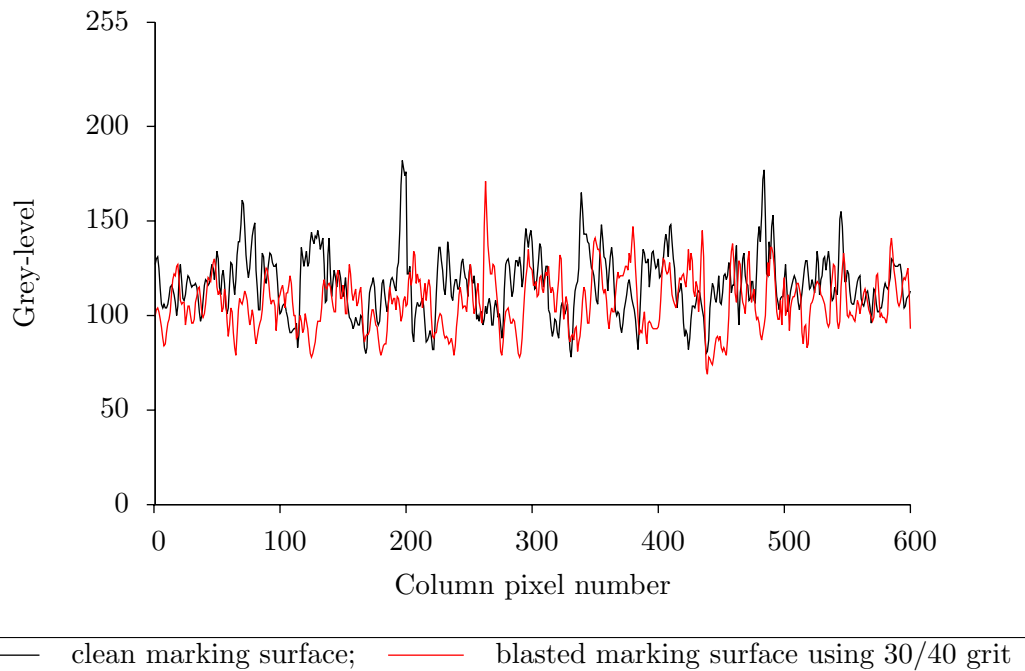
Figure 3.25: Intensity data showing the relative reflectance of two symbols after blasting having been marked on a clean and rough surface respectively – 12 mm matrices – clean and blasted marking surfaces (*Degradation:* shot blasting with 30/40 grit – three passes)

3.5.2.2 Data Matrix codes applied to a rough surface

Given that the manufacturing finish of parts can vary, in terms of roughness (e.g. casting versus machining), some plates had their surface shot blasted prior to the Data Matrix codes being applied. Legibility of these codes did not suffer significantly – all could be scanned successfully barring two out of three of the smallest 4 mm symbols applied to the plate that had been blasted with the coarser 30/40 grit (this gave rise to a surface roughness of $\sim$ 4 R_a). The data discussed previously shows that increasing surface roughness has a detrimental effect on symbol legibility. This situation is subtly different in that the codes have been applied to an already rough surface. Dot peen was used for marking, which involves forcing a stylus into the plate surface to leave an indentation. This application of pressure means that the surface within each dot has been compressed, reducing its roughness and so improving its reflective qualities compared to when shot blasting has been applied after marking. This is born out in the grey level profiles where distinct peaks still exist in relation to the dots of the upper clock track – see figure 3.24 for an example. There is increased noise in relation to the plain surface, but it is sufficiently minimal to not interfere with the read performance.

Subsequent shot blasting of the codes that were applied to a rough surface show the same reduction in legibility as do the codes applied to a clean surface. With the finer grit the scanning results were comparable to the initially clean plates; if anything they were actually slightly improved. For the coarser grit size, in some instances, less of the symbols remained legible. Because roughness was not varying with increasing exposure to shot

blasting, then one could reasonably expect the results to be comparable between those plates that had their codes applied to a clean surface against those when it was rough. Some deviation does exist, but not consistently so. At least part of the reason for this will likely lie with the blasting being a manual process. Figure 3.25 compares two grey level profiles to illustrate the similarity in reflectance despite having been initially marked on a clean versus a rough surface.

3.5.3 Geometry data

The geometry data is comprised of two elements: surface roughness measurements using a profilometer and three-dimensional data of an individual dot from each matrix. The former is an important parameter regarding reflectance from a metallic surface while the latter is necessary to understand any geometry effects that may be occurring.

Four locations were defined for sampling roughness, two along each axis in the plane of the plate's surface – these are indicated in figure 3.26. Table 3.16 indicates the roughness values measured. It can be seen that the roughness varies with the grit size, but otherwise remains reasonably constant. This is due to the air pressure and distance between the nozzle and plate being kept constant (the distance approximately so as the plate and shot blaster nozzle had to be handled manually).
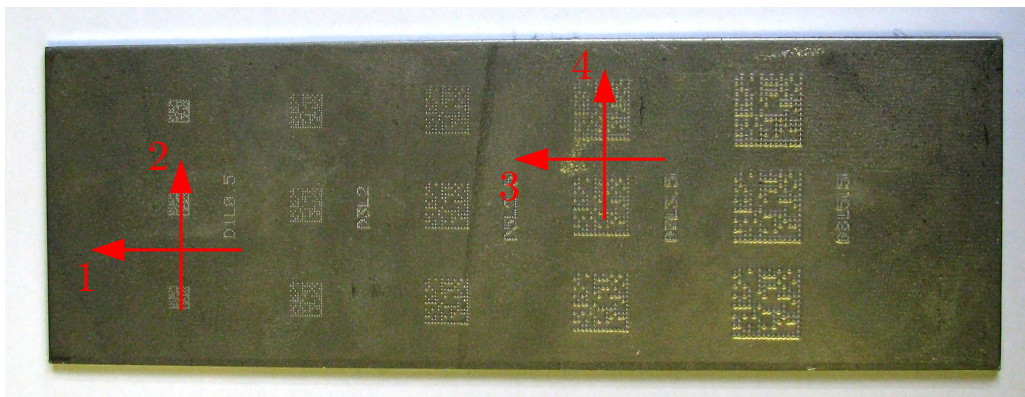
Figure 3.26: Roughness measurement locations

For the two different grit sizes employed, Data Matrix exposure was varied by traversing the nozzle across the surface up to six times. To assess the effect this had on dot geometry, a confocal microscope was used to capture three-dimensional data. The same dot, indicated in figure 3.27, was measured in each matrix. This position was selected as it is near to the centre of each symbol where the marking machine completes the auto-sense step for determining the surface location, and therefore should provide the most consistent measurement point. From the three-dimensional data a cross-section through the approximate centre of the dot was constructed for examining the effects of shot blasting. Figure 3.28 shows the cross-section through a dot for each size of matrix marked (after application to a clean surface).

With regard to material loss, a significant change was not observed. The amount of material removed was largely constant for each grit size and so it was typically the smaller dots that suffered as it represented a more significant proportion of their depth. As

Plate condition		Roughness, R_a (μm)				
		Pos. 1	Pos. 2	Pos. 3	Pos. 4	Avg.
Clean		0.84	0.76	0.88	0.82	0.83
Blasted – 60/80 grit	×1	2.86	3.00	2.52	2.84	2.81
	×2	3.00	2.74	3.00	2.84	2.90
	×3	2.34	2.48	2.78	2.92	2.63
	×4	2.86	2.72	2.64	2.86	2.77
	×5	2.94	2.98	2.72	2.76	2.85
	×6	2.78	2.88	2.60	2.76	2.76
Blasted – 30/40 grit	×1	3.86	4.22	4.48	4.50	4.27
	×2	4.18	3.84	4.12	3.92	4.02
	×3	4.06	4.18	4.32	4.14	4.18
	×4	4.34	4.02	4.68	4.46	4.38
	×5	4.06	4.42	4.52	4.10	4.28
	×6	4.26	4.08	4.40	3.96	4.18
Pre-blasted (60/80 grit)		2.94	2.72	2.80	3.00	2.87
Blasted – 60/80 grit	×1	2.92	3.00	3.10	2.76	2.95
	×2	3.12	2.88	3.06	3.16	3.06
	×3	2.76	2.92	2.72	3.06	2.87
	×4	3.06	2.98	3.16	2.98	3.05
	×5	2.96	2.56	3.06	2.76	2.84
	×6	2.86	2.72	2.96	2.74	2.82
Pre-blasted (30/40 grit)		4.46	3.94	4.56	3.90	4.22
Blasted – 30/40 grit	×1	4.48	4.16	4.14	3.74	4.13
	×2	4.06	3.76	4.44	3.88	4.04
	×3	4.08	4.46	3.86	4.14	4.14
	×4	4.14	3.92	3.86	3.84	3.94
	×5	4.16	3.88	4.36	4.30	4.18
	×6	4.00	4.14	4.14	4.16	4.11

Table 3.16: Surface roughness measurements (*c.f.* figure 3.26)
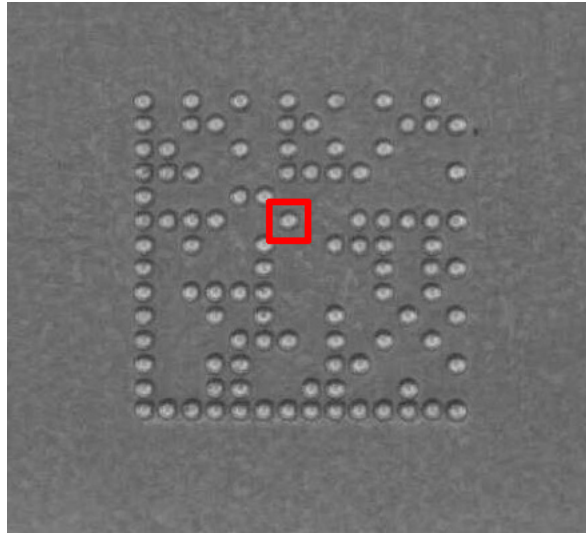
Figure 3.27: Position of the dot measured in each matrix using a confocal microscope

expected, the samples blasted with the coarser grit showed greater material loss occurring – see figure 3.29. What can be observed is that the shape of the dot becomes less distinct, specifically the rim becomes more rounded. This has the effect of causing the transition from plain surface to dot to become less distinct in the image captured by the scanner. Exacerbating this issue is the increased roughness of the surface, which can be seen to introduce noise into the surface profile of the dot. This is interesting because the profiles show how this noise has a far greater effect on smaller rather than larger dots in terms of disguising the underlying shape. Because the surface roughness remains approximately constant for each grit size, the added noise introduced will essentially have a fixed magnitude. Therefore as dot size increases the signal-to-noise ratio reduces. This behaviour is illustrated by figure 3.30 and figure 3.31.

The rounding of the dot lip and the noise added to the surface profile through increased roughness are both contributing factors to the changes in the grey level profiles discussed in section 3.5.2. These changes are evidenced, in part, by a less distinct transition in the corresponding grey level profile from surface to dot. The increased noise/roughness of the surface profile manifests itself as increased noise in the grey level profile too as the increase in diffuse reflection causes a more irregular pattern of light to be received by the scanner's CCD sensor. Further, the reduction in signal-to-noise ratio observed as dot size increases corroborates the assertion in such standards as SAE AS9132 [57] that the relative scale between dot size (such as diameter) and surface roughness is important in determining symbol legibility.

The measurements obtained using the confocal microscope indicate that the profile of the dots after the oxide has grown remains similar (see figure 3.32 for an example). This is commensurate with the scanning results in the sense that it adds weight to the assertion that the oxide and its effect on surface reflectance is sufficient to cause read failure, irrespective of dot size.
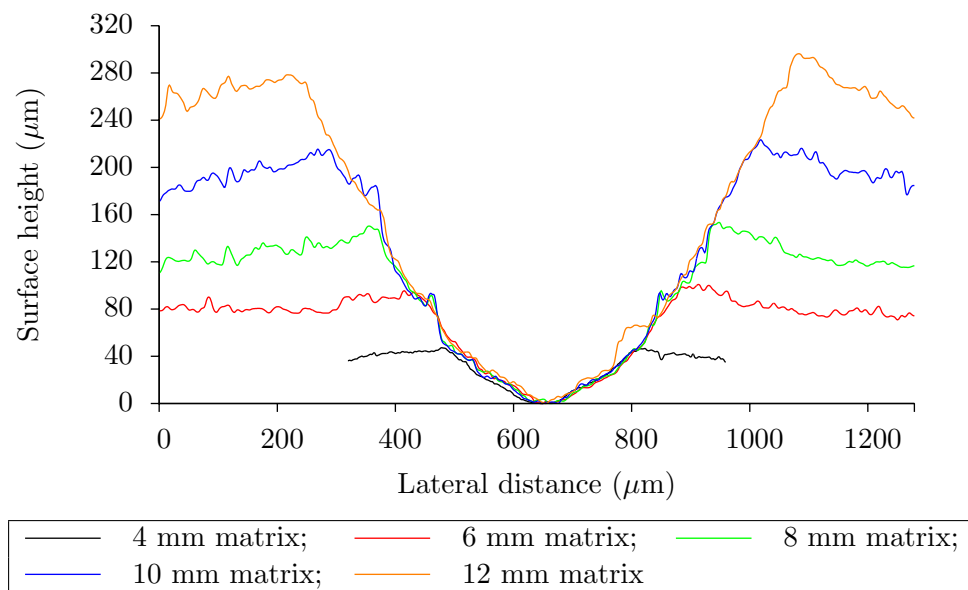
Figure 3.28: Dot profile data – clean marking surface (*Degradation:* none)
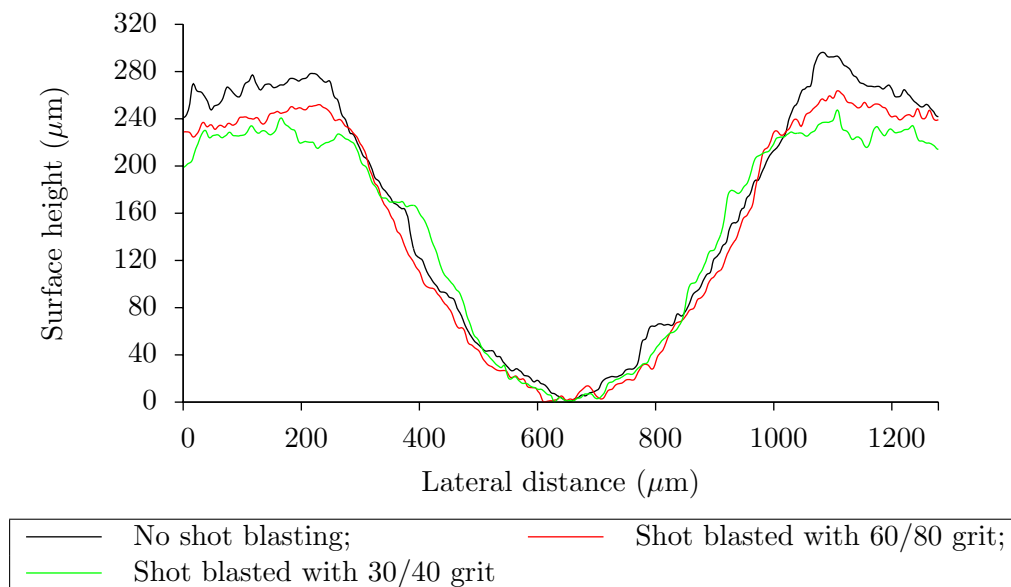
Figure 3.29: Dot profile data showing the variation in material loss for different grit sizes – 12 mm matrices – clean marking surface (*Degradation:* shot blasting with 60/80 or 30/40 grit – five passes)
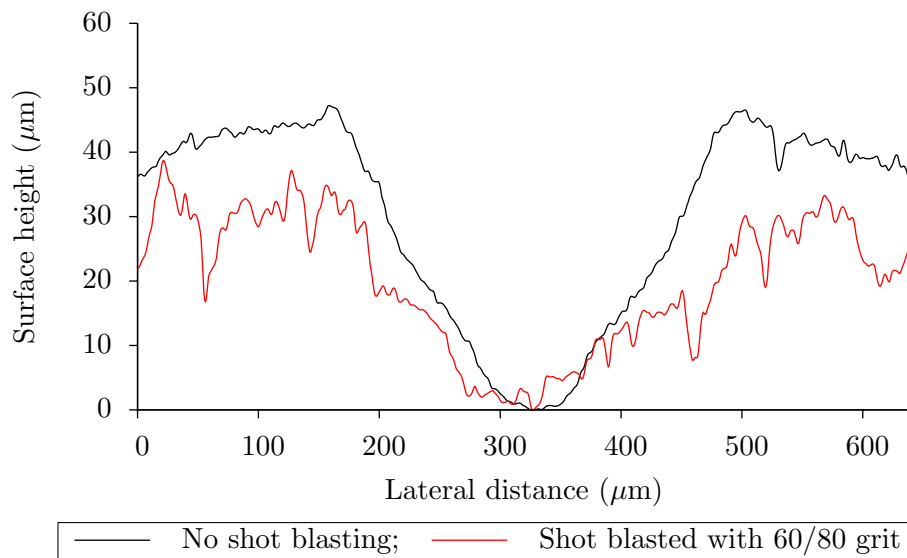
Figure 3.30: Dot profile data showing the relative impact of increased roughness for smaller matrices – 4 mm matrices – clean marking surface (*Degradation:* shot blasting with 60/80 grit – five passes)
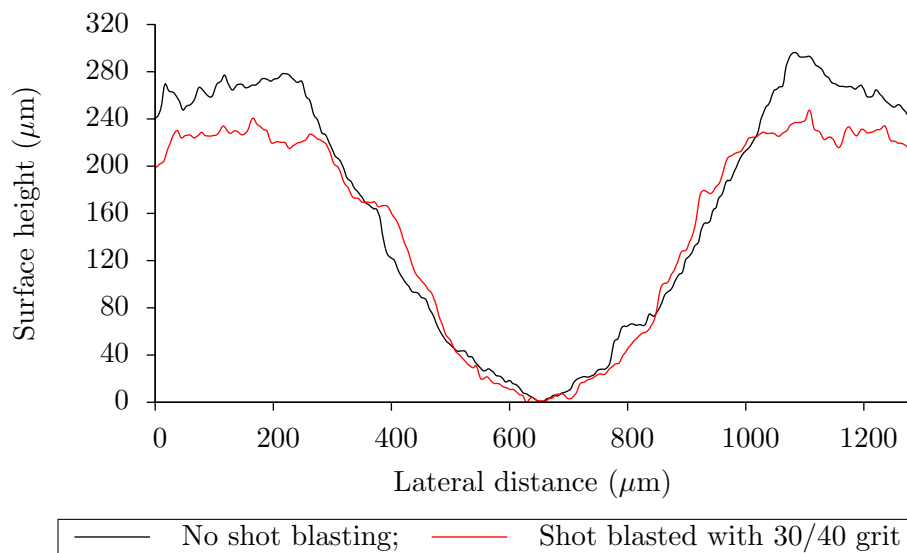
Figure 3.31: Dot profile data showing the relative impact of increased roughness for larger matrices – 12 mm matrices – clean marking surface (*Degradation:* shot blasting with 30/40 grit – five passes)
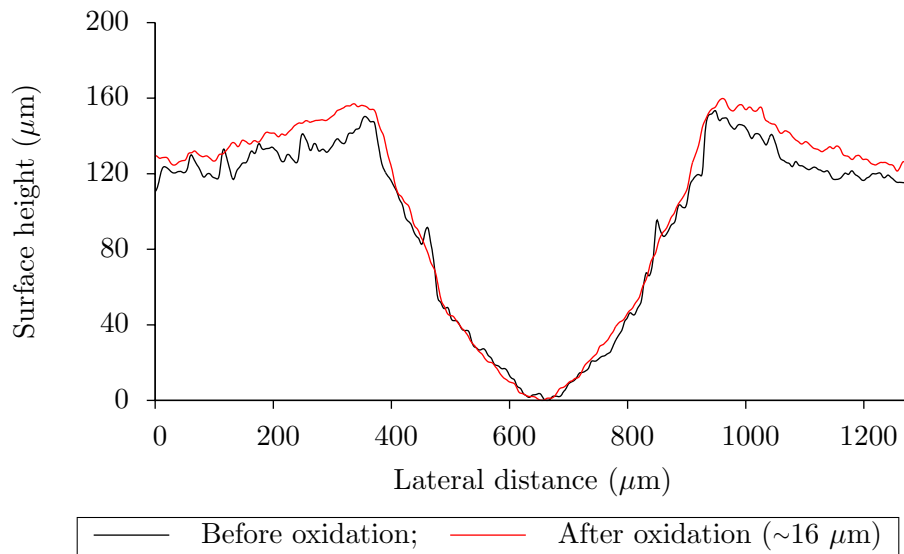
Figure 3.32: Dot profile data before and after oxidation – 8 mm matrix – clean marking surface (*Degradation:* oxidation)

3.5.4 Section conclusion

Section 3.5.2 included both the presentation and discussion of results from the Data Matrix tests. Consequently, only a summary of the key points is presented here:

- Those symbols applied to a clean surface, with no degradation applied, were all readable. Specular reflection dominates in this situation, which helps the dots of the matrix to direct more of the incident illumination back towards the scanner's sensor compared to the plain surface (the majority of the incident illumination is at a glancing angle to the plate).

  - Shot blasting samples that have been applied to a clean surface reduces their legibility. The increase in surface roughness causes the incident illumination to scatter more upon reflection from the surface – this increased randomness is true for both the dots and plain surface, meaning that they become less distinct in the captured image (i.e. the symbol contrast reduces). The coarser grit caused more read failures. The larger matrices were more resilient to increased surface roughness, suggesting that the scale of the roughness relative to the dot size is important with respect to legibility.
  - Of the plates that were oxidised, the tint caused no ill effect in terms of legibility. The 4 μm samples remained largely readable as the oxide had not developed consistently across the surface, enabling the incident illumination to continue to reflect via the bare metal in places. However, the two thickest oxide layers caused a severe reduction in symbol legibility – a combination of increased absorption due to the dark colour of the oxide and diffuse reflection caused the symbol contrast to reduce significantly. In this case, the larger matrices seemed to offer no mitigation against the effects of the surface degradation.

- Some plates were shot blasted prior to being marked so that the surface was already

rough. Initially, the impact on legibility was negligible as the compression of the surface at each dot served to smooth it, thereby improving its reflectivity (more specular than diffuse). However, further blasting of these samples produced results comparable to the case where the surface was clean prior to marking.

- The material loss observed after shot blasting was typically modest. The confocal microscope data showed that those samples which had received more blasting were losing most of their material at the rim of the dot, serving to make the transition from plain surface to dot appear less distinct. Further, it was clear that the scale of the roughness versus the dot size is significant. After blasting, the dot profile is less evident in the smaller rather than the larger dots (i.e. the signal-to-noise ratio improves with dot size for a given surface roughness).

- Those samples that were oxidised have a dot profile that remains similar to the clean condition. This suggests that the oxide alone is responsible for the read failures through alteration of the surface reflectance – this is in agreement with the scanning data.

Deposition was not investigated directly. This was because a method to apply a deposit consistently to the surface of the samples was not readily available. However, this is not meant to suggest that deposition is not important. Some conclusions can be drawn based on the definitions for marking a Data Matrix symbol. For example, the SAE standard AS9132 [57] indicates that dot diameter at the surface should not be less than 60% of the nominal module size. This relates simply to the fact that for any diameter smaller than this the scanner would be mistaken into assuming the matrix is twice the resolution it actually is, leading to a read failure as it will interpret the spaces as missing dots (such as in the finder pattern). This would be one example of inferring a limit to deposition. This does not, however, give any regard to the reflective properties of the deposit. This will be important, and some of the likely issues can be inferred from the presented test data because it is probable that any deposit encountered will affect the roughness and colour of the surface in some way. The oxidation data is a good example of how a non-metallic deposit will affect symbol legibility. The surface is significantly darkened and diffuse reflection dominates meaning that symbol contrast is severely reduced despite little change to dot size and shape. This is, of course, conjecture on the part of the author. Further tests would be necessary to confirm or reject these statements. Further, such tests should investigate not only cases where a consistent layer of deposit is applied, but also where the dots are partially filled to see if this has a significant effect on legibility.

Chapter 4

Risk Matrix System

The main contribution of this thesis has been to develop the cause and effect relationship that exists between degradation of a Data Matrix and its subsequent legibility to a scanner. This theory serves as the basis for developing the framework for a tool – referred to as a Risk Matrix System – intended to help characterise the condition of Data Matrix codes after exposure to degradation mechanisms such as deposition, erosion and corrosion. This chapter presents the phases of development of said tool.

Typical FMEA analysis – see section 2.6 – has been considered as a means to assess damage to Data Matrix codes. However, FMEA requires the rating of potential failure modes and to do so accurately requires a detailed understanding of the topic at hand and/or an extensive database of information with respect to the failure mechanisms under review. Neither of these requirements can be fully satisfied at present. Instead, the Risk Matrix System has been developed progressively as our understanding of the issues at hand has increased. That is not to say the tool presented later in section 4.3 is complete, but rather demonstrates a method by which Alstom may, if they choose, use to better estimate the life of machine readable codes marked directly on engine parts. The following sections present the three main phases of development.

4.1   Potential Failure Modes

Early in the project, the main aim was to develop a better understanding of the mechanisms affecting symbol legibility. To this end, possible sources of read failure were identified by the author, but stopped short of rating their severity due to a lack of quantitative data with respect to their effects. A structured approach to identifying and analysing the parameters relevant to code legibility was utilised because it would help to ensure robustness of the causal relationship presented in section 3.4, and in turn aid development of the Risk Matrix System.

Symbol legibility was assessed from two perspectives, that of marking and scanning (see table 4.1 and table 4.2 respectively). For each of these, relevant parameters were identified that may have an impact on the ability to successfully scan a Data Matrix. Each parameter was broken down further to identify specific issues related to it, and possible root causes identified. A summary of the information presented in these two tables follows.

Parameter	Issue(s)	Root cause(s)
Dot shape	Oversized – dots impinge into adjacent modules	1. Excessive force used during marking process 2. Incorrect stylus angle
	Undersized – adequate cell fill is not achieved (minimum of 60% required)	1. Insufficient force used during marking process 2. Incorrect stylus angle 3. Degradation may cause a reduction in dot size (e.g. removing material through erosion or filling through deposition)
	Distorted – incorrect dot shape	1. Stylus tip may be damaged 2. Degradation may cause distortion of the matrix's dots
Dot position	Dots are not correctly aligned within the matrix	1. Part not secured correctly during the marking process 2. Excessive play in the dot peen machine guide mechanism
Dot geometry	Dot shape is ineffective for trapping and reflecting light	1. Inappropriate marking force 2. Degradation may cause a reduction in dot size (e.g. removing material through erosion or filling through deposition)
Surface finish	Surface is too rough for the selected dot size	1. Dot size inappropriate for the manufacturing finish 2. Degradation through service may increase surface roughness beyond acceptable limits
	Highly reflective surfaces can cause glare (thereby obscuring the matrix)	1. Design may require a high gloss finish to the part (with no possibility of locating the symbol elsewhere on the part) 2. Processes not employed to reduce surface gloss in the vicinity of the code (e.g. shot blasting)
Surface colour	Dark colours reduce image contrast due to increased light absorption	1. Design may require a dark finish to the part 2. Degradation, such as deposition or corrosion may lead changes in surface colour

Table 4.1: Failure mode analysis from the marking perspective

Table 4.1

The parameters identified in this table all relate to symbol legibility, and encompass two main issues: Data Matrix marking specifications (e.g. dot size) and surface reflectance (e.g. surface roughness).

Dot shape is relevant to ensure that modules are identified correctly as 'on' or 'off' – particularly with respect to the finder pattern of a Data Matrix as if this is illegible then the decode process cannot continue. Dot position is a related issue as Data Matrix codes are based on a uniformly arranged grid of modules. Excessive misalignment, such as skew, will further prevent successful decoding. Dot geometry was identified as a possible issue because, in the case of marking metallic surfaces via dot peen, it is this property in relation to the incident lighting that generates the required contrast in the image captured by the scanning device (there is no surface colouring to aid legibility). Surface finish is also an important factor with respect to symbol legibility. Surface roughness, for example, can have a detrimental effect if the scale of the dots is too similar. Equally, it can be beneficial, in moderation, in the case of highly polished surfaces by reducing image glare that would otherwise hamper the scanning process. In such cases, roughening the surface in the area of the symbol, prior to marking, can provide benefits to symbol legibility. Finally, surface colour has been highlighted due to the manner in which it can affect the light reflected from a surface. Dark colours imply a surface is reflecting less light than a lightly coloured equivalent, which can reduce the contrast of the symbol. This situation is quite likely to occur as a result of damage mechanisms such as thermal oxidation.

Table 4.2

The parameters identified in this table relate to the decoding process, including image capture.

The issues categorised under the parameter "Data Matrix" relate to the decoding process. Every Data Matrix includes a finder pattern, comprised of two main features: an 'L' boundary and clock track. These are essential to the decode process – they signify important information such as location, size and data capacity – and are identified prior to attempting to decode the data region itself. If these features cannot be identified correctly then the decode process will fail. The CCD sensor of the scanner is a key part of the image capture process. It is important that it has sufficient resolution and sensitivity so as to not hamper this process. Maximising image quality will help to reduce the burden on the decoding process as there is a limit to how much correction pre-processing can achieve. The light source used and image focus are both important in this regard. For bare metals, suitable lighting is essential for generating contrast between the symbol and plain surface. Some scanners offer an adjustable lighting system so that they are better able to cope with various surface finishes. Achieving an in-focus image will aid clarity, but typically scanners have a fixed focal length that will dictate the distance at which it should be held from the symbol. Issues can occur if there are obstructions preventing adherence to the focal distance; this may be particularly relevant if one wishes to scan parts in situ.

Parameter	Issue(s)	Root cause(s)
Data Matrix	Can't detect 'L' boundary of finder pattern	1. Poor image capture 2. Vision of code obstructed 3. Physical degradation to code
	Can't detect clock track of finder pattern	1. Poor image capture 2. Vision of code obstructed 3. Physical degradation to code
	Can't decode data region	1. Poor image capture 2. Vision of code obstructed 3. Physical degradation to code
CCD (of scanner)	Poor image clarity	1. Insufficient resolution 2. Poor dynamic range (preventing differentiation between regions of similar light levels) 3. Focal distance not respected (leading to a blurred image)
	Insufficient sensitivity	1. Poor dynamic range 2. Excessive noise levels
Scanner	Poor light source	1. Not strong enough to generate sufficient contrast between the dots of the matrix and the surrounding surface 2. Not suitable for the given surface finish (e.g. no diffuse light source for high gloss surfaces)
	Focal distance – typically fixed – is not respected	1. Physical obstructions may prevent optimal positioning of the scanner relative to the code 2. Operator error

Table 4.2: Failure mode analysis from the scanning perspective

4.2   Ranking Failures

In addition to the analysis summarised in section 3.3, Faivre [27] looked to develop the author's failure mode analysis discussed in the preceding section. This was based on a report by Alstom [7] that presents data regarding the ability to read Data Matrix symbols after exposure to a number of different reconditioning processes (particularly those that are most aggressive). Faivre [27] took Alstom's work a step further by introducing an FMEA-esque system of ranking the observed damage to highlight severity, and the consequent effect on code legibility. This was achieved in cooperation with the author to ensure a positive outcome for both parties and enable the bilateral exchange of ideas and knowledge. A summary of the analysis completed by Faivre [27] follows.

4.2.1   Reconditioning processes

The reconditioning chain that engine parts are processed through is comprised of three main stages:

A. Incoming inspection
B. Cleaning of parts and detailed inspection
C. Repair and final inspection

For the incoming inspection parts are received directly from the field and visually assessed for damage. Those deemed too severely damaged for repair are scrapped. For the remaining parts the overall repair cost is estimated and the parts logged (in this case by scanning the Data Matrix code). The next stage involves cleaning the parts in order to remove surface contamination, such as deposition, erosion or corrosion, and any coatings applied previously (note that all parts are not exposed to all cleaning processes). These cleaning processes include:

- Sandblasting
- Alumina blasting
- Ultra-sonic salt bath cleaning and drying
- Chemical etching
- Chemical stripping
- Vacuum heat treatment

Once a part has been cleaned, its surface is then inspected for the presence of cracks. As not all cracks will be visible to the naked eye, a process called fluorescent penetrate inspection (FPI) is used. This involves soaking parts in a dye, called the penetrate, which is then washed from the surface and then a powder applied. The combination of penetrate and powder left in the cracks reveals them to the naked eye when the part is exposed to a UV light. Following inspection, repair processes are employed to restore the condition of parts so that they may see further service (note that all parts are not exposed to all repair processes). These repair processes include:

- Grinding
- Welding
- Electro-discharge (for cleaning cooling paths)
- Brazing
- Re-application of coatings

- Air and water flow tests
- Fluoride ion cleaning (FIC)
- Shot peening
- Balancing
- Frequency testing

Having reviewed the reconditioning processes that parts are exposed to, Faivre [27] identified the prevalent degradation mechanism applicable to each process – see table 4.3 for a summary.

Degradation mechanism	Reconditioning processes			
Erosion	Alumina blasting	Sandblasting		
Abrasion	Grinding	Trovalization		
Corrosion	Chemical etching	Chemical stripping	Salt bath	Fluoride ion cleaning
Depostion	Welding	Brazing	Coatings	
Plastic deformation	Shot peening			
Crack opening	Vacuum heat treatment			
None	Air and water flow tests	Electro-discharge	Balancing	Frequency testing

Table 4.3: Summary of reconditioning processes and their associated degradation mechanisms [27]

4.2.2 Severity scales

Faivre [27] sought to introduce a system of scales to rate the severity of the damage occurring; focusing on those parameters that would impact the reflection of light from the part's surface. This is so that the impact of surface damage can be more readily compared between Data Matrix symbols. The parameters he utilised were: dot diameter, dot depth, surface roughness and surface colour. This stage of the development process introduced a system similar to that seen in FMEA whereby the relative severity of different effects can be identified through the application of a scale (see table 4.4 for an example). In doing so, Faivre [27] differentiated between the severity of the degradation itself and the consequent effect on code legibility. This is a useful distinction to make because each of the degradation mechanisms will act differently upon the surface – meaning a universal scale would be difficult to define. However, as they all ultimately impact surface reflectivity, a common scale for indicating code legibility is not an unreasonable suggestion and enables the ultimate effect of each mechanism to be more readily compared.

Having defined scales for indicating the severity of damage present, Faivre [27] then sought to assess the effect each of the reconditioning processes has on Data Matrix symbols applied

Severity scale number	Module fill (%)
4	< 60
3	67.5–60
2	75–67.5
1	82.5–75
0	90^*–82.5

* Limit corresponds to module fill when symbol was marked

Table 4.4: Dot size severity scale – an example assuming an initial module fill of 90% [27]

via dot peen marking. Based on his findings he then proposed which processes presented the most potential for severely reducing legibility of the Data Matrix symbol. Those processes are highlighted in red in table 4.5.

Degradation mechanism	Reconditioning processes			
Erosion	**Alumina blasting**	Sandblasting		
Abrasion	**Grinding**	Trovalization		
Corrosion	Chemical etching	Chemical stripping	Salt bath	Fluoride ion cleaning
Depostion	**Welding**	**Brazing**	**Coatings**	
Plastic deformation	Shot peening			
Crack opening	Vacuum heat treatment			
None	Air and water flow tests	Electro-discharge	Balancing	Frequency testing

Table 4.5: Summary indicating the most severely damaging reconditioning processes [27]

The analysis by Faivre [27] of the damage caused by the reconditioning processes was limited to comparing photographs of the codes before and after having been exposed to each process. It was necessary to estimate from these, changes in the parameters identified for characterising Data Matrix symbol degradation. As such he was only able to highlight possible trends without being able to confirm his conclusions with empirical data. One such analysis is shown in table 4.6.

Process	Degradation mechanism	Effect on marking	Severity	Effect on scannability	Observations
Alumina blasting		Dot diameter	Decreases	4^*	1	* After 1 run. Brittle material. Nozzle perpendicular to surface.
		Dot depth	Decreases	4^*	2	* After 1 run. Brittle material. Nozzle perpendicular to surface.
	Erosion	**Surface roughness – plane surface**	Increases up to limit	0–3	3 or 4	Limit mainly depends on grain size (3–6 R_a).
		Surface roughness – dot	Increases up to limit	0–3	3 or 4	Limit mainly depends on grain size (3–6 R_a).
		Surface colour – plane surface	Metal colour restored	–	**	** Depends on colour prior to blasting.
		Surface colour – dot	Metal colour restored	–	**	** Depends on colour prior to blasting.

Table 4.6: Risk matrix example – estimation of damage to Data Matrix symbols by alumina blasting [27]

4.3   A Framework

In this section the author discusses how the ranking system of Faivre [27] may be extended to provide a complete solution for assessing symbol durability through the life of a part – dubbed a "Risk Matrix System". In doing so, three main questions will be answered:

- What is the purpose of such a tool?;
- Why would one want it?; and
- How can one realise it?

What

The proposed Risk Matrix System would provide Alstom a means to anticipate the degradation expected to befall Data Matrix symbols applied to their engine parts and therefore the likelihood of them remaining legible. This would be achieved by identifying scales of severity with respect to parameters relevant to symbol legibility – such as surface roughness – in tandem with the rate at which such parameters degrade through the life of the part. The latter should preferably be defined in a manner that is constructive to the end user, such as equivalent operating hours (EOH).

Why

Currently engine parts typically have a number of human readable alphanumeric codes applied to them starting from initial production and continuing through their useful life. In the future, it would be possible to replace these various codes with a single Data Matrix that contains a unique serial number. All other pertinent information about the part could then be recorded and stored in a database, accessible by this unique identifier. If no human readable identifiers are to remain on the parts then maintaining Data Matrix legibility is key to achieving such a system. Development of the proposed tool will help to reduce the guesswork involved in applying codes to parts and hence improve the implementation of the part tracking system as a whole.

Implementing a framework that incorporates an FMEA-esque rating system helps to make the tool more easily accessible to staff who may otherwise be insufficiently familiar to understand the significance of the parameters alone. As such, this requires that the scales defined to indicate the severity and rate at which degradation occurs are sufficiently robust to allow their use by non-experts.

How

The risk matrices drafted by Faivre [27] – see figure 4.6 for an example – serve as a good starting point from which a more expansive and robust system can be developed. The two main shortcomings of these are that they only account for reconditioning processes (engine operation can have a profound effect on symbol legibility) and the scales were defined in a rather arbitrary manner, largely due to a lack of data. Including the effects of engine operation opens up a number of additional factors that may contribute to the degradation imparted onto Data Matrix codes applied to engine parts. Some of the more pertinent issues include:

Engine duty cycle
    The manner in which the engine is operated will affect the conditions that parts

are exposed to, mainly in the form of varying temperatures and pressures. The operation of power plants is changing due to the growing use of renewable energy sources. The latter are not typically able to provide a constant output, such as wind energy, and as such gas turbines that may have otherwise been run continuously for base-load generation are more often being operated at part-load, only being turned up to compensate for supply shortages and peak demands as they occur.

Atmospheric conditions

The local atmospheric conditions will affect the degradation of internal components, particularly with respect to the main gas path. Filtration systems that are in place will not be able to prevent all of the particulate matter present in the atmosphere, such as sand or salt, from entering the engine. These particles won't be confined to the main gas path, but will also be entrained into secondary cooling flows and therefore may impinge upon Data Matrix symbols applied to blade roots, for example, causing erosive damage. Contaminants such as salts can also cause corrosive damage in combination with high temperatures.

Fuel type

The cleanliness of the fuel will dictate the extent to which particulates are released during the combustion process. These particulates may then subsequently deposit on downstream surfaces, discolouring them in the process. Depending on the extent to which this occurs, symbol legibility can be adversely affected. Fuels such as natural gas offer a relatively clean burn in terms of particulates, whilst at the other end of the spectrum we find heavy fuel oils that can leave substantial, darkly coloured, deposits on engine parts. The main gas path components are of course most susceptible to this, but areas such as the hub region are not completely impervious to penetration by the main gas path (particularly so in extreme cases where sealing components fail).

Pressures and temperatures

The pressures and temperatures engine components are exposed to will depend upon the engine's design point and the manner in which it is operated (i.e. its duty cycle). These will in turn affect degradation processes that may be occurring. For example, pressure gradients will affect the velocity of suspended particles and hence the rate it which erosion may occur, whilst temperatures can impact the rate of corrosion.

Of course the issues noted above will not have a consistent effect throughout the engine. The degradation of Data Matrix codes will also depend not just on the location of the part – compressor versus turbine, for example – but also where on the part the symbol is located. The latter can be used to help minimise the worst effects of the degradation that is occurring.

Fundamental to maximising the usefulness of such a tool lies in expanding the knowledge base. Primarily, this will involve recording data with respect to the effect of varying forms and degrees of degradation on the legibility of Data Matrix codes. Means of improving the tool's robustness include:

Test data

Where possible, degradation can be induced in samples to mimic the condition of parts received back from service – in a similar fashion to the test data discussed in section 3.5 of this thesis. A major benefit of this approach is that the legibility of Data Matrix symbols degraded to various degrees can be assessed in a relatively short space of time. However, it may not be possible to accurately mimic all possible surface conditions and it cannot directly inform the rate at which degradation

accumulates without the use of accelerated ageing techniques that can prove costly and complex to implement.

Operational feedback

Applying Data Matrix codes to parts that will be exposed to typical service patterns in customer engines is the best way to understand the conditions codes will be exposed to during their life and the degradation that results. At service intervals the codes can be inspected in terms of symbol characteristics (such as dot diameter) and surface degradation (such as thermal oxidation) as these will correlate with legibility in terms of achieving a successful read with the scanning device. The drawback of this approach is that service intervals are typically measured in years for the industrial engines that Alstom markets and so there will be a lack of rapid feedback; at least initially until a number of engine installations have received marked parts, such as blade sets.

Theory and simulation

Theory pertinent to the legibility of Data Matrix codes has been outlined as part of the literature review of chapter 2. An understanding of these factors can help to identify the issues relevant to maintaining symbol legibility as the surface of a part degrades through its service life. Further, it may be possible to simulate the impact of the degradation mechanisms occurring, such as the loss of material via erosion, to then assess the change in symbol legibility that results. Theory and/or simulation cannot be relied upon alone and should of course be backed up with real data of some form, but it can improve the efficiency of any research initiative by serving to direct resources appropriately.

Tacit knowledge

In any organisation it is difficult, and perhaps not always desirable, to record all knowledge in an explicit manner. It is inevitable that some knowledge will remain tacit in nature, typically realised in the experience employees gain in the use of systems and processes. Implementing a tool such as the Risk Matrix System discussed here will no doubt benefit from the experience gained by users who are then able to feedback their knowledge in order to improve the process. This may become explicit, such as in the form of revised procedures, or remain tacit, such as advising colleagues in the best use of the tool.

Figure 4.1 shows how data held regarding the durability of Data Matrix codes should be updated via a feedback system. Parts can be marked and then, based on current knowledge, the impact of their service conditions estimated using FMEA-esque scales derived to account for severity of the potential degradation mechanisms, the period over which degradation will accumulate and the subsequent effect on symbol legibility. As parts are received back from service the actual condition of the symbol can be compared to that which was estimated before installation and the data repository adjusted where necessary to improve the accuracy of the tool. As noted earlier, other methods of identifying the effects of degradation on symbol legibility can be used to increase the rate of feedback. Fundamentally, the feedback loop is used to infer legibility limits with respect to the effects of degradation and the rate at which the degradation occurs. This information will help to provide more accurate measures of the degradation a symbol will undergo during its service life and hence improve survivability by allowing better choices to be made regarding symbol parameters and marking location, for example.

Severity scales are necessary to indicate the degradation that accumulates through the service life of a Data Matrix symbol. The severity parameters indicated in table 4.6 are perfectly valid in themselves; however they do not necessarily represent measures that
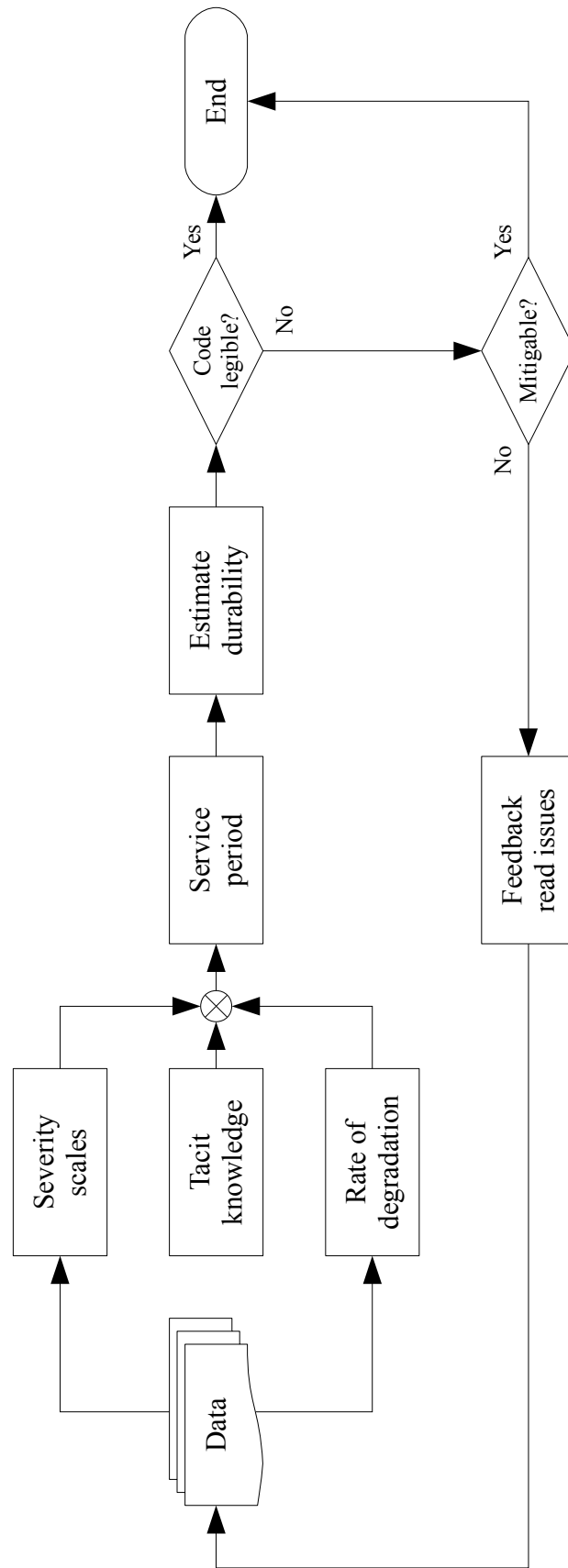
Figure 4.1: Risk matrix system development process

are readily understood by 'experts' and 'non-experts' alike. As the proposed tool would be used by both, it is important to ensure that it does not cause unnecessary confusion. One such way to achieve this is to relate each of the severity scales to a parameter that is conceptually easy to comprehend, such as equivalent operating hours (EOH) – see table 4.7 for an illustrative example. Introducing EOH means that whilst the user applying the tool may not fully comprehend the implications of the degradation that is occurring, they can still see whether it will introduce a read issue. This is achieved by identifying the severity rating and its corresponding EOH value and comparing the latter to the expected lifetime of the part. The final step is to then cross-reference the severity factor against a legibility scale to understand whether the expected damage will prevent the Data Matrix symbol from being read successfully. The accuracy of such a system is of paramount importance, particularly for 'non-experts' who will have to trust that the scales used to assess the risk to Data Matrix legibility are sufficiently robust. As noted previously, this will rely on the productive application of feedback to improve the Risk Matrix System.

Oxide thickness (μm)	Severity scale number	EOH
8	4	32,000
6	3	18,000
4	2	8,000
2	1	2,000
0	0	0

Table 4.7: Oxidation severity scale with corresponding EOH data – *illustrative example only*

The data held regarding the degradation of Data Matrix codes will be necessarily broad. This is due to the effect of various factors on the degradation processes occurring, including (but not limited to): engine type, engine duty cycle, fuel type, part type and installation environment. Whilst it should be possible to define universal severity and legibility scales for each degradation process, the rate at which degradation occurs (the EOH parameter) will vary. This means that for each use of the Risk Matrix System, the scales used to rank the impact of the expected degradation processes should be calibrated to the particular engine's operating parameters. Table 4.8 on page 99, derived by the author, is an illustrative example of a template for recording Data Matrix durability assessments (which may then be reappraised when parts return from service to assess accuracy). As knowledge and experience improves, the process of assessing symbol durability may be streamlined where commonalities are identified. For example, common severity scales for parts that suffer similar degradation, both in type and rate (although care should be taken to assess exposure correctly under such circumstances).

The proposed construction of the Risk Matrix System is essentially a modification of the FMEA process. FMEA utilises three parameters: severity, occurrence and detection (refer to section 2.6). Two of these have been translated directly to the Risk Matrix System here: severity, in the form of degradation parameters that affect symbol legibility; and occurrence, in terms of the EOH parameter that informs the service period required for each value in the severity scale to occur. Detection has been replaced in the Risk Matrix System by the legibility parameter. The former would be difficult to implement as once

parts marked with Data Matrix symbols are installed, the condition of the codes cannot be assessed until the next service cycle (i.e. not until it is too late). Instead, legibility has been utilised to indicate the effect each degradation parameter has in order to infer prior to use the expectation of read failures occurring during service.

4.4 Conclusion

This chapter has presented the development process for a tool – loosely based around FMEA techniques – intended to aid the implementation of a part tracking system that utilises machine readable codes. Whilst originally developed for improving safety, FMEA has since seen broader adoption in tackling issues ranging from product design to marketing, illustrating its versatility. The success of a part tracking system relies on the Data Matrix codes that are applied to engine parts remaining legible through their service life. The Risk Matrix System is intended to help the owner of the part tracking system assess the issues relevant to symbol legibility, such as surface degradation, so that durability can be maximised.

Initially, a simple failure mode analysis was carried out to better understand the issues that hinder symbol legibility. This was assessed from both the marking and scanning perspectives. The former largely focused on symbol quality in terms of both the marking process and the surface finish, whilst the latter looked to the scanning process and hardware. This analysis was used as a starting point by Faivre [27] to begin development of the risk matrix tool itself, under supervision of the author. This was limited in scope, focusing only on the reconditioning processes that engine parts may be exposed to, and accuracy was lacking due to much of the assessment being qualitative in nature. Nonetheless, the outcome illustrated well the intended concept of a tool to assess the impact of surface degradation on symbol legibility.

The final component presented summarises how one might develop the approach of Faivre [27] into a complete tool that can, importantly, account for the entire service period of a part and the symbol degradation that may result. Key to this is the introduction of the EOH parameter that serves to indicate the rate at which degradation occurs, which is important to understand whether it will accumulate to a critical level within the life of the part. Further, for each severity scale there is a matching one for legibility to indicate its effect on the ability to read the code. However, defining the severity, EOH and legibility scales accurately is a significant undertaking and so a feedback process has been proposed that will help to improve this aspect of the tool as experience grows. It has been noted that feedback for improvement can, in fact, come from a number of sources, both practical and theoretical. Further, as the tool becomes more familiar to its users, tacit knowledge will help to improve effectiveness, which may then be further spread through the organisation by explicit means, such as instructional documentation.

The Risk Matrix System is largely an empirical tool and as such relies on data and experience for accuracy. However, if it is accepted that time will be required for full maturation, then ultimately it could prove an excellent way of maximising the overall effectiveness of gas turbine part tracking.

Engine model: _____   Part (#): _____

Fuel type: _____   Part condition: New/reconditioned

Engine application: _____

Component: _____

Degradation mechanism	Dominant effect	Severity	EOH	Symbol legibility	Additional notes
For example: erosion	For example: change in surface roughness	scale value	value	scale value	For example: degradation source (such as service or reconditioning), damage mitigation strategies, assumptions, etc.
...	...	...	...	...	...

Table 4.8: Risk matrix system template – *illustrative example only*

Chapter 5

Knowledge Transfer

A cornerstone of the EngD programme is to address managerial issues in addition to the technical analysis such research projects require. This chapter presents the work undertaken to satisfy this requirement – the topic selected for study being knowledge transfer.

Firstly, a brief review of relevant literature is presented, followed by a summary of the product development quality (PDQ) process currently in use by Alstom. Additional requirements are then proposed for the PDQ process that would enable Alstom to harness knowledge transfer more effectively in developing new products, services and technologies.

5.1   Literature

Fender [29, pp. 15–25] highlights innovation as often being incorrectly considered a panacea. He argues that innovation is, in fact, a process built upon a base of knowledge requiring specific skills to address a particular problem. He goes on to identify the importance of knowledge transfer in innovation by saying that creativity, whilst essential to innovation, does not itself necessarily lead to a benefit, rather the role of knowledge transfer is to enable the outcomes of an innovative process to bring about commercial or societal benefits. Further, the application of knowledge transfer is not confined to new innovations, but is equally applicable to the process of exploiting existing innovations from one field to another.

Fender [29] points to the realisation that successful knowledge transfer depends upon the quality of personal interactions, which has led to a growth in the number of practitioners specialising in the field of knowledge transfer. In light of this he proposes a set of core competencies important for such practitioners [29]:

- Good communication and interpersonal skills
- Management skills
- Commercial awareness
    - New business development skills
    - Negotiating skills
    - Understanding of IP and licensing
    - Discipline/industry specific knowledge
    - Understanding business (and innovative) model options
- Personal CPD plan

- Personal library and information access strategy or plan
- Personal networking – use of social network skills
- Creation of networks to build collaboration

Gilbert and Cordey-Hayes [30] argue that the importance of knowledge transfer in modern business is due to the climate of constant change that has become the norm and that an ability to take advantage of this change has become an essential part of organisational development. There is no single definition for a learning organisation, but Gilbert and Cordey-Hayes [30] suggest there is a commonality in that an organisation "must be adaptive and be able to respond to both the internal and external environment, and it must be open and able to communicate." They present a five-stage model (see figure 5.1) that identifies the processes of knowledge transfer within an organisation, such that the knowledge becomes part of its core routines (i.e. assimilation, or learning, has occurred successfully).
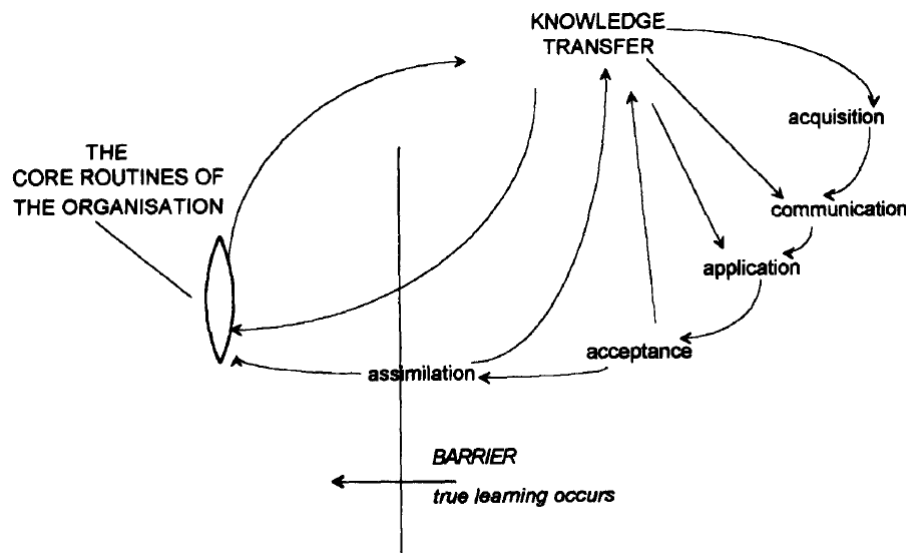
Figure 5.1: The five-stage model [30]

A brief description of the five stages [30]:

Acquisition Before it can be transferred, knowledge must be acquired. An organisation may learn from its past, by doing, by 'borrowing', by acquiring individuals with new knowledge or by a continuous process of searching/scanning. A major influence is 'congenital learning' whereby an organisation is profoundly influenced by its founders and that this prior knowledge held at birth will influence how it moves forward.

Communication Communication of knowledge may be written or verbal. Organisations should be aware of the possible barriers to the dissemination of information in order to encourage knowledge transfer.

Application In order to retain knowledge it must be applied. It is the application of knowledge that enables an organisation to learn, rather than the knowledge itself.

Acceptance Once knowledge has been applied, it must be found to be acceptable to the individuals of an organisation – a necessary step prior to assimilation.

Assimilation Key to the process of knowledge transfer is assimilation of the results and

effects of applying new knowledge – evidenced by modification of the organisation's core routines accordingly.

There are two fundamental approaches to knowledge management: tacit knowledge versus explicit knowledge. Sanchez [58] presents a comparison of these, stating that the former assumes knowledge is personal in nature and therefore difficult to extract from the minds of individuals, whereas the latter assumes knowledge is something that can be explained by individuals and therefore the useful knowledge in an organisation can be articulated and made explicit.

If one adheres to the tacit knowledge approach then typically the dissemination of knowledge within an organisation is best achieved by the transfer of individuals (or 'knowledge carriers') within the organisation in order to share their knowledge with a broader range of colleagues. However, it is difficult for managers to know what kinds of knowledge individuals hold and as such some organisations have sought to improve the understanding of who knows what within an organisation – so called "know who" knowledge. This can take the form of a contact directory that lists the experts within an organisation along with their respective knowledge areas.

On the other hand, the explicit knowledge approach leads to the belief that formal organisational processes can be used by individuals to articulate their knowledge in the creation of knowledge assets. Explicit knowledge may then be disseminated through an organisation via documents, drawings, operating procedures, or similar. Information systems often play a key role in the dissemination process, a company intranet that allows wide access to knowledge assets, for example.

Clearly the tacit and explicit knowledge approaches have distinctly different natures, with neither being 'right'. Instead, a hybrid design is preferred for knowledge management practice that balances the two approaches appropriately for the situation at hand. Sanchez [58] proposes advantages and disadvantages of the two different approaches to knowledge management – reproduced in table 5.1.

Cohen and Levinthal [23] discuss the role absorptive capacity plays in the process of knowledge transfer. They suggest that the absorptive capacity of an organisation as a whole depends upon the absorptive capacity of its individual members (although not simply a sum). Absorptive capacity is not only concerned with the acquisition or assimilation of information, but also an organisation's ability to exploit it. To understand the sources of a firm's absorptive capacity they focused on the structure of communication between the external environment and organisation, as well as among the subunits of the latter, and also on the character and distribution of expertise.

Cohen and Levinthal [23] considered that a firm's R&D not only generates new knowledge, but also contributes to its absorptive capacity. This suggests that absorptive capacity can be influenced by R&D expenditure. Their model of how absorptive capacity affects the determination of R&D expenditure is shown in figure 5.2. They postulate that learning incentives will have a direct effect on R&D spending. Where the effect of other determinants, such as technological opportunity and appropriability, depend on the firm's or its rivals' assimilation of knowledge, absorptive capacity will mediate those effects. Further, appropriability conditions will be conditioned by competitor interdependence (the extent to which a rival's technical advances diminish the firm's profits).

Cohen and Levinthal [23] suggest there are two factors that will affect a firm's incentives to learn and, therefore, its desire to invest in absorptive capacity via R&D expenditure: *i*) the quantity of knowledge to be assimilated and exploited; and *ii*) the difficulty of learning –

	Advantages	Disadvantages
Tacit knowledge approach	• Relatively inexpensive and easy to begin • Employees may respond well to the recognition of the (claimed) knowledge • Likely to create interest in further knowledge management processes • Important knowledge kept in tacit form may be less likely to 'leak' to competitors	• Individuals may not have the knowledge they claim to have • Knowledge profiles of individuals need frequent updating • Ability to transfer knowledge constrained to moving people, which is costly and limits the reach and speed of knowledge dissemination within the organisation • Organisations may lose key knowledge if key people leave the organisation
Explicit knowledge approach	• Articulated knowledge (explicit knowledge assets) may be moved instantaneously any time any where by information technologies • Codified knowledge may be proactively disseminated to people who can use specific forms of knowledge • Knowledge that has been mad explicit can be discussed, debated and improved • Making knowledge explicit makes it possible to discover knowledge deficiencies in the organisation	• Considerable time and effort may be required to help people articulate their knowledge • Employment relationship with key knowledge workers may have to be redefined to motivate knowledge articulation • Expert committees must be formed to evaluate explicit knowledge assets • Application of explicit knowledge throughout the organisation must be assured by adoption of best practices

Table 5.1: Advantages and disadvantages of the tacit versus explicit knowledge management approaches [58]

some types of information are more difficult to assimilate than others. A firm such as the Alstom Group relies heavily on R&D investment to remain competitive within its sectors of power, transport and grid. Over the 2009/10 period Alstom Group's R&D expenditure totalled €614m (excluding Alstom Grid), which equates to ~ 35 % of their income from operations [4]. To further highlight their reliance on R&D expenditure the 2009/10 figure is approximately double that from just five years ago.
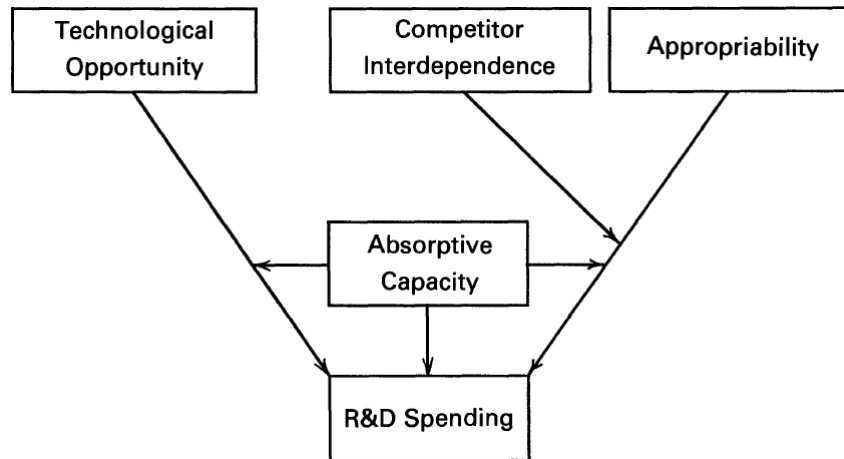
Figure 5.2: Model of absorptive capacity and R&D incentives [23]

5.2   Current Process

Alstom have a product development quality (PDQ) process (see figure 5.3 for a summary) to increase efficiency and ensure high quality of products throughout their life-cycle (from initial development to recycling/disposal). Maximising quality helps to minimise total life-cycle costs, which leads to satisfied customers (be they internal or external).

Alstom state the following major targets with respect to their PDQ process [3]:

- Global standardisation of R&D process with gate reviews
- Standardised interfaces towards interfacing processes
- Transparent tracking of R&D projects worldwide
- Increased quality of process outputs
- Reduction of cost of poor quality (COPQ) caused during the R&D process

The PDQ process is applied to all R&D projects globally. Projects are required to be planned, budgeted and scheduled over the entirety of its duration, with project planning frozen at the point of approval of the project proposal. Gate reviews and assessments are planned and tracked via internal information systems that enable all participants to follow the progress of the project, such as the status of corrective actions. As part of standardising the product development process, common templates and check lists are used.

The PDQ process is not a pure R&D tool; emphasis is placed on other relevant interfaces throughout the product development process. These may include:

- Business planning to ensure a viable business case is maintained
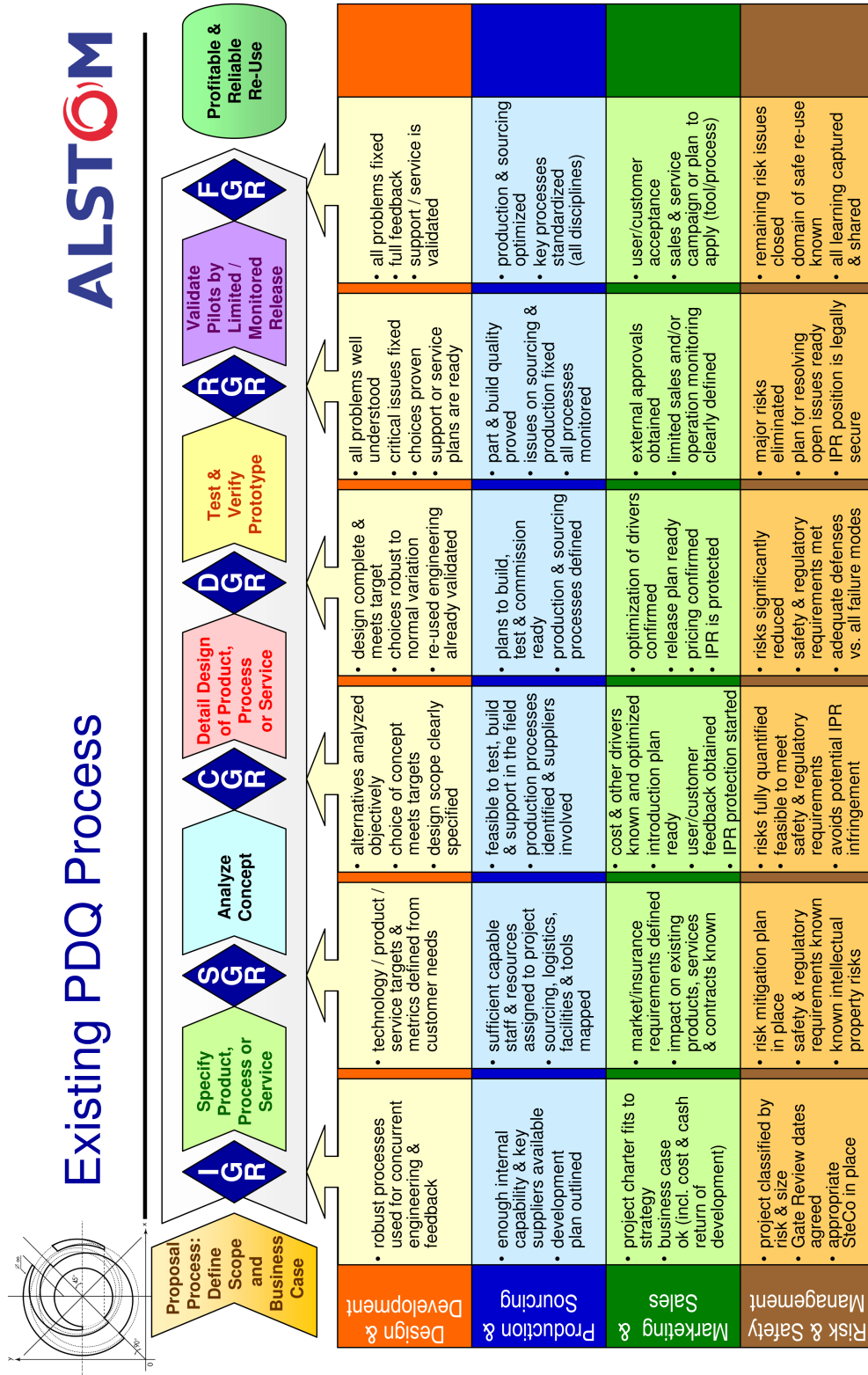
Figure 5.3: Alstom PDQ process [3]

- Monitoring intellectual property rights (IPR) to prevent infringement of third parties' IPR and identify opportunities for new patents
- Supply chain planning to ensure the new product can be accommodated
- Training planning to ensure employees are able to utilise the new product effectively
- Product documentation to ensure effective dissemination of knowledge throughout the organisation

A brief summary of the processes associated with each gate review [3]:

Proposal and IGR
- Collect market requirements and project ideas
- Prepare project proposals (including budgets, schedule and business case/plan)
- Assess technical and commercial risks
- Finalise project proposal and send for approval

Specification and SGR
- Detailed technical targets and metrics (including critical path for project completion)
- Detailed development plan, including: scope, schedule, milestones, deliverables and costs
- Sufficient resources assigned
- Detailed product specification

Concept and CGR
- Alternative designs/methods to satisfy product specifications
- Reasoning for arriving at chosen design/method
- Full assessment of technical risks (FMEA), including a mitigation plan
- Identify involvement of potential customers/suppliers

Detail design and DGR
- Final, detailed product design
- Freeze product specification/design and release design manuals
- Production and performance risk assessment (FMEA), including a mitigation plan
- Prototype release plan (ensure risks have been assessed and financial provisions are in place)

Prototype and RGR
- Gain sufficient operating experience to ensure all major problems are known
- Demonstrate the design specification has been met
- Implement feedback and make necessary modifications to meet specification
- Agree on limited and general release criteria

Validation and FGR
- Collect and analyse feedback from pilot – validate product performance
- Build sufficient operating experience to minimise commercial risk of a general release
- Provide feedback for process improvement to appropriate departments
- Ensure general release criteria are met

Note that it is not necessary for all projects to follow the PDQ process in its entirety – a minimum requirement (in terms of gate reviews) is specified with respect to the project budget.

5.3   Proposal

As it stands, Alstom's PDQ process does not explicitly account for knowledge transfer management. In this section some additional processes are described to help Alstom promote best practice with regard to knowledge transfer. Knowledge transfer will almost certainly occur regardless of the formal processes in place – particularly in tacit form. However, the proposed additions to the PDQ process – summarised by figure 5.4 on page 110 – are intended to promote constructive knowledge transfer, in both tacit and explicit forms.

Assess learning incentives

In the first instance it is important to consider the expected learning outcomes associated with the project and the incentives associated with achieving them. Cohen and Levinthal [23] cite two factors that will influence a firm's incentives to learn: *i*) the quantity of knowledge to be assimilated and exploited; and *ii*) the difficulty of learning – some types of information are more difficult to assimilate than others. They further explain the latter in terms of unit knowledge, with the cost of absorption depending on the characteristics of the knowledge to be assimilated. As learning becomes harder to achieve, more prior knowledge is required via R&D to ensure effective assimilation. Hence, the overall learning process becomes more costly. As such, for a given level of R&D expenditure, absorptive capacity diminishes with increased learning difficulty. Further, Cohen and Levinthal [23] suggest that as the difficulty of learning increases, the marginal effect of R&D expenditure on absorptive capacity increases.

In much the same way that the rigour of the PDQ process is assessed based on the value of the project, then this may be a reasonable way to assess the associated learning incentives given the relevance of R&D expenditure to achieving successful assimilation of knowledge. This should not be the only criterion, however, as the quantity and relevance of knowledge should also be considered, for example.

Allocate resources

In accordance with Alstom's existing PDQ process, resources should be allocated in order to ensure successful knowledge transfer. This will include assigning appropriate personnel who possess the right knowledge and skills, ensuring they are equipped to achieve the required learning (tools for documenting knowledge, for example). Further, it is of course necessary to ensure there is sufficient time to successfully assimilate the required learning. The R&D expenditure associated with the project helps to ensure that the resource requirements discussed, amongst others, can be achieved.

KT methods (bias)

The manner in which knowledge is required to be assimilated should be clearly defined. There will be distinctly different requirements depending on whether knowledge is to be assimilated tacitly versus explicitly. The former revolves around the individuals, including their capacity/suitability for learning and the support mechanisms in place, such as structured training processes. Explicit knowledge requires defined processes in terms of how it is recorded and accessed by colleagues.

Define communication channels

Gilbert and Cordey-Hayes [30] have defined communication as one of the steps in their five-stage model. This includes both the manner of communication (dealt

with by the previous step in this proposed process), but also the process of dissemination. The latter should lever employee familiarity with existing processes, where appropriate. It is important to ensure that communication takes place with the frequency and rigour appropriate for the learning incentives identified prior.

Define assimilation process

Gilbert and Cordey-Hayes [30] cite the assimilation process as being a key part of knowledge transfer. They propose that the success of this process is evidenced by a change in the core routines of the organisation in response to the knowledge gained. Thus, it is important to define those processes that will be effected and the manner in which those changes will be realised to ensure a constructive outcome for the firm as a whole.

Validate outcomes/metrics

It is important to validate the success, or otherwise, of the knowledge transfer process. Metrics should reflect parameters such as the expected learning outcomes defined early in the process and whether assimilation has been achieved as desired. For assimilation to occur successfully, a firm's individuals will have to accept the proposed changes as a result of the learning that has occurred [30]. Without this acceptance, true assimilation cannot be achieved. Further, it would be useful to feedback shortcomings that may have been identified in the knowledge transfer process so that improvements can be instigated.

Much of the process described above should be enacted during the early stages of the PDQ process (up to the SGR). This is because sound planning plays a significant role in effective knowledge transfer management. Assuming the early planning stages are successful, then the latter phases are more focused towards monitoring the chosen conduits of knowledge transfer and their success in achieving the desired outcomes. This, in fact, reflects the purpose of the existing PDQ process, which is meant to promote early, and robust, project planning so that risks and uncertainties can be avoided or mitigated during the latter execution phases.

5.4   Conclusion

In this chapter the author has proposed an addition to Alstom's current PDQ process (reviewed in section 5.2) with respect to knowledge transfer management, of which it takes no formal account of in its current form. The author's proposal (summarised in figure 5.4) is intended to address this omission so that Alstom can realise enhanced benefits to the firm through better utilisation of knowledge transfer.

The proposal of section 5.3 is based on the literature reviewed in section 5.1. The latter identified several key elements to knowledge transfer, including: the skills relevant to knowledge transfer practitioners, the barriers to successful knowledge assimilation, the relative merits of and differences between tacit and explicit knowledge, and the relevance of R&D expenditure to a firm's absorptive capacity.

The process of knowledge transfer management summarised in figure 5.4 is largely a planning tool. As such, the majority of the phases (up to, and including, defining the assimilation process) should be completed no later than the end of the second phase of the current PDQ process – the SGR. Beyond the SGR the emphasis swings towards monitoring adherence to the processes, methods and channels of knowledge transfer that have been
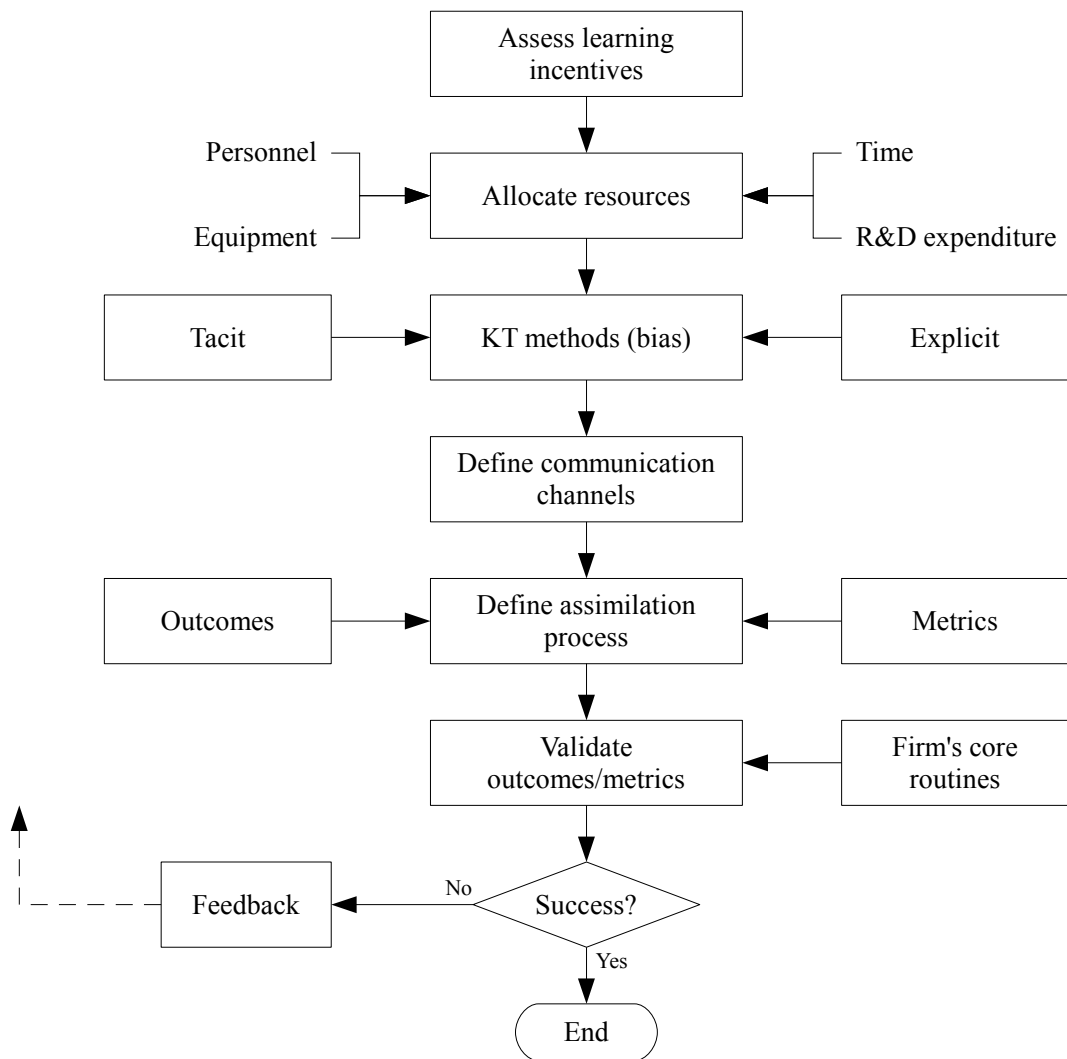
Figure 5.4: Proposed knowledge transfer management process

defined. This is important so that the benefits of the product or method being derived can be realised in the desired forms (i.e. tacit and/or explicit knowledge outcomes). Clearly, it may not be desirable or suitable to account for knowledge transfer management in all projects. Accordingly, it is suggested that criteria are derived that help clarify the need for the additional effort of including knowledge transfer management within the PDQ process.

Knowledge transfer will occur – particularly in tacit form – with or without explicit management tools in place. However, this lack of process control means that the potential benefits to the firm will be more haphazard in nature and so harder to realise. By adopting a formal knowledge transfer management process, the transfer of knowledge can be managed in such a way as to clearly define the desired outcomes of projects that are undertaken and so maximise the benefits they bring to the firm.

Chapter 6

Conclusion & Recommendations

6.1 Conclusion

6.1.1 Chapter summaries

Chapter 1

Chapter 1 introduced the topic of this thesis, including the expected benefits of the research afforded to the project sponsor – Alstom – and the main deliverables associated with achieving said benefits. This was followed by identifying the contribution to knowledge of this thesis, and the chapter concludes by presenting an overview of the research methodology adhered to by the author.

Chapter 2

Chapter 2 presents a review of the open literature relevant to this thesis. By necessity a number of areas are covered that essentially relate to either the available technical solutions for realising a part tracking system or the scanning process (in order to identify those parameters relevant to symbol legibility). Researching the elements required for a part tracking system included reviewing some of the more prevalent encoding and marking solutions available – scanners were not described in detail as they are not readily differentiated by a paper comparison. The scanning process was the focus of much of the literature, encompassing an overview of potential degradation mechanisms, the image capture process (primarily CCD operation and surface reflectance) and relevant standards with respect to the use of machine readable codes.

Chapter 3

Chapter 3 covers a number of elements that together constitute the analysis performed either by, or under the guidance of, the author. Over the course of this Engineering Doctorate the author has worked with two MSc students (Faivre [27] and Papanikolaou [54]) whose projects were defined in such a way as to contribute towards this thesis. Whilst the work itself was their own, the author was involved in directing their expected deliverables – the intention being to maintain cogency as much as possible with the author's requirements so that their work could contribute in a positive way.

The process that was followed in order to identify suitable technical solutions for each

element of the part tracking system (namely encoding, marking and scanning) is presented. The purpose of this process was not just to understand the advantages and disadvantages of each option with respect to gas turbine part tracking, but also their compatibility with other elements. The author drew particular attention to the issue of compatibility as it is an important consideration in defining a part tracking system. It suggests that to select elements in a purely sequential fashion can lead to errors; rather, an awareness of how the technical solutions relate to one another will help to ensure a robust decision making process. Those technical solutions selected for Alstom's part tracking system are identified and the justification for each is presented.

A concept is presented that identifies the causal relationship between the degradation mechanisms occurring during engine operation and the legibility of Data Matrix symbols that may be applied to parts. This concept is based on the theory presented in the literature review of chapter 2 with respect to the scanning process, specifically image capture. Surface reflectance is shown to provide a link between the degradation mechanisms and the quality of image captured. Several key physical properties (surface roughness, dot geometry and surface colour) are common in the sense that they can be used to characterise both the degradation and reflectance of the surface. Ultimately, surface reflectance has a direct influence on the legibility of the code to the scanner.

Finally, the tests are described that were undertaken to demonstrate practically some of the theoretical concepts that were identified as being important from the open literature. Erosion and oxidation were focused on (independently) because they could be readily reproduced, in a controlled manner, with the equipment available. This was not possible with deposition and so it was excluded for these tests. Once the samples had been degraded they were scanned to check whether the symbol had remained legible or not. Further, the images captured by the scanner as part of this process were saved to see how the grey levels varied. This information was used to demonstrate how the reflectance of the surface changes as it is degraded. A confocal microscope was employed to measure the geometry of the dots in order to assess any changes that may be occurring during degradation that could be significant with respect to symbol legibility.

Chapter 4

Chapter 4 presents the development of a framework for a tool referred to as a "Risk Matrix System". Its purpose is to aid the assessment of the expected durability of Data Matrix symbols applied to engine parts (with respect to scanning legibility). This tool has been inspired by failure mode and effect analysis (FMEA) where, in simple terms, potential failure modes are ranked against one another to help identify those that are most critical. A similar principle has been adopted for the Risk Matrix System, whereby it is suggested to rate the severity of each relevant degradation mechanism. Each scale should then be associated with a time-scale that identifies how long each specific level of degradation takes to occur during engine operation and finally these are further related to a legibility scale that indicates whether scanning failure is likely to occur.

The framework was not developed directly, but rather in a number of stages. Firstly, possible failure modes were identified from two different perspectives: that of scanning and marking. This initial assessment was then developed further by an MSc student – Stéphane Faivre [27] – who began the development of scales, similar to that seen in a typical FMEA, with respect to the degradation of engine parts during reconditioning. The author then developed the framework presented in section 4.3, based not just on the work of Faivre [27], but also the theory developed with respect to symbol legibility (i.e. those

parameters affecting surface reflectance). A current issue is the lack of data with regard to symbol degradation during engine operation – theory alone is not sufficient. Accuracy cannot be expected to be high until such time as more data can be gathered to better understand the rate at which different degradation processes occur. This is made more time consuming by the fact that not all engines, even those of the same model, will expose their parts to exactly the same conditions during operation.

Chapter 5

Chapter 5 addresses the requirement of an Engineering Doctorate to consider a management issue in addition to the main thesis topic. Knowledge transfer was chosen for this purpose. A brief review of relevant open literature is presented, which serves as a basis for subsequent discussion. This is followed by a summary of Alstom's current product development quality (PDQ) process – this process is applicable to all R&D projects. It was noted that there were no specific guides or controls in place to ensure effective knowledge transfer (in either explicit or tacit forms). The author then went on to describe how Alstom could develop their PDQ process to better account for knowledge transfer. Maximising the potential benefits is particularly relevant given their reliance on significant R&D investment to remain competitive. This proposal was largely based on those key areas of knowledge transfer identified as part of the literature review. A knowledge transfer management process was proposed, including suggesting at which points in the existing PDQ process different phases could be integrated. It was recognised that to manage knowledge transfer in this way will require additional resources, meaning the return may not be worthwhile for all projects. As such, it is suggested that criteria be developed to identify the need for its inclusion in the PDQ process on a case-by-case basis.

6.1.2 Contribution to knowledge

In section 1.1.1 of this thesis, a number of ways in which a contribution to knowledge can be achieved were highlighted. Of these, this thesis predominantly represents an "...application of existing knowledge to new situations...". The main issue to overcome with respect to using machine readable codes for gas turbine part tracking is their through-life legibility. Understanding the cause of read failures involved identifying how the image capture process works, which in turn indicated surface reflectance as being a key parameter. Much of the relevant open literature identified by the author was from a number of disparate sources that provided information with respect to parts of the problem at hand, but never in a complete fashion as presented in this thesis. As such, it was necessary to collate this varied information, identify the relevant aspects and then decipher how they all fit together in relation to understanding the legibility of machine readable codes applied to gas turbine parts. A brief summary of the relevant issues is presented:

Image capture

Two-dimensional symbols require an image to be captured for subsequent decoding. This is typically achieved by the use of a charge-coupled device (CCD). A CCD comprises a number of elements, referred to as pixels, that accumulate an electrical charge proportional to the degree of incident illumination. Once the desired exposure has been achieved, the charge at each pixel is then read-out and converted to a voltage so that a digital image

can be formed. Image quality is important for successfully reading a Data Matrix symbol, and, given that a CCD can only respond to the light incident upon each of its pixels, this led to investigating the properties that will affect how light reflects from a surface. The most significant parameters identified were surface roughness, surface colour and the geometry of individual dots that compose a Data Matrix.

Surface roughness

Surface roughness is a prime driver with respect to specular versus diffuse reflection. Specular reflection is associated with smooth surfaces, and diffuse rough. These modes of reflection are not always mutually exclusive; a surface can exhibit a mixture of the two, depending on its roughness. This behaviour is particularly evident with metals, whereby highly polished surfaces can appear mirror-like. However, for non-metallic materials this effect becomes less pronounced. For example, consider highly polished marble where the surface does exhibit gloss, however, no matter how smooth, it will not act like a mirror. Most non-metallic materials behave in this way because they allow light rays to penetrate their surface. Those rays that reflect via the sub-surface are more likely to escape via a different vector to other incident rays and it is this increased randomness that leads to diffuse reflection.

This specular/diffuse behaviour is important for image capture as it will affect the proportion of light incident upon the Data Matrix symbol that is reflected back towards the scanner's CCD. Contrast between the individual dots of a matrix and surrounding surface is key to achieving a successful read. Excessive roughness will weaken the clarity of important features, such as the edges of dots, through increased scattering of incident light. Similarly, a highly polished surface can be problematic if it results in glare, which will cause the image of the Data Matrix to be over exposed. Understanding these effects will enable controls to be put in place so as to ensure they remain within acceptable limits to safeguard symbol legibility.

Dot geometry

Roughness, and its effect on how light scatters from a surface, is essentially a micro-scale parameter. However, the macro-scale is also important, in this case the geometric features of a Data Matrix's dots. Larger scale features, such as dot diameter, depth and inclination of its face, will combine to affect symbol legibility. Some of these parameters, most notably diameter, are required to be a certain scale as defined in specifications such as SAE AS9132 [57], but these larger geometric features will also serve to affect how incident illumination is reflected back towards the scanner's CCD sensor or otherwise. As the scale of these features is much greater than the wavelength of the incident illumination it is their orientation that serves to determine the scattering that occurs [6].

These geometric features are largely fixed by the size of matrix that is marked, however they will affect the way in which light reflects from the surface and as such should not be ignored, particularly with respect to those symbols that have been degraded. When using the dot peen marking method the dots are not coloured to help differentiate them from the surrounding plain surface, instead it is their geometry that causes light to reflect differently, thereby enabling them to appear distinct.

Surface colour

Regarding colour, reflection and absorption are most significant for Data Matrix symbols that have been applied to opaque surfaces. With respect to this thesis, colour has been considered as an indicator of surface reflectance. For example, a surface that absorbs all wavelengths will appear black.

Colour as an indicator of absorption is a simplification to a degree, but does serve to aid identification of which surface conditions will be conducive to achieving a successful read. Thermal oxidation is particularly relevant as it will cause a change in colour of the part surface. The samples used in the tests for this thesis were mild steel and so the oxide that grew was a dark red/brown. This suggests that the spectrum of light being reflected by the surface is limited both in terms of the frequencies, but also the power of those frequencies.

The ratio of absorption to reflectance will, like surface roughness, impact the image captured by the scanner. In those situations where the surface tends to absorb more incident illumination (after thermal oxidation, for example) then there will be a reduction in light reaching the CCD sensor. As a result, image contrast is likely to be reduced and therefore the decoding process is more likely to fail.

6.2 Recommendations

It would be unrealistic to expect to answer all relevant questions regarding the legibility of machine readable codes with respect to gas turbine part tracking. As such, this section presents a number of recommendations that should help to provide further clarity of relevant issues for anyone wishing to investigate this topic further.

6.2.1 Engine operation

The severity of the main degradation mechanisms – deposition, erosion and corrosion – that will affect the legibility of machine readable codes applied to gas turbine parts will, in part, depend on the way in which the machine is operated. The GT24/26 model produced by Alstom is typically installed as part of a combined-cycle power plant (CCPP). In the past, power plants such as these would be operated in a base-load generation role, involving the engine running at approximately constant (design) load for extended periods. However, the increase in use of renewable energy sources has seen a change in the way CCPPs are operated. Many renewable energy sources, such as wind power, cannot provide a constant output due to their reliance on ambient conditions. Accordingly, more reliable energy sources, such as CCPPs, are increasingly being used for covering sudden supply shortages, peak demands or simply following the automated generation control over a wide range of relative load [36]. This changing role means that part-load efficiency is becoming more important in many cases than base-load efficiency. Increased daily stop/starts and part-load operation is being further driven by the need for increased efficiency (including reduced emissions of NOx, CO, etc.) and the shift to de-regulated (open) power markets.

In response to the changing requirements of their customers, Alstom have developed an upgrade for their GT24/GT26 engine line and associated combined-cycle power plants. This upgrade includes typical performance improvements and reduced emissions, but also directly addresses the need for improved operational flexibility. This improved operational flexibility includes enhanced turn-down capability and low-load operation

capability (LLOC) [36] – LLOC enables the CCPP to be 'parked' at a minimum load point to allow fast response from standby. An overview of the main design modifications are shown in figure 6.1.
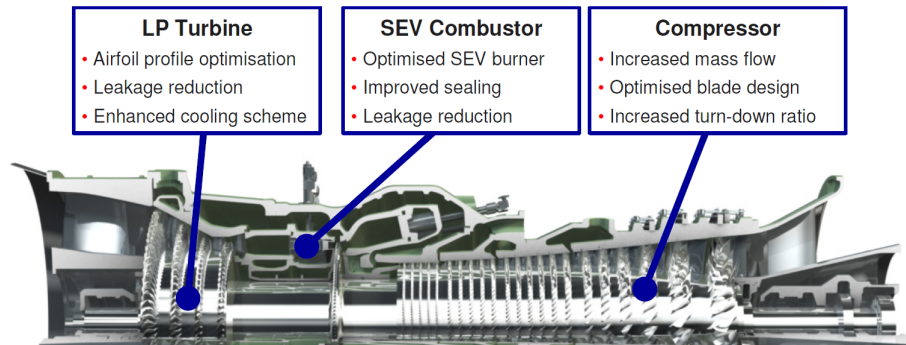
Figure 6.1: Overview of major areas of evolutionary design modifications [36]

Understanding the relevance of these changing operating conditions on the degradation mechanisms occurring will be important for accurately predicting the legibility of Data Matrix codes when parts are returned from service. Regardless of whether increased part-load operation is positive or negative with respect to code legibility, such knowledge will enable the implementation of a more robust part tracking system through improved understanding, which in turn enables mitigating actions to be implemented where necessary.

6.2.2   Surface properties

Scanning Data Matrix codes involves the use of a CCD to capture an image for decoding. CCDs are comprised of a number of individual pixels, that accumulate a charge proportional to the light incident upon them. This charge is then converted to a voltage for digitisation so that an image can be constructed. The light received by the CCD sensor will depend upon the condition of the matrix surface. Surface roughness, dot geometry and surface colour have been identified as key contributors to the way in which light is reflected and hence the likelihood of achieving a successful read.

Surface roughness

The intensity profiles extracted from the images captured by the scanner (see section 3.5.2) are susceptible to noise, meaning that the variation in reflectance between dots of the matrix and plain surface can be difficult to identify. This is because the roughness of the surface causes a variation in the light reflected back towards the scanner and is particularly evident in those images of symbols where the bare metal surface has been shot blasted.

To help reduce this noise in the intensity profile, filtering can be used. Linear low-pass filters (the Wiener filter, for example) are suitable for such a purpose, but can cause significant blurring as a fixed filter is used throughout the image – they assume that the characteristics of the signal and noise do not change over different regions. However, linear filters can be adapted to account for the local characteristics of the image, known as adaptive filtering. The software MATLAB offers an adaptive Wiener filter [45] that calculates the mean and variance in the neighbourhood of each pixel (the size of the

neighbourhood can be defined by the user); where the variance is large little filtering is performed, and vice versa. Adaptive filters such as this often perform better than a linear filter as they are more selective, helping to retain edges and other high-frequency image information. Figure 6.2 shows the improvement in signal clarity brought about by applying an adaptive Wiener filter to the image from which the data in figure 3.19 (see page 73) was extracted. More thorough treatments of adaptive filtering can be sought in the open literature, Lim [42] for example.
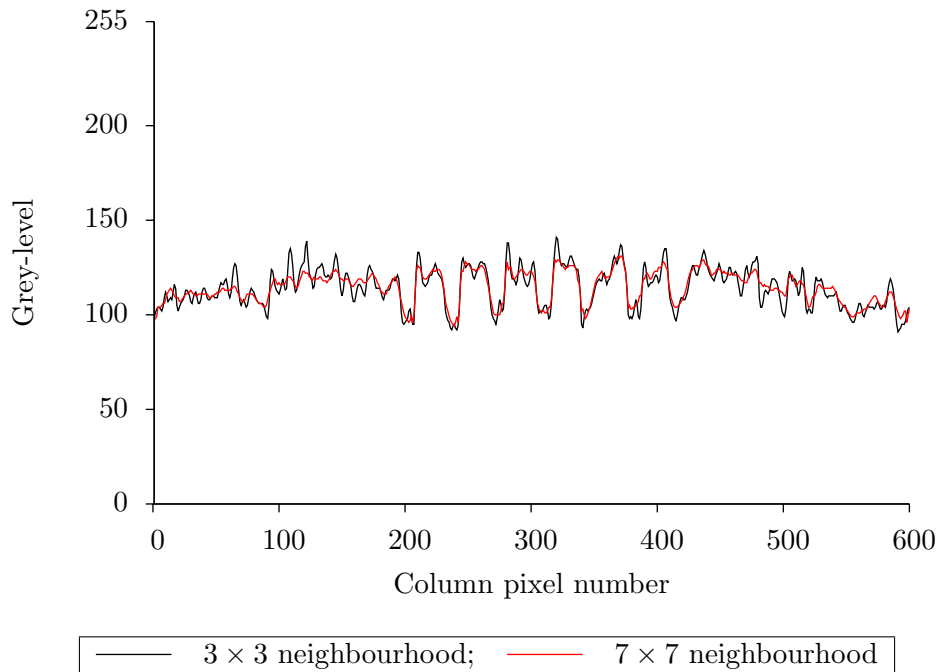
Figure 6.2: Intensity data after applying a Wiener filter to the image – (*c.f.* figure 3.19 on page 73)

The intensity profile information presented as part of the analysis in section 3.5.2 has been assessed qualitatively. What would be useful is to have more specific information regarding how light is scattered by the surface in and around the Data Matrix symbol. Computer modelling may offer a means to achieve this based on bi-directional reflectance distribution functions (BRDFs) [52]. Simply, a BRDF takes an inward and outward light direction – the angles of which are defined with respect to the surface normal – and returns the ratio between the reflected radiance in the outward direction and the incident irradiance that produces it. In the field of computer graphics, BRDFs are used to enable realistic reproduction of complex surfaces (see figure 6.3 for an example). This is made possible because BRDFs allow accurate mapping of the light scattered by a surface. Using such a technique to model varying surface conditions would enable a better understanding of the way in which light is reflected through the ability to trace individual incident rays of light. This information could then be used as an indicator of the likelihood that a Data Matrix symbol will be legible to the scanning device or not.

Figure 6.3: Anisotropic alloy wheel [73]

Dot geometry

For the test data presented in this thesis only a single marking stylus was available (90°
internal angle with a 0.3 mm tip radius). Dot diameter is effectively fixed by the required
module size, however depth will be a function of this value and the cone angle – typically
styli can be specified as 60, 90 or 120°. Dot depth was varied during testing as a result of
changing the overall size of the matrix, however it was not possible to assess the effect of
varying depth on symbol reflectance for a fixed module size with the available equipment.
Further, the angle itself may also be significant with respect to the light received by the
scanner's image sensor from the symbol surface (this will likely depend on the lighting
arrangement employed, such as its relative inclination).

The tip radius of the stylus can lead to a noticeable change in reflective characteristics
towards the dot's nadir. Typically, a radius of 0.2 mm, or less, is preferred for exactly
this reason so that the geometry, through the depth of the dot, remains as consistent as
possible. Whilst a sharp point can be specified, this is not advisable because the durability
of the stylus tip will be compromised (which will be further exacerbated if marking hard
materials such as gas turbine alloys). When a stylus tip becomes damaged (chipped, for
example) this will compromise symbol quality and hence necessitate replacement of the
stylus.

The geometric parameters described here should be developed to further understand their
significance with respect to symbol legibility, both pre and post degradation. Focusing on
the reflectance of an individual dot rather than a whole matrix may facilitate this as it
will allow greater freedom to test varying geometries. Assessing the reflectance of a single
dot should be sufficient to infer overall symbol legibility so long as quality parameters,
such as cell fill, are subsequently respected.

Surface colour

The surface of a Data Matrix is not self-luminous, but rather a so called indirect source or non-self luminous stimulus object. That is to say light reaches the observer (or scanner in this case) indirectly via an object (the part's surface where the symbol has been applied). Burnham et al. [21, p. 28] state that when light is incident upon a non-fluorescent object or material, three things can occur: the energy can be reflected, transmitted or absorbed. Typically all three will occur, but the proportion of each will be different, often varying with wavelength as well. An example of this is illustrated in figure 6.4. This behaviour will dictate the perceived colour of an object, such as a Data Matrix symbol. As the symbol degrades, for example, due to thermal oxidation, the response of the surface to incident illumination will vary leading to a change in colour relative to the original bare metal.
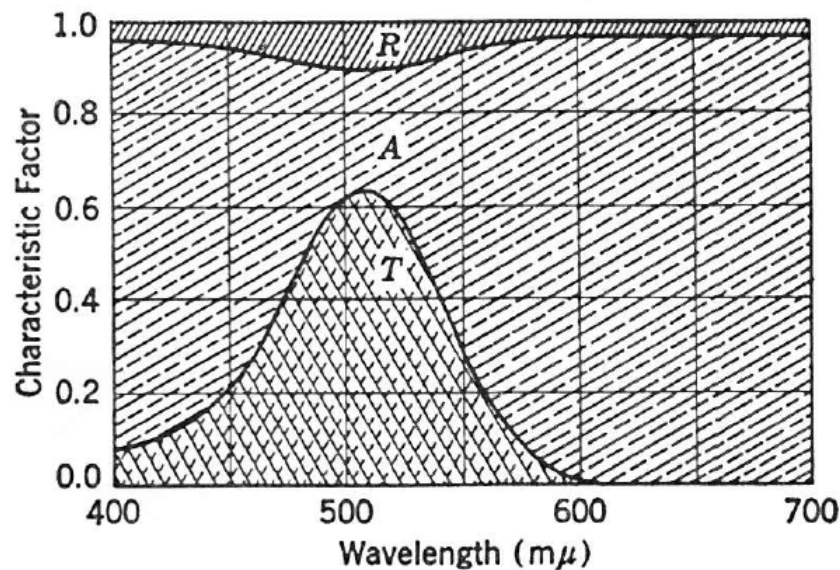
Figure 6.4: Curves showing the reflectance (R), absorptance (A) and transmittance (T) of a substance dyed with green dye [21, p. 28]

Colour is important because it indicates the proportion of incident illumination being received by the scanner. Simply, lighter colours imply much of the incident illumination is being reflected, whilst darker ones suggest absorption is dominating. Absorption hinders the image contrast that can be achieved and so reduces the likelihood of being able to read the Data Matrix symbol.

It would be useful to identify how the reflectance of different gas turbine parts varies when returned from service (due to changes in colour), to help determine the legibility of the symbols that may be applied to such parts. Further, colour is not entirely distinct from surface roughness. Surface roughness will determine the gloss of the surface, which, if excessive, can be detrimental to the scanning process. Equally, excessively diffuse reflection can also be undesirable as it causes a surface to appear uniformly luminous, which can serve to suppress the appearance of surface features such as the dots of a Data Matrix.

The parameters discussed in this section have largely been considered in isolation throughout this thesis. In reality it is likely that more than one of them will be affected at

any one time as a Data Matrix symbol degrades through its life. Investigating the relative impact of changes to these parameters with respect to symbol legibility would help to determine mitigation techniques for maintaining symbol legibility.

6.2.3 Modelling degradation

Part of the MSc thesis by Papanikolaou [54] involved investigating the possibility of modelling degradation, specifically erosion, using the software Fluent. The reasoning behind this approach was in part to offer a more rapid method of understanding how the surface of a Data Matrix may degrade during the service life of the part it has been applied to. This information could then be used as an input for assessing symbol legibility.

Papanikolaou [54] produced a simplified model of a blade foot that was exposed to an air flow containing erosive particles. The model was relatively simple to aid completion within the time available, but also because at this stage the main intention was to assess the practicality of such an approach. At the time it was concluded not to pursue it further as there were reservations regarding the absolute accuracy of the results (erosion rates, for example). The non-trivial nature of the problem meant it was likely that a reasonable amount of time would be required to resolve this in addition to developing other parameters, such as the geometry.

Computational modelling of surface degradation was not pursued for practical reasons with respect to a lack of time and specific expertise that would have been required to have confidence of a successful outcome (not because the principle showed no promise). The models of Papanikolaou [54] largely indicated the expected behavioural patterns with respect to the physical processes occurring, it was mainly outright accuracy that was lacking. With the right resources and expertise, a more fruitful outcome could be achieved.

Of course, Fluent is not the only software suitable for such an analysis. The approach described has been provided as an example of how a computational tool can be utilised to model one of the degradation processes Data Matrix symbols may be exposed to during their life. It is quite right that other tools be assessed for their applicability.

6.2.4 Mitigation techniques

Data Matrix codes applied to engine parts are expected to degrade during service. As such, it is necessary to consider how to mitigate against this in order to maximise legibility of the symbols applied.

Broadly speaking mitigation may be preventative or reactive. Preventative mitigation techniques involve employing strategies to prevent either degradation occurring in the first place or limiting its effect when it does. Reactive mitigation techniques involve developing methods that improve symbol legibility, perhaps only temporarily, despite the accumulation of surface degradation during service.

Preventative methods have already been considered to an extent as part of the selection process described in section 3.2, which resulted in dot peen being identified as the preferred marking method, in part because of its greater durability against a wider range of degradation mechanisms. Further measures should include the strategic placement of the symbols on parts, within manufacturing constraints, to help shield them from the worst effects of the engine operating conditions. There may be an element of trial and error as to the exact placement of symbols to maximise their durability because parts will be marked so as to avoid the main gas path, preferring areas such as the hub region where

conditions are less easily predicted.

As part of their ongoing trials Alstom have used a reactive method of improving symbol legibility. This involved the use of an erasable whitener (chalk or marker) to temporarily improve the symbol contrast [43]. For example, one such symbol had been degraded through a mixture of thermal oxidation and lubrication oil that had been baked onto the surface – resulting in insufficient contrast for the scanner to decode it successfully. However, this was mitigated by the application of whitener to the surface, enabling the symbol to be read. An example of this process is illustrated in figure 6.5.

(a) Before whitener **(b)** After whitener
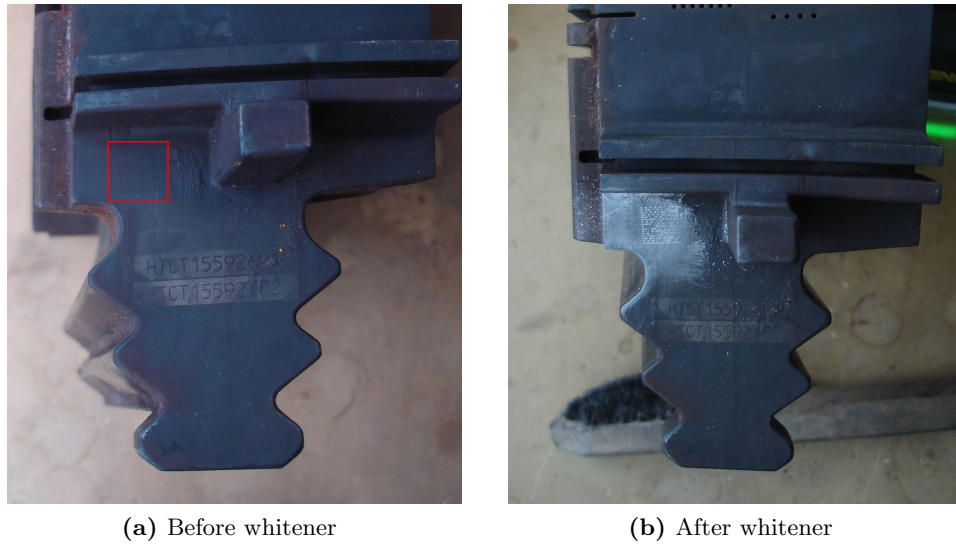
Figure 6.5: Improving the legibility of a degraded Data Matrix by applying whitener [43]

One of the benefits to Alstom of the enhanced part tracking system is to reduce the costs associated with recording part histories. Any future proposals for mitigation techniques (be they preventative or reactive) should account for this through minimal time and cost requirements over and above that which is already incurred as part of the part tracking system – the whitener method described is a perfect example.

6.2.5 Scanning parameters

For the test data presented in section 3.5 the scanner was held in a fixed position (see figure 3.14 on page 67), for the sake of consistency. However, the Cognex model used (the DataMan 7500) is designed to be hand-held and as such can be orientated towards the Data Matrix symbol in more than one way. It is possible that the perpendicular orientation utilised may not be optimum for all conditions. Further tests could incorporate different orientations of the scanner with respect to the code to better understand this effect.

Correct illumination of the symbol can greatly enhance its legibility. Lighting systems are often incorporated into the scanning device, although they can be augmented by, or substituted for, standalone equipment, which may offer more flexibility. The Cognex scanner used, for example, incorporates a variable lighting system that includes a central diffused source surrounded by a 'light pipe' separated into quadrants – these elements can be switched on or off as desired. The default settings were maintained for the

presented test data as the lack of experience using such a device meant it would have been difficult to justify one setting over another, not to mention the possibility of inadvertently compromising its performance as a result. However, much as in the case of the scanner's orientation towards the code, the optimum lighting requirements will likely change with the surface condition of the Data Matrix. So again, further tests could be undertaken to better understand the effect this may have on symbol legibility.

Understanding how best to handle the scanner would enable the production of a best practice method based on the condition of the symbol being read. Scanners will need to be handled by a variety of staff, not all of who will be experienced in doing so. By offering advice on best practice, acceptance amongst users of the enhanced part tracking system can be maximised by reducing their frustration in learning to use what will initially be an unfamiliar system.

6.2.6 Risk matrix system

Chapter 4 proposes a framework for a tool referred to as a Risk Matrix System. Its purpose being to aid implementation of a gas turbine part tracking system.

At present, the practical implications of marking gas turbine parts with machine readable codes are not fully understood – specifically with regard to maintaining symbol legibility. So, to improve the accuracy of the tool, and hence its usefulness, will require a feedback system (see figure 4.1 on page 96). As knowledge is gained with respect to symbol legibility under varying conditions, time periods, and so forth, this learning is fed back to improve the scales used to represent the severity of degradation occurring and the symbol legibility that results. The legibility scale is an indication of how the degradation affects the reflectance of the symbol and its surrounding surface, which has a direct influence on the image captured by the scanner for subsequent processing.

Developing the knowledge to improve the efficacy of the Risk Matrix System may be achieved through a number of means, including:

- Test data
- Operational feedback
- Theory and/or simulation
- User feedback (tacit knowledge transformed to explicit knowledge) and mentoring

These means of developing the efficacy of the Risk Matrix System have already begun, but are in their infancy. For example, Alstom have performed a number of tests to assess symbol durability (such as their reconditioning trial [7]) and are now marking blade sets for installation into customer engines to enable further understanding of the degradation to be expected under engine operating conditions. Further, this thesis provides a solid foundation regarding the theory of symbol legibility, including the effects of surface degradation, and hence can act as a basis for the development of computer simulations. Finally, as Alstom employees gain experience with the part tracking system they can begin to feedback improvements based on their experiences and promote its use (including best practice) amongst colleagues.

References

[1] AIM Inc. International Symbology Specification – PosiCode. ITS/02-001, 2002.

[2] AIM Inc. AIM Direct Part Marking Quality Guideline. Second public review draft – rev. J, 2006.

[3] Alstom. Product Development Quality (PDQ). (Unpublished), 2006.

[4] Alstom Group. The Alstom Group, June 2010. URL `http://www.alstom.com/WorkArea/DownloadAsset.aspx?id=8589941986&lang=en-GB`. (Date accessed: 20 Dec 2011).

[5] E. W. Andrews, A. E. Giannakopoulos, E. Plisson, and S. Suresh. Analysis of the Impact of a Sharp Indenter. *International Journal of Solids and Structures*, Vol. 39: pp. 281–295, 2002. Cited in [27].

[6] H. E. Bennett and J. O. Porteus. Relation Between Surface Roughness and Specular Reflectance. *Journal of the Optical Society of America*, Vol. 51(No. 2):pp. 123–129, 1961.

[7] J. Biedermann. Enhanced Parts Tracking – Reconditioning Trials. TN09S/0660, Alstom (Switzerland) Ltd., 2009. (Unpublished).

[8] N. Birks. *Introduction to High Temperature Oxidation of Metals*. Cambridge University Press, 2nd edition, 2006.

[9] R. M. Brach and P. F. Dunn. A Mathematical Model of the Impact and Adhesion of Microspheres. *Aerosol Science and Technology*, Vol. 16(Issue 1):pp. 51–64, 1992.

[10] British Standards Institute. Information Technology – Automatic Identification and Data Capture Techniques – Bar Code Print Quality Test Specification – Two-Dimensional Symbols. BS EN ISO 15415:2005, 2005.

[11] British Standards Institute. Abrasive Products – Checking the Grit Size of Superabrasives. BS ISO 6106:2005, 2005.

[12] British Standards Institute. Metallic Materials – Brinell Hardness Test – Part 1: Test Method. BS EN ISO 6506-1:2005, 2005.

[13] British Standards Institute. Metallic Materials – Vickers Hardness Test – Part 1: Test Method. BS EN ISO 6507-1:2005, 2005.

[14] British Standards Institute. Metallic Materials – Rockwell Hardness Test – Part 1: Test Method (scales A, B, C, D, E, F, G, H, K, N, T). BS EN ISO 6508-1:2005, 2005.

[15] British Standards Institute. Information Technology – Automatic Identification and Data Capture Techniques – PDF417 Bar Code Symbology Specification. BS ISO/IEC 15438:2006, 2006.

[16] British Standards Institute. Information Technology – Automatic Identification and Data Capture Techniques – Data Matrix Bar Code Symbology Specification. BS ISO/IEC 16022:2006, 2006.

[17] British Standards Institute. Information Technology – Automatic Identification and Data Capture Techniques – Code 128 Bar Code Symbology Specification. BS ISO/IEC 15417:2007, 2007.

[18] British Standards Institute. Information Technology – Automatic Identification and Data Capture Techniques – Code 39 Bar Code Symbology Specification. BS ISO/IEC 16388:2007, 2007.

[19] British Standards Institute. Quality Management Systems. PD ISO/TS 16949:2009, 2009.

[20] British Standards Institute. Geometrical Product Specification (GPS) – Surface Texture: Profile Method – Terms, Definitions and Surface Texture Parameters. BS EN ISO 4287:1998+A1:2009, 2009.

[21] R. W. Burnham, R. M. Hanes, and C. J. Bartleson. *Colour: A Guide to Basic Facts and Concepts*. John Wiley & Sons, Inc., 1963.

[22] F. Carvalho. EPT Project – Marking Test Center GT26 Components for Quick Engine Validation. TN09S/0767, Alstom (Switzerland) Ltd., 2009. (Unpublished).

[23] W. M. Cohen and D. A. Levinthal. Absorptive Capacity: A New Perspective on Learning and Innovation. *Administrative Science Quarterly*, Vol. 35(No. 1):pp. 128–252, 1990.

[24] B. Dahneke. Further Measurements of the Bouncing of Small Latex Spheres. *Journal of Colloid and Interface Science*, Vol. 51(No. 1):pp. 58–65, 1975.

[25] H. El-Batsh and H. Haselbacher. Effect of Turbulence Modeling on Particle Dispersion and Deposition on Compressor and Turbine Blade Surfaces. *American Society of Mechanical Engineers*, 2000-GT-519, 2000.

[26] U. R. Evans. *Metallic Corrosion Passivity and Protection*. Edward Arnold & Co., 2nd edition, 1946.

[27] S. Faivre. Dot Peen Markings: The Marking of Dot Peen Data Matrices and the Effect of Gas Turbine Reconditioning Processes on Markings. Master's thesis, Department of Power and Propulsion, Cranfield University, 2010.

[28] R. Farmer, editor. *Gas Turbine World 2005 Performance Specs*, volume 34 (No. 6). 23rd edition, January 2005.

[29] B. Fender. Innovation Through Knowledge Transfer. In *Smart Innovation, Systems and Technologies*, volume 5, pages 15–25. Springer-Verlag, 2010.

[30] M. Gilbert and M. Cordey-Hayes. Understadning the Process of Knowledge Transfer to Achieve Successful Technological Innovation. *Technovation*, Vol. 16(No. 6):pp. 301–312, 1996.

[31] R. C. Gonzalez and R. E. Woods. *Digital Image Processing*. Pearson Education, Inc., 3rd edition, 2008.

[32] J. E. Goodwin, W. Sage, and G. P. Tilly. Study of Erosion by Solid Particles. In *Proc. Instn. Mech. Engrs.*, volume 184(No. 15). IMechE, 1969–70.

[33] M. L. Guerrero and A. A. Soares. System and Method for Identifying a Defective Component in a Network Environment, May 2003. US Patent Application Publication No.: US 2003/0097315.

[34] A. Hamed, W. Tabakoff, and R. Wenglarz. Erosion and Deposition in Turbomachinery. *Journal of Propulsion and Power*, Vol. 22(No. 2):pp. 350–360, 2006.

[35] A. A. Hamed, W. Tabakoff, R. B. Rivir, K. Das, and P. Arora. Turbine Blade Surface Deterioration by Erosion. *Journal of Turbomachinery*, Vol. 127:pp. 445–452, 2005.

[36] M. Hiddemann, F. Hummel, M. Ladwig, and M. Stevens. The Next Generation GT26 from Alstom, the Pioneer in Operational Flexibility. In *IDGTE Conference 2011 Gas Turbines in the Markets of Tomorrow*, November 2011.

[37] H. W. Jensen, S. R. Marschner, M. Levoy, and P. Hanrahan. A Practical Model for Subsurface Light Transport. In *SIGGRAPH '01: Proceedings of the 28th Annual Conference on Computer Graphics and Interactive Techniques*. ACM, 2001.

[38] B. J. Koeppel and G. Subhash. Characteristics of Residual Plastic Zone Under Static and Dynamic Vickers Indentations. *Wear*, Vol. 224:pp. 56–67, 1999. Cited in [27].

[39] O. Kubaschewski and B. E. Hopkins. *Oxidation of Metals and Alloys*. Butterworth's Scientific Publications, 1953.

[40] G. Y. Lai. *High Temperature Corrosion and Materials Applications*, chapter 9 – Hot Corrosion in Gas Turbines, pages 249–258. ASM International, 2007.

[41] M. Lei and R. Ackaouy. Method for Data Matrix Print Quality Verification, Jun 2001. US Patent No.: 6,244,764.

[42] J. S. Lim. *Two-Dimensional Signal and Image Processing*. Prentice-Hall International, Inc., 1990.

[43] S. Lotfi. EPT Project – 2-D Data Matrix Engine Feedback. TN10S/0788, Alstom (Switzerland) Ltd., 2010. (Unpublished).

[44] J. Lu, S. Suresh, and G. Ravichandran. Dynamic Indentation for Determining the Strain Rate Sensitivity of Metals. *Journal of the Mechanics and Physics of Solids*, Vol. 51:pp. 1923–1938, 2003. Cited in [27].

[45] MathWorks. MATLAB online documentation: "wiener2". URL `http://www.mathworks.co.uk/help/toolbox/images/ref/wiener2.html`. (Date accessed: 4 Jan 2012).

[46] R. E. McDermott, R. J. Mikulak, and M. R. Beauregard. *The Basics of FMEA*. CRC Press, 2nd edition, 2009.

[47] C. McFee. An Introduction to CCD Operation. URL `http://www.mssl.ucl.ac.uk/www_detector/optheory/ccdoperation.html`. (Date accessed: 15 Feb 2010).

[48] M. A. Meyers, R. W. Armstrong, and H. O. K. Kirchner. *Mechanics and Materials: Fundamentals and Linkages*, chapter 14 – Dynamic Deformation and Failure, page 489. John Wiley & Sons, Inc., 1999. Cited in [27].

[49] S. G. Nadabar and R. Desai. Method and Apparatus Using Intensity Gradients for Visual Identification of 2D Matrix Symbols, Sep 2005. US Patent No.: 6,941,026.

[50] NASA. Application of Data Matrix Identification Symbols on Aerospace Parts. NASA-HDBK-6003A, September 2002.

[51] NASA. Applying Data Matrix Identification Symbols on Aerospace Parts. NASA-STD-6002A, September 2002.

[52] F. E. Nicodemus. Directional Reflectance and Emissivity of an Opaque Surface. *Applied Optics*, Vol. 4(No. 7):pp. 767–773, 1965.

[53] N. Otsu. A Threshold Selection Method from Gray-Level Histograms. *IEEE Transactions on Systems, Man and Cybernetics*, Vol. SMC-9(No. 1):pp. 62–66, 1979.

[54] C. Papanikolaou. A Study of the Performance and Operating Conditions of an Industrial Gas Turbine. Master's thesis, Department of Power and Propulsion, Cranfield University, 2009.

[55] P. V. Rao and D. H. Buckley. Time Dependence of Solid-Particle Impingement Erosion of an Aluminium Alloy. NASA Technical Paper 2169, August 1983.

[56] Rolls-Royce. Direct Part Marking Implementation Guide, June 2004. Issue 1.

[57] SAE Aerospace. Data Matrix Quality Requirements for Part Marking. SAE AS9132, February 2005. Rev. A.

[58] R. Sanchez. "Tacit Knowledge" versus "Explicit Knowledge" Approaches to Knowledge Management Practice. *Knowledge: Creation, Diffusion, Utilization*, Vol. 7 (Issue 5):pp. 1–22, 2000.

[59] H. I. H. Saravanamuttoo, G. F. C. Rogers, and H. Cohen. *Gas Turbine Theory.* Pearson Education Limited, 5$^{\text{th}}$ edition, 2001.

[60] M. Schütze. *Protective Oxide Scales and Their Breakdown.* John Wiley & Sons, Ltd., 1997.

[61] M. Sezgin and B. Sankur. Survey Over Image Thresholding Techniques and Quantitative Performance Evaluation. *Journal of Electronic Imaging*, Vol. 13(No. 1): pp. 146–165, 2004.

[62] L. G. Shapiro and G. C. Stockman. *Computer Vision.* Prentice Hall, 2001.

[63] G. L. Sheldon. Effects of Surface Hardness and Other Material Properties on Erosive Wear of Metals by Solid Particles. *J. Eng. Mater. Technol.*, Vol. 99(Issue 2):pp. 133–137, 1977.

[64] M. Soltani and G. Ahmadi. On Particle Adhesion and Removal Mechanisms in Turbulent Flows. *J. Adhesion Sci. and Technol.*, Vol. 8(No. 7):pp. 763–785, 1994.

[65] G. Subhash, B. J. Koeppel, and A. Chandra. Dynamic Indentation Hardness and Rate Sensitivity Models. *Journal of Engineering Materials and Technology*, Vol. 121 (Issue 3):p. 257, 1999. Cited in [27].

[66] S. Swaddiwudhipong, J. Hua, K. K. Tho, and Z. S. Liu. Equivalency of Berkovich and Conical Load-Indentation Curves. *Institute of Physics Publishing – Modelling Simu. Mater. Sci. Eng.*, Vol. 14:pp. 71–82, 2006. Cited in [27].

[67] R. J. D. Tilley. *Colour and Optical Properties of Materials.* John Wiley & Sons, Ltd., 2000.

[68] G. P. Tilly. Erosion Caused by Airborne Particles. *Wear*, Vol. 14(Issue 1):pp. 63–79, 1969.

[69] P. Tordoir. Technical and Economic Assessments of Industrial Gas Turbines. Master's thesis, Department of Power and Propulsion, Cranfield University, 1995.

[70] J. Torrent and V. Barrón. Diffuse Reflectance Spectroscopy of Iron Oxides. In *Encyclopdeia of Surface and Colloid Science*, pages 1438–1446. Marcel Dekker, 2002.

[71] US Department of Defense. Identification Marking of U.S. Military Property. MIL-STD-130N, 2007.

[72] T. Wakeman and W. Tabakoff. Measured Particle Rebound Characteristics Useful for Erosion Prediction. *American Society of Mechanical Engineers*, 82-GT-170, 1982.

[73] S. H. Westin, J. R. Arvo, and K. E. Torrance. Predicting Reflectance Functions from Complex Surfaces. In *SIGGRAPH '92: Proceedings of the 19th Annual Conference on Computer Graphics and Interactive Techniques*. ACM, 1992.

Appendix A

Turbomatch Data

This appendix details the input/output files for the design point model of the Alstom GT26 engine developed by the author.

Input data file: "ALSTOM GT26 DP - bleed.dat"

```
!TURBOMATCH SCHEME DESIGN FILE
!ENGINE TYPE: ALSTOM GT26 (Single Shaft)
////
DP SI KE CT FP
-1
-1
INTAKE  S1,2        D1-4                             R300
COMPRE  S2,3        D5-11                            R301   V5    V6
ARITHY              D101-107
ARITHY              D111-117
ARITHY              D121-127
ARITHY              D131-137
PREMAS  S3,4,13     D12-15
PREMAS  S13,14,15   D16-19
BURNER  S4,5        D20-22                           R302
MIXEES  S5,14,6
TURBIN  S6,7        D23-32                                  V23   V24
DUCTER  S7,8        D33-36                           R303
MIXEES  S8,15,9
TURBIN  S9,10       D37-44,118,45                           V37   V38
NOZCON  S10,11,1    D46                              R304
OUTPBD              D109,118,138
PERFOR  S1,0,0      D37,47-49,304,300,302,0,0,303,0,0,0
CODEND

DATA////

! INTAKE
1     0.0        ! Altitude (ft)
2     0.0        ! Deviation from ISA (K)
3     0.0        ! Flight Mach number
4     0.98       ! Pressure recovery

! COMPRESSOR
5     0.85       ! Surge margin "Z"
6     1.0        ! Relative rotational speed
7     33.9       ! Design pressure ratio
8     0.86       ! Design isentropc efficiency
9     1.0        ! Error "switch"
10    3.0        ! Compressor map number
11    0.0        ! Stator angle relative to design point

! COMPRESSOR BLEED (for cooling)
12    0.92       ! Lambda (W) = Wout1/Win
13    0.0        ! Delta (W)
```

```
14    1.0         ! Lambda (P)
15    0.0         ! Delta (P)


! SPLIT COOLING COOLING BLEED FOR TURBINE 1 AND 2
16    0.25        ! Lambda (W) = Wout1/Win
17    0.0         ! Delta (W)
18    1.0         ! Lambda (P)
19    0.0         ! Delta (P)


! COMBUSTOR 1
20    0.05        ! Pressure loss
21    0.99        ! Combustion efficiency
22    -1.0        ! Fuel flow


! TURBINE 1 (modelled as a free turbine)
23    150.0E6     ! Auxiliary work (W)
24    -1.0        ! Design relative non-dimensional inlet mass flow
25    -1.0        ! Design relative non-dimensional speed
26    0.88        ! Design isentropic efficiency
27    1.0         ! Relative rotational speed
28    0.0         ! Driven compressor number
29    3.0         ! Turbine map number
30    1000.0      ! Power law index
31    -1.0        ! Compressor work
32    0.0         ! NGV angle relative to design point


! COMBUSTOR 2 (modelled as a duct)
33    2.0         ! Reheat requirement
34    0.05        ! Pressure loss
35    0.99        ! Combustion efficiency
36    1.0E5       ! Limiting value of fuel flow (or 1.0E5 if not needed)


! TURBINE 2 (modelled as a power turbine)
37    288.3E6     ! Auxiliary work (W)
38    -1.0        ! Design relative non-dimensional inlet mass flow
39    -1.0        ! Design relative non-dimensional speed
40    0.88        ! Design isentropic efficiency
41    -1.0        ! Relative rotational speed
42    1.0         ! Driven compressor number
43    3.0         ! Turbine map number
44    1000.0      ! Power law index
45    0.0         ! NGV angle relative to design point


! CONVERGENT NOZZLE
46    -1.0        ! Exit area "switch"


! PERFORMANCE
47    1.0         ! Propeller efficiency
48    0.0         ! Scaling "switch"
49    0.0         ! Design-point net thrust


! CONVERT TURBINE 1 AUX. WORK FROM W TO CHU/s
101   4.0         ! Divide
102   -1.0
103   109.0       ! OP(1): place result in BD109
104   -1.0
105   23.0        ! OP(2): turbine 1 aux. work (W)
106   -1.0
107   108.0       ! OP(3): division factor from BD108
108   1899.105    ! Division factor


! CALCULATE THE COMPRESSOR WORK FOR TURBINE 2
111   2.0         ! Subtract
112   -1.0
113   118.0       ! OP(1): place result in BD118
114   -1.0
115   301.0       ! OP(2): compressor work (CHU/s)
116   -1.0
117   109.0       ! OP(3): turbine 1 compressor work (CHU/s) from BD109
```

```
! SUM INDIVIDUAL TURBINE COMPRESSOR WORK VALUES
121   1.0         ! Add
122  -1.0
123   128.0       ! OP(1): place result in BD128
124  -1.0
125   109.0       ! OP(2): turbine 1 aux. work (CHU/s) from BD23
126  -1.0
127   118.0       ! OP(3): turbine 2 compressor work (CHU/s) from BD118

! CHECK COMPRESSOR WORK AGAINST VALUE OUTPUT BY TURBOMATCH
131   2.0         ! Subtract
132  -1.0
133   138.0       ! OP(1): place result in BD138
134  -1.0
135   301.0       ! OP(2): compressor work (CHU/s)
136  -1.0
137   128.0       ! OP(3): sum of the turbine compressor work (W) from BD128

-1
1 2 633.0
5 6 1565.0
8 6 1565.0
-1
-3
```

Output data file: "ALSTOM GT26 DP - bleed.tmr"

```
                   The Units for this Run are as follows:-

 Temperature = K   Pressure = Atmospheres   Length = metres

 Area = sq metres  Mass Flow = kg/sec       Velocity = metres/sec

 Force = Newtons   s.f.c.(Thrust) =  mg/N sec   s.f.c.(Power) = mug/J

 Sp. Thrust =    N/kg/sec    Power =   Watts
1

      ***** DESIGN POINT ENGINE CALCULATIONS *****



 ***** AMBIENT AND INLET PARAMETERS *****
 Alt. =     0.0      I.S.A. Dev. =    0.000      Mach No. =  0.00
 Etar = 0.9800       Momentum Drag =     0.00

 ***** COMPRESSOR  1 PARAMETERS *****
 PRSF = 0.45028E+01     ETASF = 0.10246E+01     WASF =  0.64730E+01
 Z = 0.85000           PR = 33.900            ETA = 0.86000
 PCN =   1.0000        CN = 1.00000           COMWK =  0.36680E+09

 ***** COMBUSTION CHAMBER PARAMETERS *****
 ETASF = 0.99000E+00
 ETA = 0.99000        DLP = 1.6611          WFB = 12.7711

 ***** TURBINE  1 PARAMETERS *****
 CNSF = 0.10831E-01    ETASF = 0.98157E+00    TFSF = 0.56817E+00
 DHSF = 0.47135E+04
 TF =  430.924         ETA = 0.88000         CN = 2.750
 AUXWK = 0.15000E+09

 Additional Free Turbine Parameters:-
 Speed = 100.0%        Power = 0.15000E+09

 ***** DUCT/AFTER BURNING 1 PARAMETERS *****
 ETA = 0.9900         DLP = 0.7992          WFB = 4.1609

 ***** TURBINE  2 PARAMETERS *****
 CNSF = 0.10744E+03    ETASF = 0.98157E+00    TFSF = 0.25772E+00
 DHSF = 0.15084E+05
 TF =  430.924         ETA = 0.88000         CN = 2.750
 AUXWK = 0.28830E+09

 ***** CONVERGENT NOZZLE  1 PARAMETERS *****
 NCOSF = 0.10000E+01
 Area = 44.8040        Exit Velocity =   36.70 Gross Thrust =  23158.66
 Nozzle Coeff. = 0.97104E+00

   BD(109) = 0.789846E+05   BD(118) = 0.114160E+06   BD(138) = 0.000000E+00


 Scale Factor on above Mass Flows, Areas, Thrusts & Powers =    1.0000
```

Station	F.A.R.	Mass Flow	Pstatic	Ptotal	Tstatic	Ttotal	Vel	Area
1	0.00000	633.000	1.00000	1.00000	288.15	288.15	0.0	******
2	0.00000	633.000	******	0.98000	******	288.15	******	******
3	0.00000	633.000	******	33.22202	******	841.56	******	******
4	0.00000	582.360	******	33.22202	******	841.56	******	******
5	0.02193	595.131	******	31.56092	******	1565.00	******	******
6	0.02146	607.791	******	31.56092	******	1551.07	******	******
7	0.02146	607.791	******	15.98472	******	1354.35	******	******
8	0.02893	611.952	******	15.18548	******	1565.00	******	******
9	0.02719	649.932	******	15.18548	******	1526.28	******	******

```
10   0.02719   649.932   ******    1.00226   ******   893.66   ******   ******
11   0.02719   649.932   1.00000   1.00226   893.09   893.66     36.7   44.8040
12   0.00000     0.000   ******    0.00000   ******     0.00   ******   ******
13   0.00000    50.640   ******   33.22202   ******   841.56   ******   ******
14   0.00000    12.660   ******   33.22202   ******   841.56   ******   ******
15   0.00000    37.980   ******   33.22202   ******   841.56   ******   ******


  Shaft Power = 288300000.00
   Net Thrust = 23158.66
 Equiv. Power = 289793184.00
    Fuel Flow = 16.9320
       S.F.C. = 58.7306
      E.S.F.C. = 58.4280
Sp. Sh. Power = 455450.25
Sp. Eq. Power = 457809.16
Sh. Th. Effy. = 0.3948
```

Appendix B

Scan Results

The remainder of this page has been left blank intentionally.

Degradation applied	Matrix size (mm)	Result		
		1	**2**	**3**
None	4 × 4	Success	Success	Success
	6 × 6	Success	Success	Success
	8 × 8	Success	Success	Success
	10 × 10	Success	Success	Success
	12 × 12	Success	Success	Success
Shot blasting 30/40 grit (×1 pass)	4 × 4	Failure	Failure	Failure
	6 × 6	Failure	Failure	Failure
	8 × 8	Failure	Failure	Failure
	10 × 10	Success	Success	Success
	12 × 12	Success	Success	Success
Shot blasting 30/40 grit (×2 passes)	4 × 4	Failure	Failure	Failure
	6 × 6	Failure	Failure	Failure
	8 × 8	Failure	Failure	Failure
	10 × 10	Success	Success	Success
	12 × 12	Success	Success	Success
Shot blasting 30/40 grit (×3 passes)	4 × 4	Failure	Failure	Failure
	6 × 6	Failure	Failure	Failure
	8 × 8	Success	Failure	Success
	10 × 10	Success	Success	Success
	12 × 12	Success	Success	Success
Shot blasting 30/40 grit (×4 passes)	4 × 4	Failure	Failure	Failure
	6 × 6	Failure	Failure	Failure
	8 × 8	Failure	Failure	Failure
	10 × 10	Success	Success	Success
	12 × 12	Success	Success	Success
Shot blasting 30/40 grit (×5 passes)	4 × 4	Failure	Failure	Failure
	6 × 6	Failure	Failure	Failure
	8 × 8	Failure	Failure	Failure
	10 × 10	Success	Failure	Success
	12 × 12	Success	Success	Success
Shot blasting 30/40 grit (×6 passes)	4 × 4	Failure	Failure	Failure
	6 × 6	Failure	Failure	Failure
	8 × 8	Success	Success	Success
	10 × 10	Success	Success	Success
	12 × 12	Success	Success	Success

Key:

- Success
- Intermittent
- Failure

Table B.1: Scan results after shot blasting (30/40 grit) – clean marking surface

Degradation applied	Matrix size (mm)	Result		
		1	**2**	**3**
None	4 × 4	Failure	Success	Failure
	6 × 6	Success	Success	Success
	8 × 8	Success	Success	Success
	10 × 10	Success	Success	Success
	12 × 12	Success	Success	Success
Shot blasting 30/40 grit (×1 pass)	4 × 4	Failure	Failure	Failure
	6 × 6	Failure	Failure	Failure
	8 × 8	Failure	Failure	Failure
	10 × 10	Success	Success	Intermittent
	12 × 12	Success	Success	Success
Shot blasting 30/40 grit (×2 passes)	4 × 4	Failure	Failure	Failure
	6 × 6	Failure	Failure	Failure
	8 × 8	Failure	Failure	Failure
	10 × 10	Failure	Failure	Failure
	12 × 12	Success	Success	Success
Shot blasting 30/40 grit (×3 passes)	4 × 4	Failure	Failure	Failure
	6 × 6	Failure	Failure	Failure
	8 × 8	Failure	Failure	Failure
	10 × 10	Failure	Failure	Failure
	12 × 12	Success	Success	Success
Shot blasting 30/40 grit (×4 passes)	4 × 4	Failure	Failure	Failure
	6 × 6	Failure	Failure	Failure
	8 × 8	Intermittent	Intermittent	Success
	10 × 10	Success	Success	Success
	12 × 12	Success	Success	Success
Shot blasting 30/40 grit (×5 passes)	4 × 4	Failure	Failure	Failure
	6 × 6	Failure	Failure	Failure
	8 × 8	Intermittent	Failure	Failure
	10 × 10	Success	Success	Success
	12 × 12	Success	Success	Success
Shot blasting 30/40 grit (×6 passes)	4 × 4	Failure	Failure	Failure
	6 × 6	Failure	Failure	Failure
	8 × 8	Failure	Failure	Failure
	10 × 10	Success	Failure	Failure
	12 × 12	Success	Success	Success

Key:

Success
Intermittent
Failure

Table B.2: Scan results after shot blasting (30/40 grit) – shot blasted marking surface (30/40 grit)

Degradation applied	Matrix size (mm)	Result 1	2	3
None	4 × 4			
	6 × 6			
	8 × 8	*Refer to table B.1*		
	10 × 10			
	12 × 12			
Shot blasting 60/80 grit (×1 pass)	4 × 4	Failure	Failure	Failure
	6 × 6	Failure	Failure	Failure
	8 × 8	Failure	Failure	Failure
	10 × 10	Success	Success	Success
	12 × 12	Success	Success	Success
Shot blasting 60/80 grit (×2 passes)	4 × 4	Failure	Failure	Failure
	6 × 6	Failure	Failure	Failure
	8 × 8	Success	Success	Success
	10 × 10	Success	Success	Success
	12 × 12	Success	Success	Success
Shot blasting 60/80 grit (×3 passes)	4 × 4	Failure	Failure	Failure
	6 × 6	Failure	Success	Intermittent
	8 × 8	Success	Success	Success
	10 × 10	Success	Success	Success
	12 × 12	Success	Success	Success
Shot blasting 60/80 grit (×4 passes)	4 × 4	Failure	Failure	Failure
	6 × 6	Intermittent	Failure	Failure
	8 × 8	Success	Success	Intermittent
	10 × 10	Success	Success	Success
	12 × 12	Success	Success	Success
Shot blasting 60/80 grit (×5 passes)	4 × 4	Failure	Failure	Failure
	6 × 6	Failure	Failure	Intermittent
	8 × 8	Success	Success	Success
	10 × 10	Success	Success	Success
	12 × 12	Success	Success	Success
Shot blasting 60/80 grit (×6 passes)	4 × 4	Failure	Failure	Failure
	6 × 6	Failure	Failure	Failure
	8 × 8	Failure	Intermittent	Success
	10 × 10	Success	Success	Success
	12 × 12	Success	Success	Success

Key:
- Success (green)
- Intermittent (orange)
- Failure (red)

Table B.3: Scan results after shot blasting (60/80 grit) – clean marking surface

Degradation applied	Matrix size (mm)	Result 1	Result 2	Result 3
None	4 × 4	Success	Success	Success
	6 × 6	Success	Success	Success
	8 × 8	Success	Success	Success
	10 × 10	Success	Success	Success
	12 × 12	Success	Success	Success
Shot blasting 60/80 grit (×1 pass)	4 × 4	Failure	Failure	Failure
	6 × 6	Failure	Intermittent	Intermittent
	8 × 8	Success	Failure	Intermittent
	10 × 10	Success	Success	Success
	12 × 12	Success	Success	Success
Shot blasting 60/80 grit (×2 passes)	4 × 4	Failure	Failure	Failure
	6 × 6	Success	Intermittent	Failure
	8 × 8	Success	Success	Success
	10 × 10	Success	Success	Success
	12 × 12	Success	Success	Success
Shot blasting 60/80 grit (×3 passes)	4 × 4	Failure	Failure	Failure
	6 × 6	Failure	Failure	Failure
	8 × 8	Success	Success	Success
	10 × 10	Success	Success	Success
	12 × 12	Success	Success	Success
Shot blasting 60/80 grit (×4 passes)	4 × 4	Failure	Failure	Failure
	6 × 6	Failure	Failure	Intermittent
	8 × 8	Success	Success	Success
	10 × 10	Success	Success	Success
	12 × 12	Success	Success	Success
Shot blasting 60/80 grit (×5 passes)	4 × 4	Failure	Failure	Failure
	6 × 6	Failure	Failure	Failure
	8 × 8	Success	Intermittent	Success
	10 × 10	Success	Success	Success
	12 × 12	Success	Success	Success
Shot blasting 60/80 grit (×6 passes)	4 × 4	Failure	Failure	Failure
	6 × 6	Intermittent	Failure	Failure
	8 × 8	Success	Success	Success
	10 × 10	Success	Success	Success
	12 × 12	Success	Success	Success

Key:
- Success (green)
- Intermittent (orange)
- Failure (red)

Table B.4: Scan results after shot blasting (60/80 grit) – shot blasted marking surface (60/80 grit)

Degradation applied	Matrix size (mm)	Result		
		1	**2**	**3**
Oxidation (Blue tint)	4×4	🟩 Success	🟩 Success	🟩 Success
	6×6	🟩 Success	🟩 Success	🟩 Success
	8×8	🟩 Success	🟩 Success	🟩 Success
	10×10	🟩 Success	🟩 Success	🟩 Success
	12×12	🟩 Success	🟩 Success	🟩 Success
Oxidation ($\sim 4\mu$m)	4×4	🟩 Success	🟩 Success	🟩 Success
	6×6	🟩 Success	🟧 Intermittent	🟩 Success
	8×8	🟧 Intermittent	🟩 Success	🟩 Success
	10×10	🟩 Success	🟩 Success	🟥 Failure
	12×12	🟩 Success	🟩 Success	🟩 Success
Oxidation ($\sim 8\mu$m)	4×4	🟥 Failure	🟥 Failure	🟥 Failure
	6×6	🟥 Failure	🟧 Intermittent	🟧 Intermittent
	8×8	🟥 Failure	🟥 Failure	🟥 Failure
	10×10	🟥 Failure	🟥 Failure	🟥 Failure
	12×12	🟥 Failure	🟥 Failure	🟥 Failure
Oxidation ($\sim 16\mu$m)	4×4	🟥 Failure	🟥 Failure	🟥 Failure
	6×6	🟥 Failure	🟥 Failure	🟥 Failure
	8×8	🟥 Failure	🟥 Failure	🟥 Failure
	10×10	🟥 Failure	🟥 Failure	🟥 Failure
	12×12	🟥 Failure	🟥 Failure	🟥 Failure

Key:

- 🟩 Success
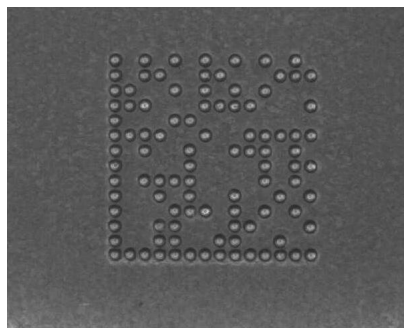- 🟧 Intermittent
- 🟥 Failure

Table B.5: Scan results after oxidation – clean marking surface
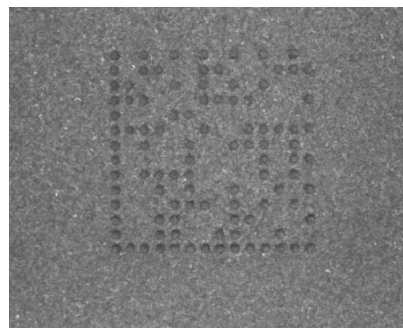
Appendix C

Scan Images

The figures included in this appendix show how the image captured by the scanner changes with the introduction of degradation to the Data Matrix surface.
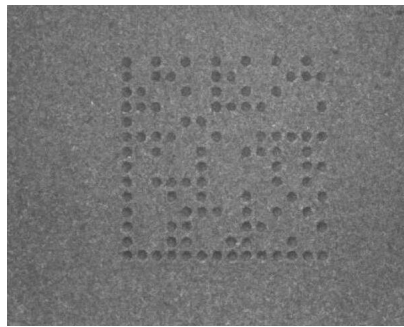
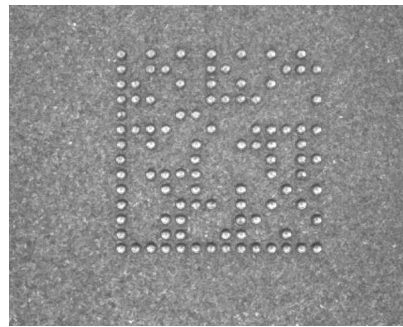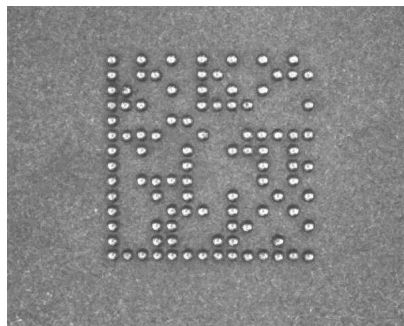*The remainder of this page has been left blank intentionally.*

(a) Clean
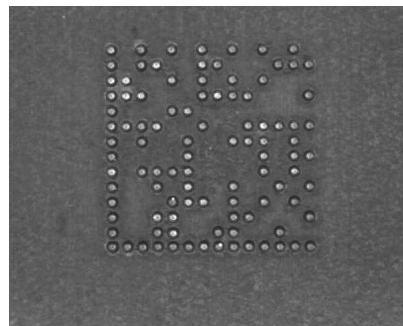

(b) Shot blasted (30/40 grit)
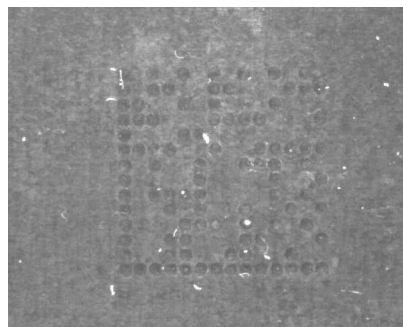

(c) Shot blasted (60/80 grit)

(d) Shot blasted (30/40 grit) before marking

(e) Shot blasted (60/80 grit) before marking

(f) Oxidised (blue tint)

(g) Oxidised ($\sim 8~\mu$m)

Note: all these images show a 10 mm matrix

Figure C.1: Scan images showing Data Matrix symbols of varying surface condition